PETROLEUM SOURCE ROCK EVALUATION AND PALYNOFACIES ANALYSIS OF BONGAYA FORMATION IN PITAS AREA, NORTHERN SABAH

NOR AAINAA FARHANA MD NOR 'AZAM

FACULTY OF SCIENCE
UNIVERSITI MALAYA
KUALA LUMPUR

2022

PETROLEUM SOURCE ROCK EVALUATION AND PALYNOFACIES ANALYSIS OF BONGAYA FORMATION IN PITAS AREA, NORTHERN SABAH.

NOR AAINAA FARHANA BINTI MD NOR 'AZAM

THESIS SUBMITTED IN FULFILMENT OF THE REQUIREMENTS FOR THE DEGREE OF MASTER OF SCIENCE.

DEPARTMENT OF GEOLOGY
FACULTY OF SCIENCE
UNIVERSITI MALAYA
KUALA LUMPUR

2022

UNIVERSITI MALAYA
ORIGINAL LITERARY WORK DECLARATION

Name of Candidate: **NOR AAINAA FARHANA**

Name of Degree: **MASTER OF SCIENCE**

Title of Dissertation ("this Work"):

PETROLEUM SOURCE ROCK EVALUATION & PALYNOFACIES ANALYSIS OF BONGAYA FORMATION IN PITAS AREA, NORTHERN SABAH.

Field of Study:

PETROLEUM GEOLOGY / GEOCHEMISTRY

I do solemnly and sincerely declare that:

(1) I am the sole author/writer of this work;
(2) This Work is original;
(3) Any use of any work in which copyright exists was done by way of fair dealing and for permitted purposes and any excerpt or extract from, or reference to or reproduction of any copyrighted work has been disclosed expressly and sufficiently and the title of the work and its authorship have been acknowledged in this work;
(4) I do not have any actual knowledge nor do I ought reasonably to know that the making of this work constitutes an infringement of any copyrighted work;
(5) I hereby assign all and every right in the copyright to this work to the University of Malaya ("UM"), who henceforth shall be the owner of the copyright in this Work and that any reproduction or use in any form or by any means whatsoever is prohibited without the written consent of UM having been first had and obtained;
(6) I am fully aware that if in the course of making this work, I have infringed any copyright whether intentionally or otherwise, I may be subject to legal action or any other action as may be determined by UM.

Candidate's Signature Date: 7 February 2022

Subscribed and solemnly declared before,

Witness's Signature Date: 7 February 2022

Name:

Designation:

PETROLEUM SOURCE ROCK EVALUATION AND PALYNOFACIES ANALYSIS OF BONGAYA FORMATION IN PITAS AREA, NORTHERN SABAH.

ABSTRACT

Bongaya Formation is Miocene sediment consisting of mostly sandstone interbedded with shale, coal, and mudstone presence and located on Borneo's northern tip. This study focuses on assessing the organic geochemistry (source rock analyzation, bitumen evaluation, and molecular analysis) of the onshore Bongaya Formation to identify their petroleum hydrocarbon potential. The quantitative pyrolysis technique and petrographic analysis (vitrinite reflectance and maceral counting) are then correlated in the study for better provision where palynology analysis is also conducted to reconstruct the paleoenvironment model of the formation. This work was prompted by the scarcity of geochemical evaluations of the Bongaya Formation in the Pitas area and seismic record suggesting hydrocarbon indicators in the adjacent unexplored offshore basin, which includes the Bongaya Formation (Mazlan et al., 1999). Bulk geochemistry results showed fair to excellent amount of carbon contains, up until 63.1 wt%. The highest TOC value is coals, followed by carbonaceous shales and shale, whereas the lowest (fair) TOC amount is mudstones. The relationship between HI and TOC brings to the identification of kerogen type possessed by Bongaya source rock, as mainly shows Type III kerogen. However, pyrolysis details analysis reveals that there is a possibility of Type II/III kerogen to be present. Bongaya Formation is dominant in generating gas-prone source rock and little oil for some samples, according to intense liptinite occurrence and Py-GC analysis. Petrographic and maceral analysis identified that some of the coal has high resinite constituents, which potentially produce waxy oil. Nevertheless, the variations of T_{max} data (369.6 –437.3 ˚C) are consistent with huminite reflectance measurements (0.32-0.43 R_o %), indicating that this formation is thermally immature to generate petroleum.

The paleoenvironment of organic matter is determined to be colonized by the mangrove area. However, besides mangroves, inland vegetation and back mangrove were also interpreted as a part of the Bongaya Formation depositional environment. The majority of the Bongaya formation was produced from terrestrial organic materials and was primarily maintained in a suboxic environment. There are some indications that some organic materials may be deposited in anoxic conditions, albeit this is not the case in the majority of cases.

Keywords: Source rock evaluation; Bongaya Formation; Type III kerogen; Immature; Miocene.

PENILAIAN BATUAN PUNCA PETROLEUM DAN ANALISIS PALINOFASIS FORMASI BONGAYA DI KAWASAN PITAS, UTARA SABAH

ABSTRAK

Formasi Bongaya adalah sedimen Miosen yang kebanyakannya terdiri dari batu pasir yang disatukan dengan syal, dan batu bara dan batu lumpur yang terdapat di hujung utara Borneo. Kajian ini memfokuskan pada penilaian geokimia organik (analisis batuan sumber, penilaian bitumen, dan analisis molekul) Formasi Bongaya darat untuk mengenal pasti potensi hidrokarbon petroleum mereka. Teknik pirolisis kuantitatif dan analisis petrografi (pantulan vitrinit dan pengiraan *maceral*) kemudian dikorelasikan dalam kajian untuk penyediaan yang lebih baik di mana analisis palinologi juga dilakukan untuk merekonstruksi model pembentukan formasi. Karya ini didorong oleh kelangkaan penilaian geokimia Formasi Bongaya di daerah Pitas dan catatan seismik yang menunjukkan kewujudan petunjuk hidrokarbon yang merangkumi Formasi Bongaya di lembangan luar pesisir yang berdekatan, (Mazlan et al., 1999). Hasil geokimia pukal menunjukkan jumlah karbon yang bagus hingga sangat baik, sehingga 63.1%. Nilai TOC tertinggi adalah arang batu, diikuti oleh syal karbon dan syal, sedangkan jumlah TOC terendah (bagus) adalah batu lumpur. Hubungan antara HI dan TOC membawa kepada pengenalpastian jenis kerogen yang dimiliki oleh batu sumber Bongaya, dimana yang terutama menunjukkan kerogen Jenis III. Namun, analisis perincian pirolisis menunjukkan bahawa ada kemungkinan adanya kerogen Jenis II/III. Pembentukan Bongaya dominan dalam menghasilkan gas dan sedikit minyak untuk beberapa sampel, berdasarkan kewujudan liptinit yang kuat dan analisis Py-GC. Analisis petrografi dan makmal mengenal pasti bahawa sebilangan arang batu mempunyai unsur konstituen *resinite* yang tinggi, yang berpotensi menghasilkan minyak lilin. Walaupun demikian, variasi data T_{max} (369.6 –437.3 ˚C) konsisten dengan pengukuran pantulan *huminite*

(0.32-0.43 R_o%), yang menunjukkan bahawa pembentukan ini tidak matang secara termal untuk menghasilkan petroleum. Persekitaran bahan organik didapati kebanyakkan berasal dari Kawasan bakau. Namun, selain hutan bakau, vegetasi pedalaman dan bakau bahagian belakang juga ditafsirkan sebagai bagian dari lingkungan persekitaran terdahulu Formasi Bongaya. Sebahagian besar formasi Bongaya dihasilkan dari bahan organik terestrial dan dipelihara dalam lingkungan suboksik. Terdapat beberapa petunjuk bahawa sebilangan bahan organik mungkin terbentuk dalam keadaan anoksik, walaupun ini tidak berlaku dalam kebanyakan kes.

Keywords: Penilaian batu sumber; Formasi Bongaya; Kerogen Jenis III; Tidak matang; Miocene.

ACKNOWLEDGEMENTS

The thesis presented here is the product of tremendous assistance supplied by individuals whose creativity, ideas, time, funding, and love were critical in its completion.

I would like to thank my supervisor, Dr Khairul Azlan Mustapha, for providing invaluable help throughout my research process, particularly during fieldwork, lab work, and writing. Dr Mohammed Hail Hakimi (my second supervisor) was extremely helpful in improving and commenting on my publication and data analysis. Thank you for taking the time to share your knowledge with me. Mr. Nura (Ph.D. student) deserves special thanks for his helpful comments and guidance from the beginning to the end.

I am grateful to the Universiti Malaya for allowing me to conduct this research and to IPPP for funding research grant N0: GPF0 19B-2018. Many thanks to Mr. Zamri, Madam Zaleha, Mr. Alif, and Mr. Aizat for their technical assistance with laboratory operations and maintenance, as well as their participation in sample analysis. I'd like to thank the entire faculty and personnel of the Department of Geology for their technical and administrative cooperation.

I am immensely thankful to Imtiyaz, Intan, Mariah, and my family, for their moral support, encouragement, and inspiration. Thank you for keeping things normal and reminding me of what is important in life. A sincere appreciation to Fatin and Najihah for their invaluable contributions to the success of this study. Also, I would like to offer my heartfelt appreciation to all of my seniors. Thank you for your time, consideration, and intellect. Everyone holds a special place in my heart, and they have helped to make my master's path less burdensome and more colourful. Finally, I thank God for His goodness in making all this possible.

TABLE OF CONTENTS

LIST OF FIGURES

LIST OF TABLES

LIST OF APPENDICES

CHAPTER 1: INTRODUCTION

1.1 Introduction

In Malaysia, the northwestern part of Borneo Island, notably the offshore region, has been subjected to more than a century of petroleum exploration and has since been identified as one of the most prolific oil-producing basins (Leong,1999). As a result, the petroleum resources in the surrounding area, especially in the provinces of Sabah, are being closely examined, however, most of the Northern Sabah oil and gas discoveries and exploration are concentrated on the west side with little insight on the east. Many studies have been conducted on the formation origin, geochemistry, structural, and sedimentation of Sabah's northern extension, especially in the Kudat region (Northwestern part). In contrast, this study focuses on the East Peninsula (Bengkoka Peninsula), specifically on the Bongaya Formation of Pitas, which is in the east northern part of Borneo, to provide a detailed study of their source rock characteristics, depositional environment condition, and resources, as no geochemistry and palynology study has ever been published on this area. The goal of this study was to investigate any potential hydrocarbon resources in this new border area on the east coast of Sabah.

According to prior research, the source rock unit in Sabah has a very similar composition and was created mostly by terrigenous organic materials. The Bengkoka shales and coal sediments, and other similar age sediments (Miocene Formation) such as Sabahat Formation, and Sandakan Formation are all regarded as potential source rock (Mazlan et al., 1999; Mustapha and Abdullah, 2013; Mustapha et al., 2017). Even though these sediments are high in organic matter, they have low thermal alteration. The source rocks are too young to yield hydrocarbons. Furthermore, their characteristics are mostly gas-prone, with little oil enclosure. So far, one palynology analysis on a Miocene age formation, the Sandakan Formation palynology study has been released, showing that the majority of the organic matter is mangrove-related substances from the transition climate

(Mustapha et al., 2017). The depositional environment extended from the mangroves to a shallow marine environment.

As discussed, this research aims to analyze the onshore source rock of the Bongaya Formation through the hydrocarbon-producing characteristics. The characteristics suggest three key criteria for determining source rock potential, which is the amount of organic matter in the rock that should be adequate to produce the hydrocarbon, the nature of the organic matter, which is dependent on their origin and affects the kerogen type, and finally, the amount of thermal the rock is exposed (Peter and Cassa, 1994). This study investigates the Bongaya Formation potential as a source rock to generate petroleum through several geochemical and petrology experiments such as using source rock analyzer, bitumen extraction, pyrolysis gas-chromatography, and vitrinite reflectance. The organic geochemistry assessment refers to the variety of organic matter origin, deposition, preservation, and transformation in sediments, where organic matter and hydrocarbon content are discovered (Tissot and Welte, 1984; Hunt, 1995; Dembicki, 2017). Second, this project aims to examine previous paleodepositional environments and paleoconditions using palynology research and their relationship with sedimentology study and biomarkers fingerprints. Palynology is important in the study of vegetation because it uses pollen assemblage profiles and the characteristic range of significant pollen to do so. Oil exploration practices have increased the use of pollen to align with oil-bearing formations for a more accurate source origin performance.

A prospective hydrocarbon plays area, and its distribution can be assessed by comparing generation petroleum potential to their depositional environment. Finally, it will serve as a guide for potential hydrocarbon discoveries in the region.

1.2 Problem Statement

Bongaya Formation in Bengkoka Peninsular is considered scarce and difficult to access, especially the tip northern part. As a result of the lack of previous research on geochemistry and its organic sources, let alone palynofacies review, hydrocarbon potential has been underestimated, and no petroleum exploration work has been done in the field. Furthermore, this work supports a prior seismic record in the offshore SubMalawi Basin that deposited with the Bongaya Formation and exhibited hydrocarbon indication (Mazlan et al., 1999), which has sparked interest in studying this formation.

The hydrocarbon Sub-Malawi Basin is a small offshore basin located between the Kudat Peninsula and the Bengkoka Peninsular that has yet to be explored and studied in depth. Because there is no access to the Bongaya sediments in the Sub-Malawi Basins, an effort was made to investigate the onshore Bongaya Formation.

1.3 Objectives

The primary purpose of this research is to evaluate the hydrocarbon generating potential of Bongaya Formation sediments and concludes the best source rock by:

1) Evaluating the petroleum source rock potential by determining the quantity, quality of organic matter, and organic matter's thermal maturity in the analyzed rock.
2) Correlating palynology data with sedimentology and biomarker fingerprints for paleoenvironmental interpretation.
3) Reconstructing the paleodepositional environment, condition, and organic source input of Bongaya Formation.
4) To predict the hydrocarbon prospectivity of Bongaya formation in the onshore northern Sabah.

1.4 Sabah in a brief

Sabah, situated in the northern part of Borneo Island along with the Sarawak state is made up of a 3,900,000 population in 2015. The total Sabah area covered 73,904 km2 with the largest city of Kota Kinabalu (capital city) and other divisions including Kudat, Sandakan, Tawau, etc. Some parts of Sabah are still inaccessible as they have long mountain ranges on the west part which is part of the Crocker Range National Park Kinabatangan River with Mount Kinabalu as the highest mount in Sabah as well as in Malaysia.

The climate of Sabah is humid hot and uniform temperature throughout the year. The average daily temperature varies from 27°C to 34°C and raindrops are approximately 1,800 millimeters to 4,000 millimeters. The variation in temperature and rainfall is due to topographical relief and the effect of tropical monsoons. The monsoons have two seasons of northeast and southeast which occurs from November to March and May to September relatively. The northeast contributes heavy rainfall however southeast prevails less rainfall.

The coastline area of Sabah is covered with mangrove (331,325 hectares) and Nipah forest. Besides that, both the west and east coast are dominated by sand beaches while the inner area is covered by sand mixed with mud.

1.5 Location of Study Area

The research area is located in northern Sabah, in the Pitas area of the Bengkoka Peninsula. The Bengkoka Peninsula is the eastern tip of the Sabah Peninsula, parallel to the Kudat Peninsula, separated by a small offshore basin called the Sub-Malawi Basin in between them. The Bongaya Formation, which was studied, was discovered in the Pitas Town area and spread to the tip of the Peninsular, which is in Kg. Malubang (Figure 1.1).

This formation was in a form of isolated basins and consist of grey sandstones interbedded with carbonaceous shales with small occurrences of conglomerate beds. Coal clast can also be found randomly in the bedding. Tongkul (1991) described that the basins are small, shallow, and nearly circular-shaped lies uncomfortably on older formations such as the Crocker, Kudat, and Chert-Spilite Formations (Figure 1.2). For the analysis, the formation has good exposure in the area and good aerial photographs. The road from Pitas town to Malubang is on gravel and winding, and the outcrop studied was discovered alongside this road. We passed through many villages along the way, including Kg. Telaga, Kg. Kandang, and Kg. Liu, and visited the Bongaya-deposited, Supirak Island, near the coast at Kg. Malubang. The study area is bounded by latitudes 06° 40'N-06° 59'N and longitudes 116° 59'E-117° 6'E.

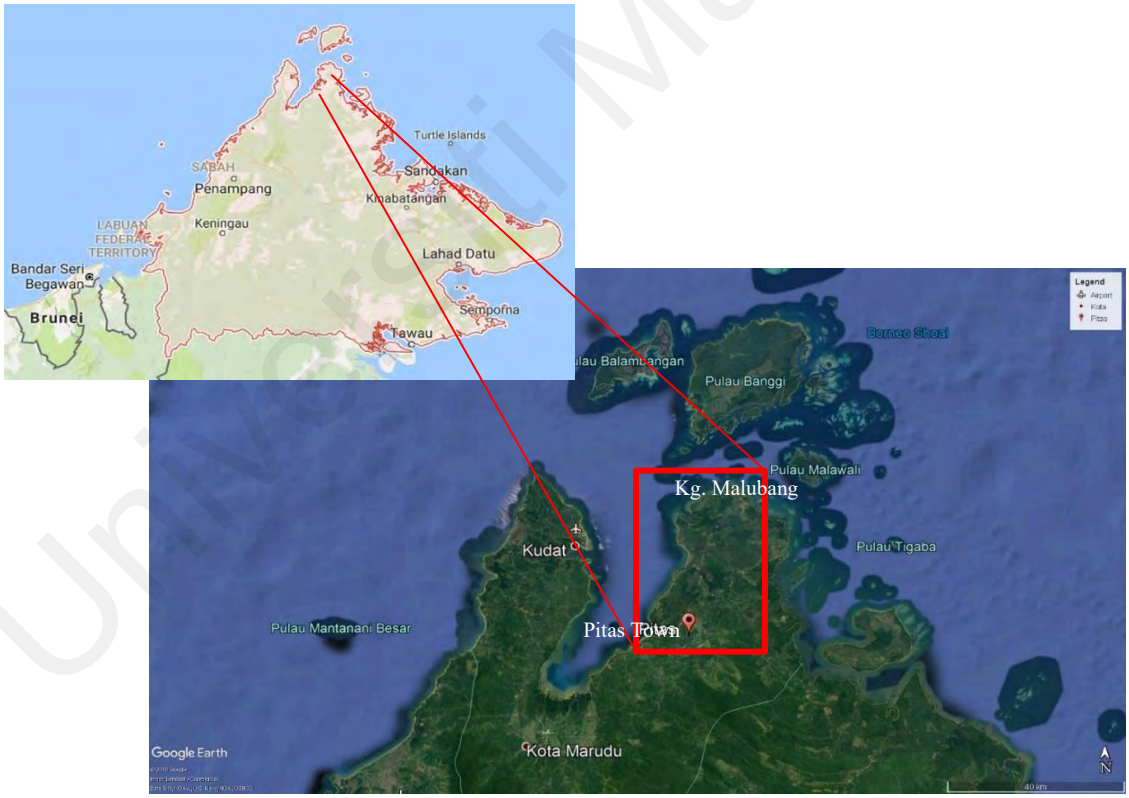

Figure 1.1: Satellite image shows the Borneo Island, and highlighted are the location of the study areas (in red rectangles).

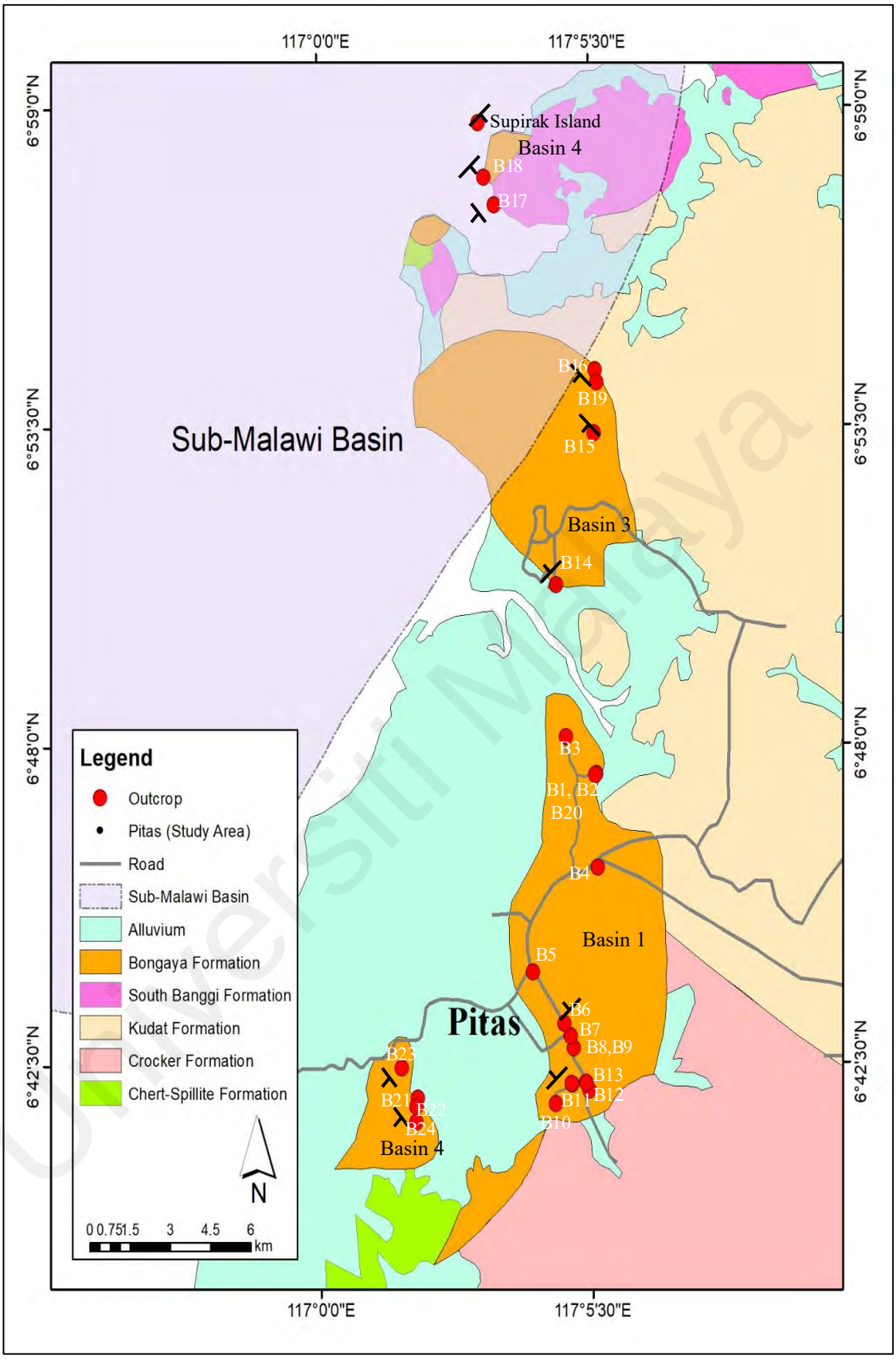

Figure 1.2: Geological map of the study area with indication of outcrop in (red dot) (Modified from Lim and Heng,1985)

CHAPTER 2: GENERAL GEOLOGY OF SABAH

2.1 Introduction

Sabah is located in the northern part of the world's third-biggest island, Borneo Island, and is flanked by three marginal basins: the South China Sea, the Celebes Sea, and the Sulu Sea. Northern Borneo then underwent significant compressional deformation, as evidenced on onshore by folded sedimentary units dating from the late early Miocene to the middle Miocene (e.g., Sandal, 1996; Morley et al., 2003; Back et al., 2001, 2005, 2008), and in offshore, by folded and thrust of middle Miocene to the present-day shelf and slope sequences (e.g., Levell, 1987; Hinz et al., 1989; Hazebroek and Tan, 1993; Morley et al., 2003; Ingram et al., 2004). Sabah's position has caused it to deform in response to the movements of the neighboring plates, and it has undergone a complex structural development and depositional framework from the early Tertiary, which has resulted in current geology (Balaguru and Hall, 2008). Therefore, Sabah has been labeled as one of Malaysia's most complex geological history settings and has been a source of discussion among fellow scholars ever since.

2.2 Tectono-stratigraphic province of Sabah.

The massive fold-thrust belt trending northeast in the west which bends east and southeast towards the north and eastern parts of Sabah is the principal tectonic event in the state (Balaguru et al., 2003). This belt is made up of the deep marine Eocene to Oligocene accretionary complex (Rangin et al., 1990; Tongkul, 1990; Hall, 1996). According to the tectonostratigraphic province of NW Sabah (Hazebroek & Tan, 1993), five aspects that contribute to the geology of Sabah are:

a) The crystalline basement of Sabah succession is also a pre-tertiary ophiolite complex. Radiometric dating was once done and indicate it to be aged around Cretaceous to Triassic (Kirk, 1962; Hutchison et. al., 1997; Leong 1974,1998)

b) The Rajang-Crocker accretionary prism consists of Chert-Spilite Formation, Sapulut Formation, Trusmadi Formation, and Crocker Formation. A study by Hutchinson (1996) has revealed a proper distinction between the older Rajang Group consisting of Sapulut, Trusmadi, and East Crocker Formation, and the younger Rajang Group which includes West Crocker and their equivalent formation. 'Sarawak Orogeny' results in the lifted older Rajang Group during Middle to Late Eocene, where only later, the younger Rajang Group (West Crocker, Temburong, Setup Shale and Kudat Formation) were deposited (Hutchinson, 1996; Tongkul,1997). During Early Miocene to Middle Miocene, the deposits also were uplifted, and their erosion sediments made up the Deep Regional Unconformity (DRU).

- Chert-Spillite Formation: dated to be Cretaceous-Early Paleogene deposits that are a complex extrusive ultra to ultrabasic igneous rock. The chaotic sediments are also composed of radiolarian cherts, limestones, and clastic sediments that exist from eastern Sabah through central Sabah and extended to the Gunung Kinabalu area.

- The Sapulut, Trusmadi, and Crocker Formation: These formations were discovered in slumps in various parts and made up from thick deep marine sediments of sandstone and shale that had partly metamorphosed into phyllite and slates.

c) Broken formations and mélanges are believed to form through a series of connected events from the Early to Middle Miocene. This formation delivered tectonic characteristics, sedimentary and diapiric origin in Sabah.

d) Neogene sedimentary rocks which are deposited after Deep Regional Unconformity (DRU) and before Shallow Regional Unconformity (SRU)

- Consists of mostly shallow marine to fluvial-deltaic facies that made up the 'circular basins' of Sabah.

- This formation is bounded as fault areas and forms the petroleum-producing basins in Sabah.

- The depositional of hydrocarbon-bearing Neogene basins was based by DRU and further deposited by deep marine shales and turbiditic sand (Setup Shale and Kudat Formations) clastic units of Middle to late Miocene Formation.

e) The Semporna-Sulu Arc comprised of andesitic to dacitic volcanic activity (Miocene) to the Dent and Semporna peninsulas (Quaternary).

- The igneous activity is represented by felsic to intermediate intrusive rocks such as Mount Kinabalu and volcanic rock in Semporna and Tawau area (Kirk, 1968; Lee,1988).

- After the Shallow Regional Unconformity (SRU), the Dent group (Sahabat and Ganduman Formations) was deposited in the late Middle Miocene to early Late Miocene. Lithostratigraphic units consist primarily of clastics with minimal carbonates, and they were formed in settings ranging from deltaic to shallow marine.

- Late Middle Miocene to early Late Miocene period is which the Dent group (Sahabat and Ganduman Formations) deposited after the Shallow Regional Unconformity (SRU). The lithostratigraphic units are made of mainly clastics with minor carbonates that made up deltaic to shallow marine environments. Later Plio-Pleistocene strata, such

as the Timohang, Togopi, and Wallace Formations, consist primarily of limestone, calcareous sandstones, conglomerates, and carbonaceous shales.

2.3 Tectonic evaluation and basin development in Sabah

2.3.1 Pre-Cenozoic

The bottom of Sabah is in line with the 'crystalline basement' which describes older 'basement' metamorphic and igneous rocks where gneiss, schist, amphibolite, and associated granite, granodiorite, and biotite tonalite was exposed. It is always associated with the Chert-Spilite Formation. Technically, the term ophiolites sequences were interpreted as the Crystalline Basement rocks that were exposed above sea level, onto the continent crustal rocks (coarse-grained ultrabasic rocks with chromite layers at the bottom overlain by 'Silumpat Gneiss') followed by fine-grained meta-basalt and topped by Chert-Spillite Formation.

2.3.2 Early Cretaceous to early Eocene (~42.5 Ma)

At this time, the Celebes Sea was closing due to southeasterly subduction of the proto-South China Sea in the NW Borneo. Parts of the oceanic basement were uplifted as a result of major tectonic compression and a newly formed oceanic basement made of deep-water mudstones and turbiditic sandstones sediments that eroded from the uplifted older oceanic basement and continental basement of Sabah were deposited. The sediments were thought to have been deposited in Crocker Basin and were highly deformed with tight isoclinal folds and thrusts (Hutchinson, 1996).

The Lubuk Antu Melange, Lupar Valley of Sarawak (Tan, 1982), and Eastern Sabah Ophiolitic Melange (Leong,1974) provided evidence of oceanic basement imbrications during a compressional event trending NE-SW in the Mid Eocene to Early Miocene. The

western of Sabah was also deformed and being uplifted at that time (Balaguru, 2006a) and was referred to as 'Sarawak Orogeny' by Hutchinson (1996). This orogeny was suggested to be driven by collision along the northern Borneo margin. Rangin et al. (1990) indicate possible unconformity formation in Paleogene turbidites succession although the contact is obscure. Evidence of reworking of nannofossil has been highlighted however it is too difficult to be recognized due to the lithologies similarities on either side and the strong Neogene deformation.

Many believe that a part accretionary complex of Sea Pacific is interpreted to be turbiditic Rajang Group that has undergone deformation. Deep marine turbidites deposition continued until the Late Eocene, while Balaguru (2006) reported that structural deformation events in the Late Eocene aided in the control of an elongated basin (trending NE-SW) development in Sabah.

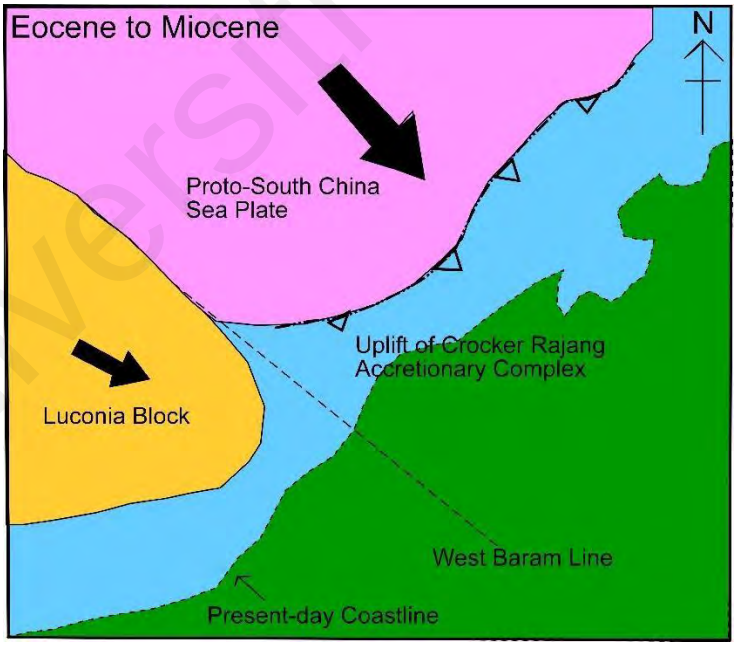

Figure 2.1: A schematic diagram depicting the plate arrangement at the NW Borneo collisional boundary from the Eocene to the Miocene periods (after King et al., 2010)

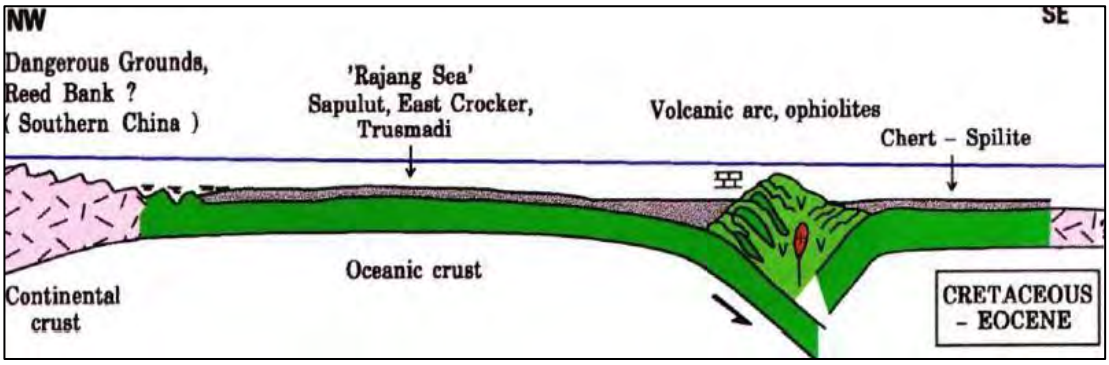

Figure 2.2: Schematic cross-section of Celebes Sea closing due to subduction in NW Sabah during Cretaceous to Eocene (Modified after Tongkul, 1991a; Petronas, 1991).

2.3.3 Oligocene-early Miocene (~42.5-20.5 Ma)

Further deformation on the basement caused by the continuing of the subduction process has resulted in sedimentation filling in the elongated basin in two ways. The sedimentation in the south and southwest filled the basin axially, while the sedimentation in the north, northwest, northeast, and east filled the basin laterally. The Crocker, Trusmadi, port of Sepulut, Kudat, Labang, Kulapis, and Temburung Formations, basically the deepwater sediments were found in the forearc basin and we see exposed in western Sabah. In contrast, the other side of the basin was formed by shallow water sediments such as Labang, Tembrung, a portion of the Kudat Formation, and the Kulapis Formation. This sedimentation process has compacted Mid Eocene to Early Miocene sediments into NE-SW and NW-SE oriented fold-thrust belts in the west and north of Sabah, respectively. During the Oligocene period, substantial regional subsidence occurred, which was attributed to an active growth fault based on numerous syn-depositional and syn-diagenetic extensional faults discovered in outcrops.

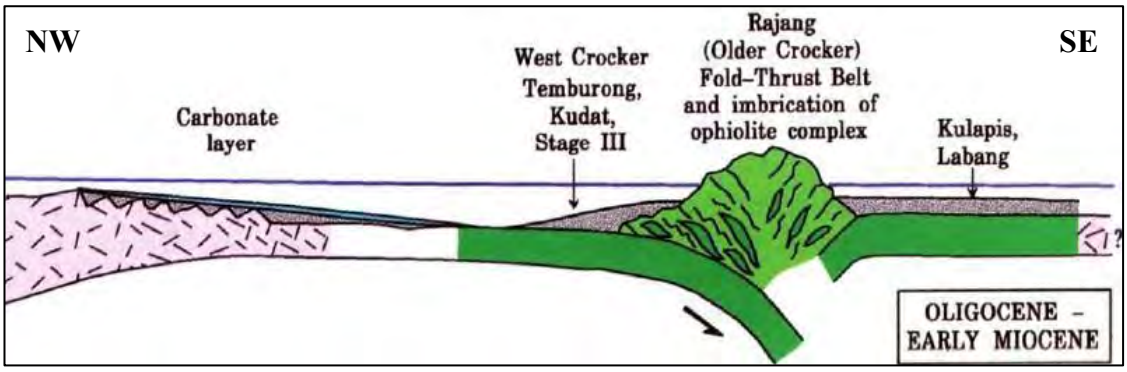

Figure 2.3: Schematic cross-section of Celebes Sea closing due to subduction in NW Sabah during Oligocene to Early Miocene (Modified after Tongkul, 1991a; Petronas, 1991).

2.3.4 Early Miocene

In Sabah, the early Miocene epoch saw widespread mélange development and rapid tectonic evolution, including major uplift and erosion. The Base Miocene Unconformity (pre-DRU or BMU) was created during this time. Hutchison (1996) refers to the tectonic events that happened at this time as the 'Sabah Orogeny,' which arose because of the Dangerous Ground Continental Block subduction and collision with NW Borneo. Continuation of uplifted and erosion events deliberately provided deltaic to shallow marine sediments that change the depositional environment from deep-water to a shallow deltaic setting. The dominant N-S compression has resulted in the formation of NW-SE fold and thrust belt, which would most likely cause subduction in the southeastern direction, resulting in the Early-Middle Miocene volcanic arc in Dent Peninsular. The onset of Tanjong, Meligan, or Kudat Formation clastic deposition marked the end of the Early Miocene period.

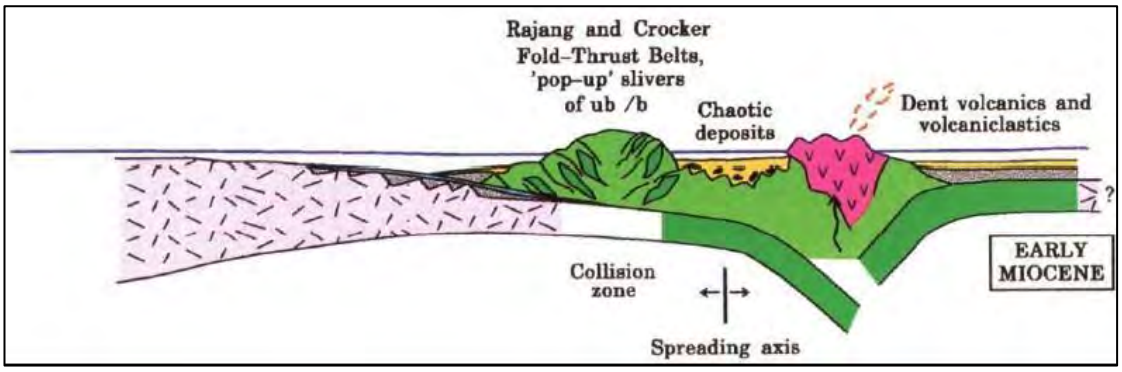

Figure 2.4: Schematic cross-section of Celebes Sea closing due to subduction in NW Sabah during Early Miocene (Modified after Tongkul, 1991a; Petronas, 1991).

2.3.5 Late early-middle Miocene

The NW-SE fold and thrust belt occurred in the Early-Middle Miocene and were followed by major NW-SE extensions. The extension caused the extensive chaotic deposits found in eastern Sabah to form as it fragmented the older imbricate sediment and underlying oceanic basement. The subsidence of the central Sabah Basin in the Middle Miocene was thought to be related to the opening of the Sulu Sea Basin in a back-arc setting or regional thermal subsidence. After the Deep Regional Unconformity (DRU) was created (Middle Miocene) by arc-continent collision, the extension stopped, and subsidence occurred and provide thick prograding post-rift deposits.

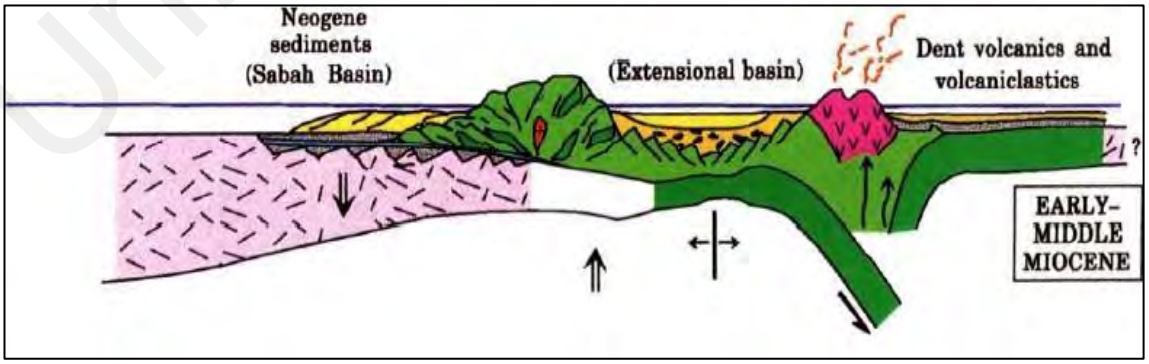

Figure 2.5: Schematic cross-section of Celebes Sea closing due to subduction in NW Sabah during Early to Middle Miocene (Modified after Tongkul, 1991a; Petronas, 1991).

2.3.5 Late Miocene- Pliocene

This epoch marked another major folding and uplift that made up the Shallow Regional Unconformity (SRU). The Maliau Orogeny was the most significant tectonic event in the Late Pliocene (Balaguru et al., 2003). The event was triggered by transpressional fault movement along with NW-SE trending strike-slip faulting, which resulted in additional orogenic deformation, elevation, and structural development in Sabah.

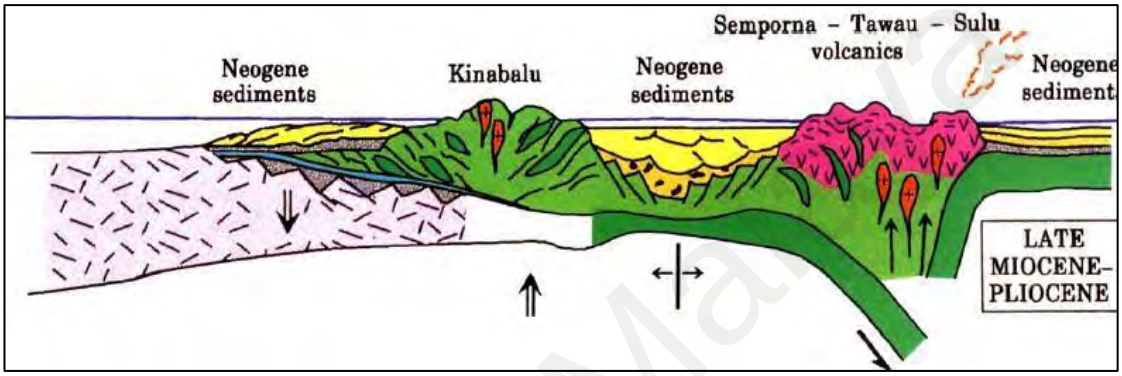

Figure 2.6: Schematic cross-section of Celebes Sea closing due to subduction in NW Sabah during Late Miocene to Pliocene (Modified after Tongkul, 1991a; Petronas, 1991).

2.4 Stratigraphy of Northern Sabah

The figure that summarized stratigraphy of northern Sabah is shown in Figure 2.7 previous studies indicate that northern parts of Sabah were filled with mostly igneous rock with subordinate metamorphic rocks and sedimentary rocks (Stephen, 1956; Collenette, 1958; Wilson, 1961; Leichti et al 1960; Stauffer, 1967; Tjia, 1974; Lee, 1979; Tongkul, 1987). The igneous rocks found to consist of serpentinites, basalts/spilite, agglomerates, gabbros, dolerites, andesites, granodiorites, and adamellites (Tongkul,1990) while metamorphic rocks are hornblende schists and gneisses. The igneous rocks made up most of the basement of the spilite formation. Whereas the

sedimentary sediments are made of dominantly sandstones and shales with subordinate cherts, limestone, and conglomerate.

The northern Sabah basins grouped of Kudat-Banggi begins with Chert-Spilite lithology since Cretaceous as the chert was considered the oldest sedimentary rocks (Basir & Sanudin, 1988). Representing the basement rocks of this region, this formation resembles the ophiolite series as these cherts are associated with other igneous rocks such as basaltic, intrusive rocks, ultrabasic rocks, and metamorphic rocks.

Separated by unconformity on the top of this basement formation, The Crocker and Kudat Formation were mainly sedimentary rocks that lay on it. The Crocker that characterized by a rhythmic alternation of sandstone and shale beds indicates deep water flysch sediments which occurred mostly in Western Sabah. As for Kudat Formation, it can be found mostly in Northern Sabah and is shallow water sediment that formed interbedded carbonaceous sandstones and shales. Some limestone lenses could be found in the bedding. Both Crocker and Kudat Formation deposited during Eocene to Early Miocene time.

Early Miocene to Early Pliocene age saw shallow-water deposits formations of South Banggi and Bongaya Formation that is made of mainly of sandstones, shales, with minor limestone and conglomerates bed. These two formations also lie unconformably on top of the Crocker, The Kudat, and basement formation. Further overlain formation by Timohing Formation which also shallow-water sediment of Pliocene-Pleistocene in age. As for igneous rocks, Miocene-Pliocene times is a time for these igneous rocks progressively intruded (Mt. Kinabalu plutonic) and extruded (Sirar Island volcanic).

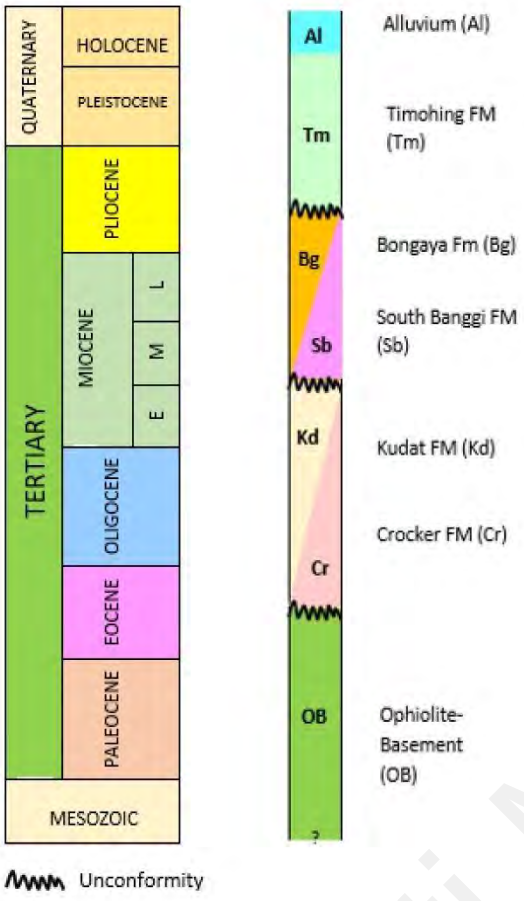

Figure 2.7: General stratigraphy of Northern Sabah (modified from Tongkul, 1990)

2.5 Bongaya Formation

Pitas is located on Sabah's right horn, in the northeastern section of the Kudat Division. The Bongaya Formation in Pitas Sabah is a Neogene deposit that exists on top of earlier sediments such as the Crocker, Kudat, and Chert-Spilite Formation in the Bengkoka Peninsular. The formation appears in a few isolated basins (Tongkul, 1991) and is bordered by the South Banggi Formation at the north and by the Crocker Formation at the south. Wilson (1961) specified that the Bongaya Formation was dated as Late Miocene to Early Pliocene material based on foraminifera discovered.

The lithology of the Bongaya Formation is primarily sandstone, shale series, and limestone facies, with a thickness of almost 750 meters (Wilson, 1961). Tongkul (1991) explained that the Bongaya Formation is mostly made up of grey sandstone interbedded

with carbonaceous shale and limited conglomerate beds, with a thickness of fewer than 200 meters that varies depending on the area. It is discussed that the sediments will be thicker at the basin's edge compared to at the center of the basin. Crocker and Chert-Spillite sediments eroded and make up the conglomerate beds in the Bongaya basin. Sedimentary characteristics include burrowing trace and rich with crossbedding structure shown to have deltaic to shallow water depositional environment influences.

Tongkul (1991) reported that the Bongaya Formation basin formed as gently dipping beds governed by ancient features on earlier formations such as the Basement and Crocker Formation. Up to the middle Miocene, early north Sabah deformations were folded and thrust faulted in NW-SE trend and were later cross-cut by various sets of NE-SW and N-S horizontal faults (Tongkul; 1990, 1994). The E-W basin is formed by N-S compression and was afterward deposited by the South Banggi Formation and Bongaya Formation. The basin contains N-S fault extensional structures; however, they do not exhibit significant deformation due to the lack of substantial folding. The Bongaya Formation's nearly circular basin was created by a mix of fault structures with NW-SE, NE-SW, and W-E trends. The existing structures were continuously extended, resulting in a V-shaped graben-type basin that seemed deeper towards the sea, approximately the northeastern part.

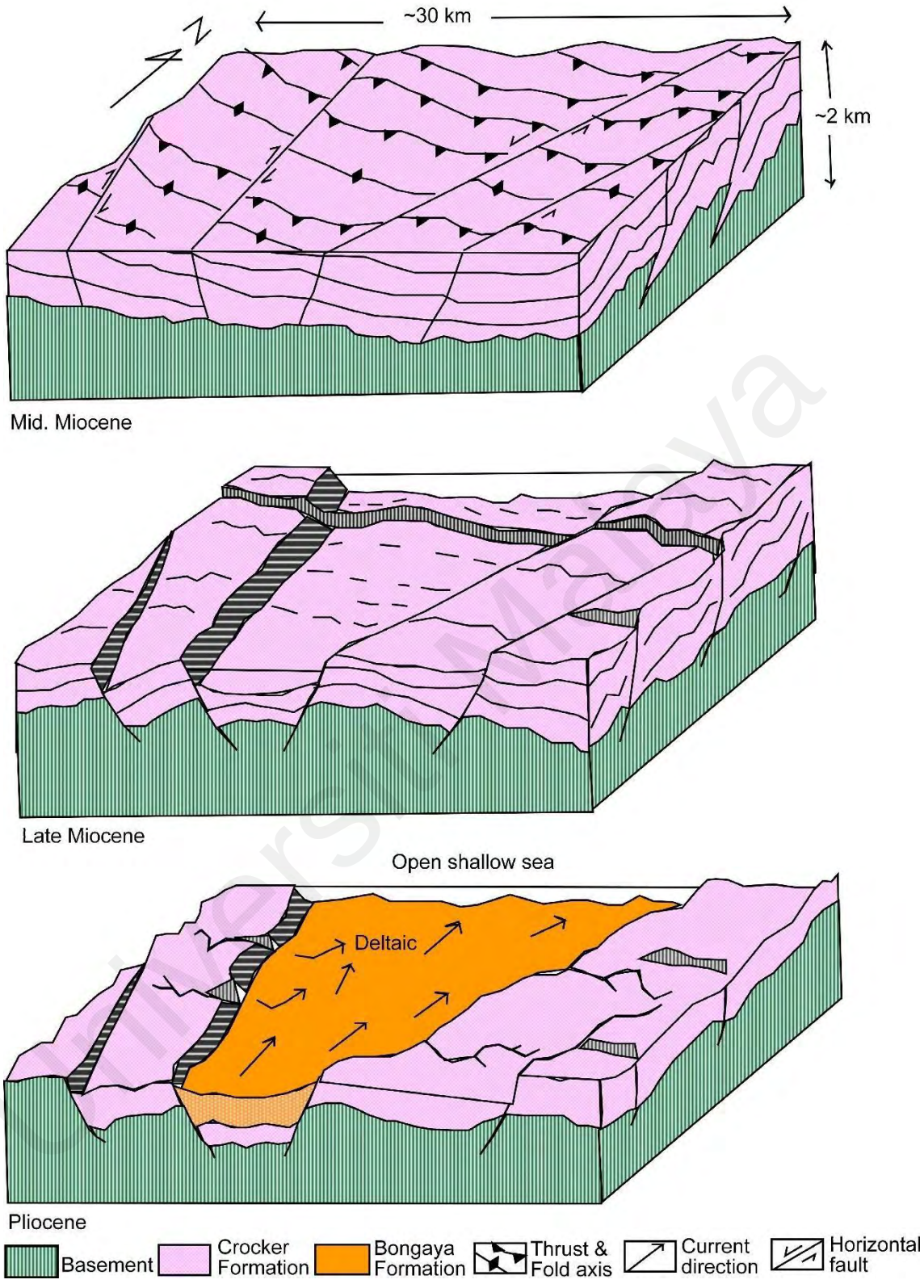

Figure 2.8: Schematic diagram of basin development and deposition of Bongaya Formation Development from Middle Miocene until Pliocene (modified from Tongkul, 1991).

CHAPTER 3: LITERATURE REVIEW

3.1 Petroleum system overview in northern Sabah

Previously, most hydrocarbon exploration in Sabah was done on West Borneo, either onshore or offshore, even though most sediments in Sabah appear to have been evaluated for their potential in petroleum production. West Borneo offshore hydrocarbons are mostly in Stages IVA, IVC, and IVD (Leong, 1999). There have been discoveries of oil seeps in North Sabah Province (Kudat Formation) that show the potential of the petroleum system in onshore sediments. Furthermore, the presence of hydrocarbon indicators on seismic studies in North offshore Sabah Basin (Bongaya deposit) plays an important role in supporting the presence of hydrocarbons in the research region, even though it is still underexplored (Mazlan et al. 1999).

3.1.1 Type of common source rock in Sabah

The hydrocarbons in the Sabah basins are composed of very similar compositions and as predicted, sourced primarily from terrestrial organic materials (Scherer, 1980; Abdul Jalil and Mohd Jamaal, 1992; Azlina Anuar and Abdul Jalil, 1997). Most of the reported source rock originates within the DRU and SRU sequences since pre-DRU marine shales are thermally over-mature to create hydrocarbon. The most prolific source rock in Sabah Basins is coal and carbonaceous shales due to their high sedimentation (>2000m thick in some areas) (Abdullah et al., 2017). These ideal source rocks were found close to an interbedded series with sandstones, which aids future hydrocarbon migration patterns when they are formed. The Miocene erosion and intensive outbuilding of the stage IV siliciclastic wedge resulted in terrigenousrich organic matter deposition that was interbedded with sand at the time (Mazlan et al., 1999).

3.1.2 Reservoirs, Traps, and Seals

The majority of hydrocarbon reservoirs are siliciclastic, created by layered shallow marine sandstones from the coast to the sea. Likewise, high-quality reservoirs can be developed from marine turbidites in phases IVC/IVD (Leong and Azlina,1999). There are a few carbonate reservoirs in Sabah, but they are not as good as siliciclastic reservoirs. According to Scherer (1980), the structural traps for the majority of hydrocarbon in west Sabah were fault propagation folds and fold anticlines. Hydrocarbons are known to occur in complex fault-related closures such as faulted anticlines and rollover anticlines associated with deltaic growth faults. With the migration of hydrocarbons via faults and interbedding movement (Nor Azidin et al., 2011), hydrocarbon in Sabah is sealed by shale and mudstone with effective top and flank sealing (Erb West, Kinabalu, St Joseph) and, to a lesser extent, by shale diapirs or shale that filled slump scars (Leong and Azlina, 1999).

3.2 Petroleum source rock evaluation

Petroleum exploration study always includes mapping of source rock where we tracked source rock characteristics that determine the source rock's ability to produce hydrocarbon at the same time to indicate the stratigraphic extent of a pod of active source rock. Petroleum source rocks were defined as sedimentary rock that commonly contained organic matters that are or were or may generate petroleum (Tissot and Welte,1984). Effective source rock is source rock that currently generating or has generated petroleum. Besides, a potential source rock preserved adequate quantities of organic matter for hydrocarbon production however, it is not yet at the proper level of thermal maturity to generate them while an active source rock is a type of source rock that can expel petroleum and currently generate them in a critical moment as they are within the oil window zone (Dow,1977a). To carefully classify the type of source rock, they need to

satisfy three geochemical parameters which include the amount of organic matter preserved in the source rock, type of organic matter, and their extent of burial heating. Further explanation regarding the parameters is elaborated below.

3.2.1 Quantity of organic matter

The fact that total organic carbon (TOC) concentration determines the richness of organic matter is no longer new. The TOC is the ideal indicator for displaying the amount of each source rock as a weight percent because the carbon in the source rock is needed to combine with hydrogen to generate hydrocarbon. The minimal TOC quantity to be considered as a prospective source rock is 0.5% for shales and 0.3% for carbonates, with shaly source rocks averaging 1.5% to 2% and carbonates 0.6% (e.g., Tissot and Welte. 1984; Peters and Moldowan, 1993; Hunt, 1996). The amount of TOC is connected to the maturity level, as TOC decreases in greater maturity rocks since the majority of the organic matter has expelled the hydrocarbon, leaving some carbon in the rock. Excellent source rocks have TOC values greater than 12%, while TOC values in the range of 2% to 10% are regarded rich enough, with TOC >10% indicating a very immature source rock for development (Alexander et al., 2011). A higher TOC value indicated a better outcome, suggesting more organic materials. However, careful consideration needs to be given because TOC alone is insufficient to generate oil or gas. According to Tissot et al., 1974, depending on the sort of organic materials, it will either produce oil or gas, while others will produce nothing. As previously stated, carbon must be coupled with hydrogen, hence the amount of hydrogen must be considered when determining hydrocarbon prospectivity. In this case, determines by the amount of GP (GP= S1+S2) (El Kammar, 2015; Dembicki, 2009). Furthermore, bitumen extraction concentration of extractable organic matter (EOM) can be used to represent the quantity of carbon richness. Low concentration percentages suggest poor potential, whereas 0.05-0.1% indicates fair, and 0.1-0.2% indicates good source rock. The quality of source rock is very good when the

percentages are between 0.2 and 0.4%, and outstanding when the percentages are greater than that (>0.4%) (Peter and Cassa,1994).

Table 3.1: Geochemical parameters describing the quantity of immature source rock by Peter and Cassa (1994).

	Organic matter			Bitumen extraction (EOM)		Hydrocarbon
Petroleum potential	TOC (wt. %)	S_1	S_2	(wt.%)	(ppm)	(ppm)
Poor	0-0.5	0-0.5	0-2.5	0-0.05	0-500	0-300
Fair	0.5-1	0.5-1	2.5-5	0.05-0.10	500-1000	300-600
Good	1-2	1-2	5-10	0.10-0.20	1000-2000	600-1200
Very good	2-4	2-4	10-20	0.20-0.40	2000-4000	1200-2400
Excellent	>4	>4	>20	>0.40	>4000	>2400

3.2.2 Quality of organic matter

Kerogen's capability in generating hydrocarbon was dependent on the organic matter chemical composition and their origin as said either derived from marine or terrestrial sources. There are four types of kerogens which are type I, II, III, and IV. The classification of kerogen type is based on their chemical composition, maceral source present, and relative amounts of carbons, hydrogens, and oxygen in the source rock. As the geochemical composition of each sample is determined by the amount of hydrogen over carbon (H/C) and oxygen over carbon (O/C), the maceral composition is identified through microscopic analysis that differentiates the relative amount between liptinite, vitrinite, and inertinite maceral. The hydrogen amount plays an important role because a higher amount will correspond to a greater oil-generating potential source rock as this is shown through an increase in the atomic hydrogen-to-carbon (H/C) ratio (Hunt,1996).

Type I kerogen is known as the best type of kerogen to be generated. This type has a hydrogen-to-carbon (H/C) atomic ratio that is high (~1.5) compared to the low oxygen-

to-carbon atomic ratio (O/C) that is under 0.1 (Peters and Moldowan, 1993). Predominantly, Type I kerogen composed the most hydrogen-rich organic matter as, in petrographically study, this organic matter indicator is represented by liptinite macerals with minor of vitrinite and inertinite present. The organic matter was derived from alginate of algal or bacteria where this kerogen often produces the best oil when mature. Although were derived from the same marine matter, Type II kerogen originates from zooplankton, phytoplankton, and bacterial debris mixtures. The composition of Type II kerogen is not as good as Type I kerogen but still produces better hydrocarbon (oil). The ratio of H/C is 1.2-1.5 and has lower O/C ratios compared to both Type III and IV (Peters and Moldowan, 1993). As for their maceral composition, liptinite still dominated however the amount of vitrinite and inertinite possessed could be more than in Type I. Type III kerogen were identified through their ratio of low H/C (<1.0) to high O/C (~0.3) (Peters and Moldowan, 1993). Type III consisted of organic matter derived from a humic plant where they mostly have a lot of vitrinite macerals in the samples. The low hydrogen content and high terrestrial plant influences contribute to more gas production. Lastly, Type IV which has a very low H/C (=0.5) and very high O/C (0.2-0.3) is an oxidized organic matter that cannot produce oil or gas.

The correlation between H/C versus O/C (van Krevelen diagram) to identify the kerogen type was further modified to hydrogen index (HI) versus oxygen index (OI) plots. Peter and Cassa (1994) mentioned that these data are more rapidly generated and less expensive when compared to atomic H/C versus O/C data. The HI derived from $S_{2,}$ and TOC amount (S_2/ TOC x 100) expressed volume of the generated hydrocarbons and as an indicator used for quantitative modeling of phase (Pepper and Corvi, 1995; Arfaoui et al., 2007). Whereas, OI represents a relationship between oxygen to carbon ratio as it was derived from S3 to TOC amount (S_3/TOC x 100). However, the HI vs. Tmax plot can substitute HI vs. OI plot when doubtful S_3 is arisen (Espitalie et al., 1984). High HI values

(>600 mg HC/g TOC) indicate Type I algal-derived kerogen while HI values of >250,150-250 and <150 mg HC/g TOC represent Type II, Type II-III and Type IV respectively (Peters and Cassa,1994; Yensepbayev et al., 2010).

Table 3.2: Geochemical parameters that describe the quality of source rock by Peter and Cass (1994).

Kerogen type	HI (mg HC/g TOC)	S2/S3	H/C	Product expelled at peak
I	>600	>15	>1.5	Oil
II	300-600	10-15	1.2-1.5	Oil
II/III	200-300	5-10	1.0-1.2	Mixed oil and gas
III	50-200	1-5	0.7-1.0	Gas
IV	<50	<1	<0.7	None

3.2.3 Thermal maturation

Catagenesis, also known as thermal maturation, is a process that breaks down organic matter through high temperatures or burial to produce commercial quantities of kerogen. When kerogen reaches 60°Celsius or above, it undergoes thermal breakdown and creates hydrocarbon under decreasing conditions (Hunt,1996). The oil is produced at its optimum when the organic matter is in the 'oil window' zone. The majority of the world's Type I or II kerogens was expelled between 60°C and 160°C, whilst temperatures above the "oil window" range produced Type III gas sources.

Tmax (the maximum release hydrocarbon temperature during pyrolysis) and vitrinite reflectance (%Ro) are two often used maturity markers. Both factors are very reliable as a thermal maturity indicator in Type II and Type III kerogen but not in Type I kerogen. The S_2 peak disappears in Type I kerogen, so the Tmax value, which was calculated from S2, cannot be obtained. The vitrinite reflectance, on the other hand, cannot be used in Type I source rocks because they lack vitrinite and are generally composed of rich marine material such as algae. The oil generation range for vitrinite reflectance is 0.6-1.35 %Ro,

while dry gas generation is greater than 1.35 %Ro (Peter and Cassa,1994; Taylor et al., 1998).

Table 3.3: Geochemical parameters shows thermal maturation stage.

	Maturation			Generation		
Thermal maturity	R_o (%)	Tmax (°C)	TAI	Bitumen/ TOC	Bitumen (mg/g rock)	PI (S1/(S1+S2))
Immature	0.2-0.6	<435	1.5-2.6	<0.05	<50	<0.10
Early Mature	0.6-0.65	435-445	2.6-2.7	0.05-0.10	50-100	0.10-0.15
Peak	0.65-0.9	445-450	2.7-2.9	0.15-0.25	150-250	0.25-0.40
Late Mature	0.9-1.35	450-470	2.9-3.3	-	-	>0.40
Postmature	>1.35	>470	>3.3	-	-	-

3.3 Biomarker

A biomarker is a molecule that occurs in the geosphere and serves as a geochemical fossil to signal source facies determination, paleoenvironment, correlation studies, biodegradation, age determination, and thermal maturity in petroleum exposure (Mackenzie et al., 1984; Simoneit, 2004; Peters et al., 2005; Hakimi et.al. 2012). This compound is regarded as one of the most potent geochemical tools because of its structural qualities, which are indisputably related to its biological origin despite having undergone some alteration due to diagenesis or other processes (Peters and Moldwon, 1993; Peters et al., 2005; Adedosu et al., 2012; Wang, 2016). For example, pristane and phytane were previously thought to be formed from the phytol side change of chlorophyll, but current findings show that pristane is a component of a-tocopherol and phytane is derived from bis-phytanyl ethers in archaebacteria (Philip,1994). Because of their preservation conditions, which are oxygenated or reductive, phytol diagenesis differentiates into two isoprenoids which are pristane and phytane respectively (Tissot and Welte,1984). M/z 191 of chromatography process present triterpenes and steranes compound which is derived from different elements. While triterpenes are thought to be

formed from the membrane lipid of bacteria (prokaryotic) (Ourisson et al., 1982), steranes are typically obtained from sterols found in higher plants and algae but are rare or absent in prokaryotic organisms (Volkman, 1986,1988). It is described that oil is common to have a wide range of terpanes distribution from C19 to C25, C29 ab- and C30 ab pentacyclic hopanes, and C23 and C24 tricyclic terpanes abundance (Wang et al., 2016). All of these constituent compositions and ratios were identified and analyzed to collect adequate and relevant data about the source rock paleoenvironment and sources.

3.3.1 Source input and environment.

N-alkanes, a widely distributed biomarker found in the majority of elements around the world, has been proved to be a very good marker in detecting the source input and the environmental condition. The distributions of the n-alkanes compound with enhancement on their odd to even carbon number (C_{25}-C_{35}) give rise to higher plants originality. The waxes of higher plants are composed of significant concentrations of the long-chain homologs n-alkanes (Gogou et al., 2000; Eglinton and Hamilton, 1967; Tulloch, 1976). Similarly, the aquatic input is based on a high concentration of low carbon number n-alkanes which are in the range of C_{15}-C_{19}. A CPI value representing an odd carbon number preference over even indicates organic matter input from the higher plant when the value does not drop below 1, and vice versa for marine input.

An isoprenoid of pristane and phytane is present in association with carbon-17 and carbon-18, and its ratio was employed to infer depositional environment and source rock organic matter origin. A Pr/Ph ratio greater than 3.0 indicates oxic depositional conditions as well as terrestrial input, whereas a ratio less than 0.8 indicates anoxic conditions present. A value between 0.8 and 3.0 indicates a suboxic transitional environment.

Furthermore, compounds detected in the ion 191 chromatogram, such as tetracyclic terpenes, hopanes, and compounds in the triterpenes group, have demonstrated a specific association between oil production and source rock (Seifert and Moldowan., 1980; Peter et al., 2005). C24 tetracyclic were studied to enhance terrestrial organic matter as evident by Australian oils studied (Philp and Gilbert, 1986). Hopanes, altered from prokaryotes membrane (Ourisson et al, 1982) shown to be part of peat and coal when extended hopane C31 are present high (Villar et al., 1988). A high abundance of moretanes is also found in terrestrial organic matter (Connan et al., 1986; Mann et al., 1987).

According to Brook (1986), the significant quantity of C29 hopanes is related to terrestrial organic matter. Because C29 and C30 17a (H) hopanes are always the major triterpenes in petroleum, the C29/30 hopanes ratio was employed to give the source input. A C29/C30 ratio less than 1.0 was found in a source rock composed of terrestrial organic materials. In three major steranes of C29:C28:C27 relative proportions in m/z 217 are considered in paleoenvironment steranes studied. Dominant C29 implies high land input compared to the others, whereas substantial marine phytoplankton input is indicated by a high C27 fraction. High C28 contributions are always rare and modest in comparison to the other two, although high C28 distributions generally suggest a substantial contribution from lacustrine algae.

3.3.2 Thermal maturity indicators

The Carbon Preference Index (CPI), which compares odd to even n-alkanes, can be used to evaluate the maturity level of sediments (Bray and Evans,1961). CPI values greater than or less than one is recommended as indicators for thermally immature source rock (Peters and Moldowan, 1993; Bray and Evans, 1961), though values less than 1.0 are shown to be exceptional and typical for low maturity carbonate oils (Peters et al., 2005). CPI values of 1.0 are thought to imply thermally mature source rock, however,

there is no convincing evidence to support this. Tissot and Welte (1984) described how a CPI value of one is caused by an equal abundance of odd to even number n-alkanes, which is always observed in high maturity samples.

Furthermore, an isoprenoid/n-alkanes ratio can be used to provide maturity stage. The plot of pristane/n-C17 versus phytane/n-C18 reflects the relative maturity stage of the samples, which normally decreases with maturity as more n-alkanes are produced owing to thermal cracking (Tissot et al., 1971). Other common indicators to evaluate maturity are based on two triterpenoids ratios which are the moretane/hopane and Ts/(Ts+Tm). The less stable Triterpenoids viz. 17β,21α(H)-moretane and C27 17α-trisnorhopane (Tm) are converted to more stable isomers, 17α,21β(H)-hopane and C27 18-α trisneonorhopane (Ts) respectively towards maturity (Peters et al., 2005; Bhattacharya et al., 2017). The ratio of moretane/hopane below 0.1 has been denoted as high thermal maturity.

Aside from saturated biomarker distributions, abundances and distributions of aromatic hydrocarbons are commonly employed for the maturation appraisal of oils, source rock, and coal (Radke et al., 1985; Radke 1988). Because their structures change with increasing maturity, aromatic biomarkers for maturity are sometimes found to be more dependable than aliphatic biomarkers (Farrimond et al., 1998; Radke, 1988). The aromatic distribution of alkyl naphthalene and phenanthrene was developed to numerous measures in determining this maturity, including the Methyphenanthrene Index (MPI 1), Trimethylnaphthalene (TMN) abundance, and DNR-1/DNR-2 ratio. The methyphenanthrene index (MPI 1), which increases with depth (maturity), is one of the most extensively used parameters. This parameter relies on a shift with maturity in the methyl phenanthrene distribution towards a preponderance of β-type isomers. MPI 1 was used due to its proven linear relationship with vitrinite reflectance throughout the conventional oil window (Radke and Welte, 1983).

3.4 Organic petrology

3.4.1 Maceral

3.4.1.1 Vitrinite

The major component of coal is vitrinite maceral, which is grey. This maceral was made up of the preservation of parenchymatous and woody tissues from humic plants such as roots, stems, barks, and leaves consisting of cellulose and lignin. This indicates that vitrinite is rich in aromatic structures, albeit the level of concentration varies according to coal rank. Low H/C and O/C atomic ratios promote aromaticity. Coal rich in vitrinite was preserved anaerobically in swamps, and vitrinite can also be found in coaly shales associated together with mineral matter and other organic material. The reflectance is in the medium range, between liptinites and inertinite, and vitrinite shows no physical attributes (opaque/blacked) when exposed to UV radiation. The elemental composition of vitrinite has a Carbon-Hydrogen-Oxygen relationship, with oxygen being considerably more abundant than the others. As vitrinite refers to medium to high-rank coal, huminite refers to low-rank coal or lignite. Huminite, often known as brown coals, is a low reflectance vitrinite maceral found in the immature source rock.

3.4.1.2 Inertinite

Inertinite, which is also found in coal source rocks (though some coal does not contain any inertinite), is composed of tissues from fungi or higher plants, amorphous material, fine detrital pieces, and cell secretions. Inertinite has a higher reflectance than liptinite and vitrinite, however, it has weak fluorescence. Because of its high carbon concentration and low oxygen and hydrogen content, inertinite is classified as a Type IV kerogen that influences maceral

3.4.1.3 Liptinite

One of the most essential macerals for identifying oil-prone source rock is liptinite macerals. Liptinite macerals, which are derived from non-huminite plant materials such as sporopollenin, resins, waxes, and fats, have a lower reflectance than vitrinite and are the darkest maceral in white light. Liptinite's finest qualities are that it will initially glow under UV/blue light, displaying a vivid greenish-yellow or yellow color. The reflectance increases as the thermal maturity increases, while the fluorescence decreases as the rank increases. All liptinite particles are relatively hydrogen-rich, implying high percentages of aliphatic to aromatic compounds (Guo and Bustin,1998), which is ideal for Type I-II kerogen indicators.

Table 3.4: Subgroup and group classification of coal maceral based on the Australian Standard System of Nomenclature AS2856 (1986) and ICCP system 1994-Classification of Huminite. (After Tissot and Welte, 1984 and Diesel, 1992).

Maceral group	Maceral group	Maceral	Kerogen type
Vitrinite / Huminite	Telovitrinite/ Telohuminite	Textinite	Type III
		Texto-ulminite	
		Eu-ulminite	
		Telocolinite	
	Detrovitrinite/ Detrohuminite	Attrinite	
		Densinite	
		Desmocollinite	
	Gelovitrinite/ Gelohuminite	Corpogelinite	
		Porigelinite	
		Eugelinite	
Liptinite		Sporinite	Type I/II

		Cutinite	
		Resinite	
		Liptodetrinite	
		Alginate	
		Suberinite	
		Fluorinite	
		Exsidatinite	
		Bituminite	
Inertinite	Teloinertinite	Semifusinite	Type IV
		Sclerotinite	
	Detroinertinite	Inertodetrinite	
		Macrinite	
	Geloinetrinite	Macrinite	

3.4.2 Vitrinite reflectance

Vitrinite reflectance (Ro) is one of the most reliable measures of a source rock's maturity. The vitrinite reflectance measurements are based on the percentage of incident light reflected from vitrinite particles, which is commonly done at a wavelength of 546mm and under oil immersion (state as o in Ro). The measurement increases with increasing maturation due to irreversible aromatization reactions from the dehydrogenation process. The maceral vitrinite was chosen because: a) vitrinite is the most prominent maceral discovered in coals; and b) it looked to be always homogeneous c) usually vitrinite is large cause it is convenient to be measured; d) vitrinite behavior represents the plastic and agglutinating qualities of coals. Telocollinite is the recommended vitrinite particle in this approach due to its homogeneous surface and high occurrence (ICCP, 1971). Aside from that, vitrinite had a wider maturity range than any other indication.

However, necessary measurements should be taken during analysis because some samples' vitrinite can be overwhelmed by recycled or caved particles, influencing the findings to high and low maturity, respectively. In addition, insufficient polishing might result in a low Ro, while a high Ro value indicates oxidized vitrinite (Peter and Cassa, 1994). The vitrinite reflectance is not suitable for samples that are lacking in vitrinite and rocks older than Devonian because plants had not yet grown during that time. Peter and Cassa (1994) classified the analysis into immature for oil generation, early mature for oil generation, the peak of oil generation, late mature and gas window in range of 0.20-0.6%Ro, 0.6-0.65%Ro, 0.65-0.9%Ro, 0.9-1.35%Ro, and above 1.35%Ro range, respectively.

Table 3.5: The vitrinite reflection value for the maturity indication (Peter & Cassa, 1994, Tissot & Welte, 1984, Taylor et al, 1998).

Maturity level (R_o)	Peter and Cassa (1994)	Tissot & Welte (1984)	Taylor et al (1998)
Immature	0.2-0.6%	<0.5-0.7%	<0.4-0.5%
Early (mature)	0.6-0.65%	-	-
Peak	0.65-0.90%	0..7-1.3%	~1.0%
Late (mature)	0.90-1.35%	1.3-2.0%	1.0-1.35%
Mature for gas	>1.35%	>2.0%	1.35-3.0%

3.5 Trace Elements

Trace elements are commonly found in saltwater, and a portion of it (dissolved trace elements) is later moved into sediments by a variety of processes. This event resulted in the enrichment of sediments with trace elements that reflect the conditions that existed during deposition and early diagenesis (e.g., among recent papers, Werne et al., 2003; Lyons et al., 2003; Riboulleau et al., 2003; Sageman et al., 2003; Rimmer, 2004; Rimmer et al., 2004; Algeo and Maynard, 2004; Nameroff et al., 2004; Tribovillard et al., 2004a, 2005; Riquier et al., 2005).

Many trace elements (redox-sensitive trace elements) respond as a function of redox status, where they are more soluble under oxidizing conditions and less soluble under reducing conditions. This provides an unequal indicator of the habitats, as oxygen-depleted sedimentary facies has more abundant trace element than in oxic conditions. Tribovillard and his colleague (2006) were able to identify numerous factors that influence the occurrence of trace elements. a) use of metals in the metabolic process of living organisms, b) the sediments conditions such as the pH and Eh, c) the presence of metals in the sedimentary environment, which will interact with the chemical composition of the fluid during deposition; d) the mineralogy of the rock, such as the kind and amount of clay in it; and e) the sort of organic matter that interacts to generate organometallic complexes. No further replenishment of oxidizing agents will ensure sulfides stability and results in no movement of elements that engaged with sulfides in the sediments (Tribovillard et al., 2006). In another word, the more reducing the environments, the more the trace elements contained in the sediments.

Trace elements including V, Ni, Cr, Cu, and Mo are commonly used as paleoredox proxies that their ratio and enrichment aid in the reconstruction of paleoenvironments (Akinlua et al., 2010; Zhao et al., 2016). These trace element concentrations are employed to quantify geochemistry studies since they will remain unaltered and ineffective to diagenetic process and reservoir alteration (Lewan, 1984; Barwise, 1990). The comparison of vanadium and nickel concentrations provides paleoenvironmental indications, with a high V/Ni ratio linked with an anoxic deposition setting (Lewan, 1984; Jia et al., 2013). The V/Ni and Co/Ni ratios are associated with oxidizing and reducing circumstances, respectively, and a cross-plot of these ratios is employed for improved early diagenesis interpretation (Jones and Manning, 1994).

3.6 Palynology

From an early age, palynology is extensively used for stratigraphic purposes where primarily it is used to assist correlation problems in respect of hydrocarbon exploration by international oil company laboratories in the Southeast Asia region. Palynology is described as the only biostratigraphic technique which permits crossfacies correlation and micropaleontological method that correlated non-marine sediments. Approaches of palynology are outlined not only for the stratigraphic purpose but also in dating sediments. However, it is emphasized that palynological zones dating is applied mostly on independent dating using planktonic microfossils associated with distal marine facies and transgressive sequences (Morley,1991). Pollen and spores are the most common organic materials extracted from terrestrial palynomorphs sources. Since they have varied stratigraphic ranges and abundances in different areas, it is mostly used to offer resolution using quantitative palynological zonation schemes. Factors such as the depositional environment will influence the composition of parent vegetation, resulting in pollen assembly during deposition (Slater &Wellman, 2016). This approach not only solves stratigraphic problems, but is also used for hydrocarbons searching in non-marine, marginal marine, and some marine depositional sequences. The diversity of palynological material is less of a worry in Southeast Asia due to the wide range of pollen and spores as to their climate, but in northern temperate affinities, these palynomorphs were demonstrated to characterize nothing more than drilling mud contamination (Muller, 1961).

3.7 Bulk Kinetic

Bulk kinetic energy analysis is a laboratory-based model of the natural petroleum generation process that provides a quantitative way of predicting the hydrogen timing on generation and expulsion from a source rock (Makeen et al., 2020), though greater

complexity is possible when compared to natural processes. This method could also be used to obtain the corresponding transformation ratio (TR) of selected samples. The analysis includes two key parameters: range of activation energies (E_{act}) and frequency factor(s)/Arrhenius constant (A), which describe the amount of energy necessary to break kerogen bonds from hydrocarbon expulsion and the frequency with which such reactions take place. These criteria are essentially determined by the sort of organic matter assemblage in the source rock (Hakimi et al., 2015). Broad activation energy distributions are common for terrigenous organic matter (Schenk et al., 1997; Abbassi et al., 2014), whereas narrow and low-frequency distributions imply an organic-rich source from lacustrine and marine; Type I and II kerogen (Abbassi et al., 2014). In terms of petroleum generation temperature prediction, a linear heating rate of 3.3 °C/My, representing the average geological heating rate in sedimentary basins, could perform both Ro percent (calibration of vitrinite reflectance) and Tmax temperatures of bulk petroleum generation. It is believed, however, that the method provides reasonably accurate modelling of Type I and II kerogen but not so effectively represented by Type III kerogen in general, particularly by open system pyrolysis kinetics.

CHAPTER 4: SAMPLES AND ANALYTICAL METHOD

4.1 Introduction

In this chapter, the outline of the process that influences research strategy is discussed, as the evaluation is based on data collected during fieldwork and laboratory analysis. The fieldwork was done to learn about the subject area's background as well as to collect samples. Meanwhile, the laboratory-based analysis is divided into two categories which are source rock characterization based on organic geochemistry and petrology study, and paleoenvironment reconstruction using gas chromatography and palynology analysis. Organic geochemistry research method comprises of total organic carbon or Source Rock analysis, bitumen extraction, pyrolysis- gas chromatography, and gas chromatography – mass spectrometry. The experiments are then enhanced by petrological analysis, which includes vitrinite reflectance identification, fluorescence analysis, and maceral point counting. Palynology studies are commonly used to determine the deposition of the paleoenvironment. A quality control approach was used in the laboratory for every quantitative analysis, which constituted of taking a mean reading for the final result to check that the result matched a standard reading and to avoid any misinterpretation or miscalculation.

Coal and carbonaceous shales are indeed the most prolific and common source rock in Sabah due to its abundance volume, which can reach >2000m thick in some regions (Abdullah et al., 2017). As a result, special attention was paid to coal, carbonaceous shale, and shale, for their petroleum potential generation and source rock features.

4.2 Fieldwork and sample collection

Prior to fieldwork, a desk study was conducted to provide a basic site appraisal and background of the research region, as well as planning the one-week field inquiry. The fieldwork, which took place in February 2020, began in the Pitas region and progressed

to the northern area, covering the farthest outcrop at Kg. Malubang. Every outcrop location was pinpointed using a Global Positioning System (GPS) and displayed as a reference on a geological map (Figure 2) to ensure correct formation. Tongkul (1990, 1991) discussed that the Bongaya formation has a gentle dip and was controlled by the former formation underneath. Strike and dip measurements, as well as images (with scale), were taken for illustration and as evidence of any structure or organic material discovered at the outcrop.

Every type of lithology found in the formation was sampled, namely sandstone, shale sediments, mudstones, and coaly sediments. Each sample was classified based on its location and layers before being placed in a different sampling bag. Any weathered components were wiped clean to avoid contamination, and samples were carefully isolated from one another.

4.3 Preparation of source rock samples

Techniques for preparing the source rock for experiments were meticulously carried out. The source rock was wire-brushed, rinsed, and dried in the oven or left at room temperature overnight. To undertake the geochemical and palynology analyses, a portion of each rock was finally ground or milled to a fine powder using both mortar and pestle. However, for palynology examination, care must be taken not to over-crush the rock because the original shape of the pollen must be preserved. The remaining source rock was mildly crushed (into 2mm-3mm) for petrography evaluation. All of the sample preparation was done in the Department of Geology's laboratory at the University Malaya.

4.4 Organic Geochemistry analysis

4.4.1 Source Rock Analysis (SRA)

The source rock analysis (SRA) pyrolyzer processes samples to evaluate the richness of organic materials as well as their thermal maturity. The quantitative values obtained are S1 (the quantity of free carbon), S2 (the amount of hydrocarbon created by non-volatile organic matter thermal cracking), and S3 (carbon dioxide amount). This method also yielded TOC (total organic carbon) and Tmax (highest temperature), which were later converted into the hydrogen index (HI) and oxygen index (OI). Fine powder samples (50mg to 100mg) prepared were heated in an inert environment in the Weatherboard SRA under TOC/TPH mode. The initial temperature was set at 340°C and gradually increased to 700°C. This procedure takes about 2 hours and was conducted in Department of Geology, University of Malaya.

4.4.2 Bitumen Extraction

Bitumen extraction, as the name implies, is a process of isolating kerogen from its parent rock using a pure solvent, commonly known as the Soxhlet extraction method. This approach, which makes use of the reflux and siphon principle, is inexpensive, quick, and a common experiment in the subject of organic geochemistry which was done in the Petroleum Laboratory I of the Department of the Geology University of Malaya. This experiment employs a quantitative approach because each bitumen amount provides information about the richness and type of kerogen (Peter and Cassa, 1994). As a result, to acquire a trustworthy result, a very careful and attentive treatment of the sample is required.

The chosen sample was grounded and make sure thimble, thimble with the sample, and round bottom flask were weighted and recorded before the experiment. The amount

of sample placed in the thimble must be equivalent through every sample depending on their lithology type. Coal sediment will require an average of 5g of weight, whereas shale will require 10 to 15g.

Bitumen extraction consisted of three major components: 1) extractor, 2) reflux condenser, and 3) solvent storage. The first component, the extractor, was formed of a Soxhlet with a thimble filled with bituminous sample and cotton (to prevent the sample from flinging out of the thimble) inside. The extractor section was introduced using a reflux condenser at the top and was connected by a round bottom flask holding solvent (150 ml) at the bottom and heated. The solvent used is a 93:7 mixture of dichloromethane and methanol. Before the experiment, an anti-bumping granule (to lessen pressure from overshooting) and a few copper sheets (to absorb sulfur) were introduced to the solvent.

Figure 4.1: Complete apparatus used during the bitumen extraction process. The

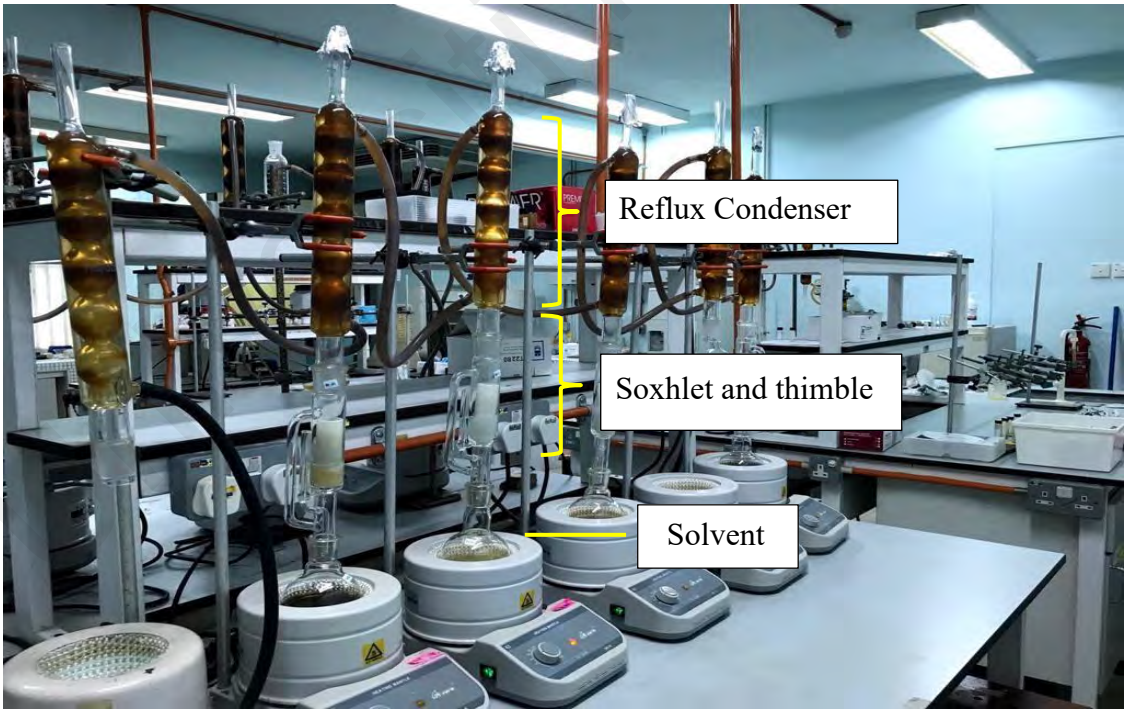

picture included the three major components: 1) extractor, 2) reflux condenser, and 3) solvent storage.

The extraction was allowed to run for 72 hours, or until the sample in the thimble was clear. The vapor from the boiling solvent is condensed and dropped back to the solid in

the thimble for extraction via the extractor arm. When the solvent containing the extraction reached the highest point of the siphon, it was sucked back and concentrated inside a bottom flask. The solvent in the bottom flask was then evaporated with the Butchi rotary evaporator, leaving just the bitumen inside, which was pipetted into vials (weighted beforehand) and left to dry. The weight of the bitumen is calculated and reported.

4.4.3 Column Chromatography

The bitumen extraction extracts were further separated into aliphatic, aromatic, and NSO (nitrogen, sulfur, oxygen) by column chromatography which was also conducted in Petroleum Laboratory I of the Department of Geology, University of Malaya. In the laboratory, a cleaned and rinsed cotton wool-packed column was installed vertically, and a silica gel slurry substance was poured within, followed by alumina gel until the column was covered for roughly one-third of the way. To remove air bubbles, the column side was gently tapped until the materials were seen to settle correctly. These materials serve as a filtration layer to separate the extracts, and cotton wool aids in preventing any extracts from falling on the residue. To extract aliphatic, a low polar solvent (hexane or petroleum ether) was utilized for the initial separation. The method was repeated by diluting bitumen with dichloromethane and methane, to extract aromatics and NSO, respectively.

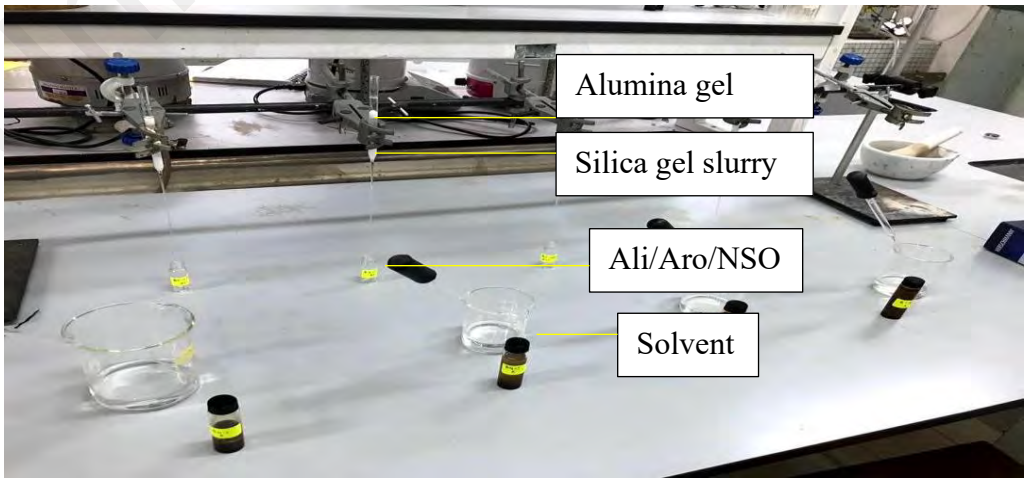

Figure 4.2: Short column chromatography setup for separating aliphatic, aromatic, and NSO compounds.

4.5 Gas Chromatography- mass spectrometry

Gas Chromatography-Mass Spectrometry (Figure 4.3) was used to further investigate the saturates and aromatics. The analysis is carried out using gas-liquid chromatography (GC) to separate the compound, and mass spectrometry (MS) using an Agilent V 5975B MSD to ionize the compound with an electron beam. The hydrocarbon samples are dissolved in a solvent and injected into the furnace using a syringe. The sample was ramped from 40°C to 300°C in 30 minutes before being vaporized and mixed with He before being transferred to the column for separation. This process takes around 95 minutes and produces a chromatograph, which is used to identify biomarkers in the formation. The mass-of-charge of ionized ions employed in mass spectrometry was shown in the form of a chromatogram. The fingerprint demonstrates how the ions react to the function of time. The image below depicts a GCMS unit in a University of Malaya Department where the experiment was conducted.

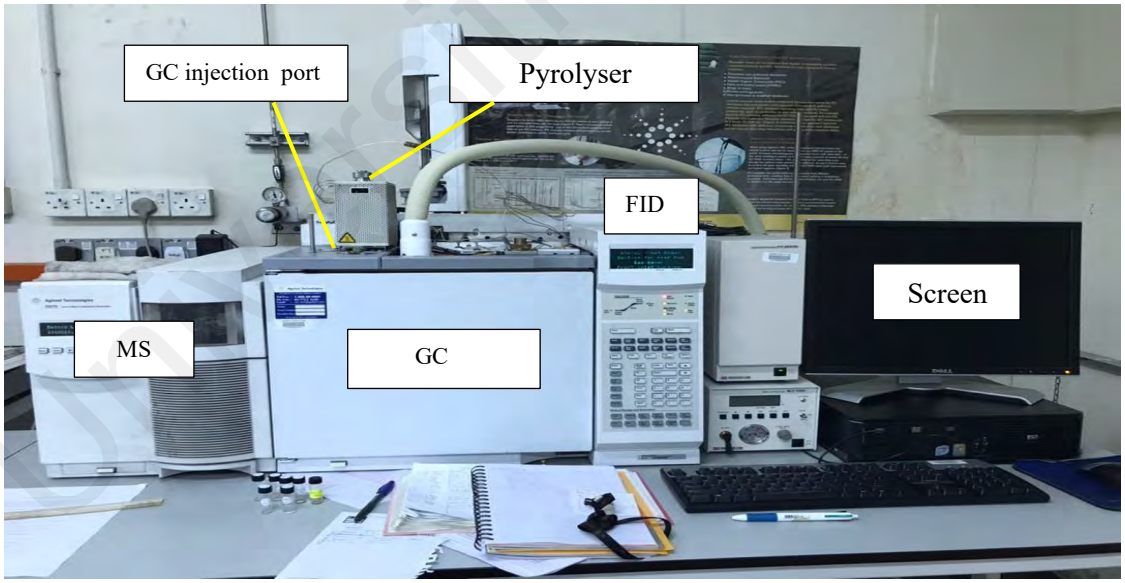

Figure 4.3: An Agilent 6890N Series gas chromatograph (GC) and pyrolysis unit shown here is also installed at the Geology Department, University of Malaya as an attachment.

4.6 Pyrolysis Gas chromatography (Py-GC)

Pyrolysis Gas Chromatography (Py-GC) analysis is another method for detecting the kerogen type and was analyzed in Petroleum Laboratory II of Department of Geology University of Malaya. This method permits a tiny sample (4-8 mg) to be placed in the probe of the Double-Shot Pyrolyzer Py-2020iD and then lowered into a furnace heated to around 54°C. The pyrolysis process of converting the powder sample to gas happens concurrently as the temperature is ramped up to 20°C each minute until the temperature reaches 600°C. Helium gas is utilized to flush pyrolysate into the column to be separated (GC phase) before it is identified by FID for identification. The separated carbon peaks are turned into a pyrogram, which shows peaks ranging from the lighter compound to the higher compound, n-alkenes/n-alkanes, with aromatic peaks in between. An organic sulfur component may also be present in some samples.

4.7 Petrographic Analysis

The petrographic analysis aids comprehension of the organic matter (maceral matter) contained in the samples chosen. The samples are manufactured as a polished block in which 2-3 mm of rock chips were immersed in epoxy resin mixed with hardener liquid for 48 hours. Each block was ground and polished with 350, 800, and 1200 carbide paper and alumina powder until the samples were exposed. This ensures that the blocks are smooth and flat so that they can operate effectively during microscopic examination by microscope Leica CTR 6000 photometry (Figure 4.5) situated in the Organic Petrology Room in Geology Department University of Malaya. The three petrographic analyses are as follows:

4.7.1 Vitrinite/ huminite reflection

Vitrinite/huminite reflection is a maceral analysis technique used to determine the thermal maturity of a formation. Tissol and Welte (1984) highlight that this approach

outperforms others, such as SRA recognition of Tmax and hydrocarbon extraction maturity measurement. This technique offered valuable information on the organic maturation and evolution of petroleum generating capability in comparison to others (Sweeney and Burnham, 1990; Waples, 1994). The reflectance of vitrinite was determined using Fossil Software, specifically on the homogeneous surface of vitrinite. The reflectance data is represented as average reflectance %Ro and was compared using Peter and Cassa's (1994) technique; (<0.5Ro=immature, >0.5Ro=mature).

4.7.2 Maceral counting

The quantity of macerals in samples reflecting paleo-organic matter resources aids in determining the type of kerogen and depositional environment creation. This method employs point selection of macerals' kinds in the form of percentages. A Maceral Software was designed to aid in the calculation of 500-1000 points per sample.

4.7.3 Macerals Fluorescence

In addition to point measurements, the fluorescence of macerals (liptinite) under UV light was monitored and photographed (for documentation purposes) to estimate hydrocarbon potential and maturity (Taylor et al., 1998). The luminous strength of liptinite in the source rock serves as a hydrogen indicator and is utilized to assess the presence of oil.

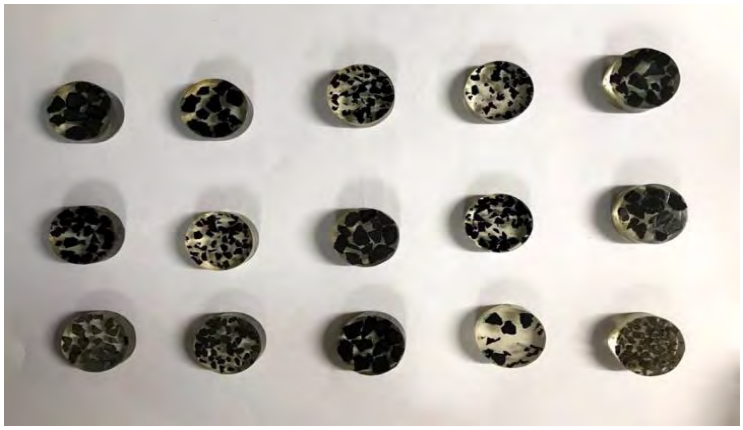

Figure 4.4: Polished block composed of shale and coal source rock

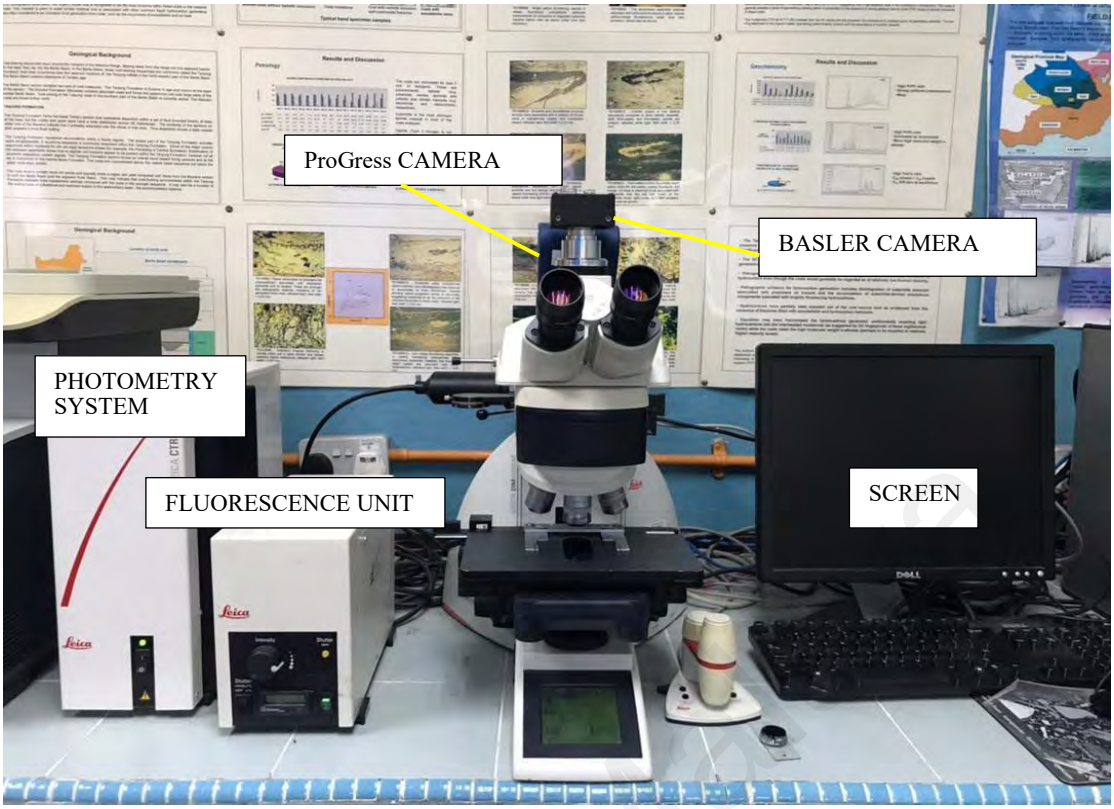

Figure 4.5: A LEICA DM6000M microscope and a LEICA CTR6000 photometry system with fluorescence illuminators were employed at the University of Malaya's Geology Department.

4.8 Palynology

The standard technique of palynology analysis by Tyson (1995) and Wood et al. (1996) was employed with some modification of enhancement on pollen recovery. The sample preparation phase of this method permits the fine-grain sample to be soaked in hydrochloric acid (HCL) and hydrofluoric acid (HF) to ensure that no calcite and silicate components accumulate in it. The remaining material full of palynological matters was neutralized several times with distilled water before being treated with a little amount of ZnBr2, concentration 2:3, and centrifuged. The tube contained layers of kerogen (at the top), ZnBr2, and residue. Kerogen was collected and diluted with distilled water before being placed on the slide for pollen microscopy examination (under transmitted light).

Powdered samples were sent to Orogenic Resources Sdn Bhd for sample preparation as well as pollen identification analysis.

4.9 Inductively Plasma Mass spectrometry (ICP-MS)

The trace element concentrations were determined using an Agilent Technologies 7500 Series Inductively-coupled plasma mass spectrometer (ICP-MS) in the Department of Chemistry, Faculty Science, University Malaya. The analysis was performed by a science officer in the Chemistry Department. Before ICP-MS could be done, the samples required to be digested according to Pi et al. (2013) procedures. Before digestion, the materials were pulverized into a fine powder and processed in an Anton 3000 microwave oven with chemicals such as HNO_3, HF, and $HClO_4$. The acidic HF in the solution was repeatedly neutralized in the solution by adding $HClO_4$ before being left to near dryness and adding 10 ml of 5 M HNO_3 to allow digestion to take place. The sample was diluted with a dilution factor of 100 using deionized water before ICP-MS analysis. The study yielded ppb unit detection, which was subsequently corrected to the bulk rock weight.

4.10 Bulk Kinetic Energy

Weatherford SRA was used to select and analyze samples for bulk kinetic pyrolysis analysis. Fine ground whole-rock samples of 10-20 mg were heated at different heating rates of 1,5,10, 25, and 50 °C/min. Helium served as a carrier gas, transporting the pyrolysis product (S2) to the FID, which was calibrated with a hydrocarbon standard, yielding a quantitative yield of the S2 component and the real temperature (Tt) (Jarvie et al.,1996). The kinetic model used the bulk petroleum formation curved recorded at the five heating rates as input. KINETICS 2000 and KMOD software were used to assess the activation energy distribution (Ea) and frequency factor (A). The discrete energy model is based on kinetic analysis as described by Burnham et al. (1987,1988).

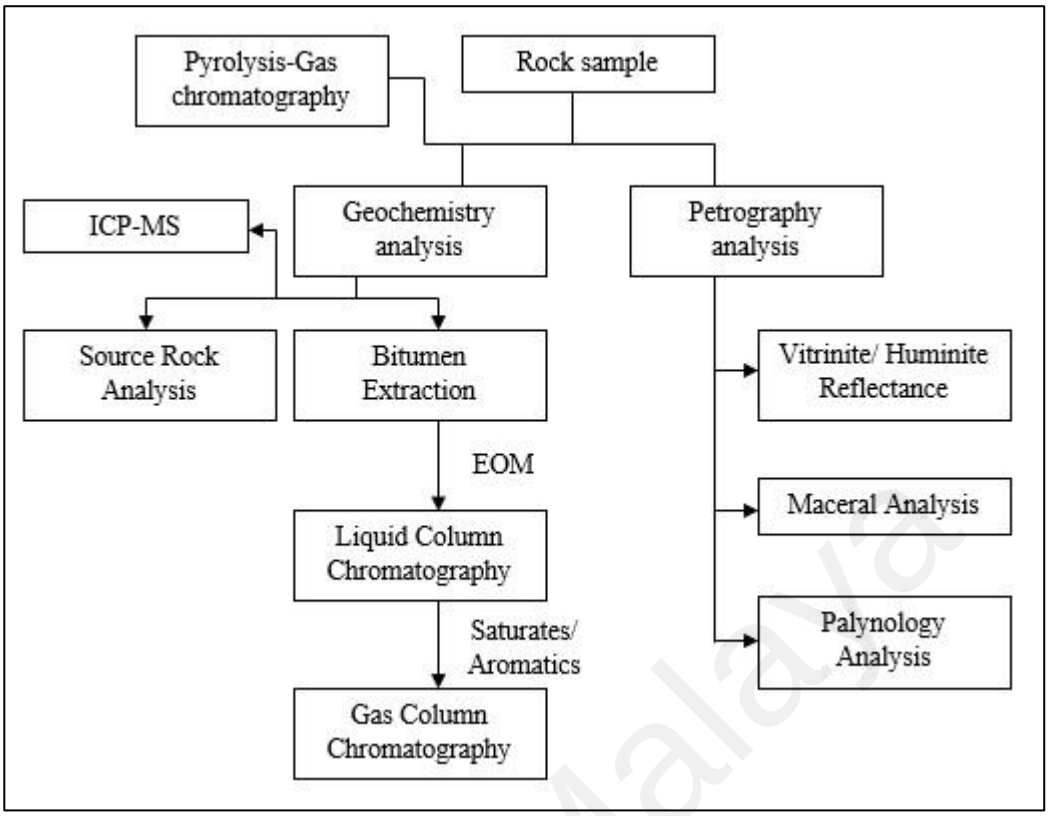

Figure 4.6: Flowchart of the methodology adopted in this research.

CHAPTER 5: RESULT

5.1 Introduction

This chapter combined all the geochemical and microscopic analysis results, including both petrographic and palynology studies. There are also further analyses such as elemental analysis and bulk kinetic energy. The samples for this analysis were gathered at several locations on the Bongaya Formation, as shown in Figure 1. This chapter also analyzed lithofacies discovered during the fieldwork.

5.2 Outcrop and Lithofacies description

Total of 16 outcrops (as labeled in Figure 1) were visited, and 2 selected sedimentology logs were selected to be discussed in this section. The lithologic log done during the fieldwork is shown in Fig 5.2, 5.3, and 5.5. The lithologic sequence of the Bongaya Formation is identified and analyzed in this section, which leads to the identification of lithofacies and depositional environment identification.

Four Bongaya Basins are distinguished as Basin 1, Basin 2, Basin 3, and Basin 4. Sediments in Basins 1 and 2 are composed of typical thick Bongaya Sediments, the sandstones and shale sequences, where coal lenses were found between the layers. A thin lenticular layer of interbedded grey sandstones and shale sediments up to 2 meters thick was also found on a prominent outcrop of Basin 1 and 2. In one of the outcrops, the minor conglomerate layer was also discovered, as stated by the previous researcher (Tongkul,1991). The lithologies, however, changed towards the sea (north). The northern basins (Basin 3 and 4) are dominated mainly by thick white sand, where the sandstone occurred coarser compared to sediments in Basin 1 and 2. The seaside observed a small folding comprised of coarse sandstone rich in fossils in the mangrove area near Kg. Malubang.

5.2.1 Outcrop B13 and sedimentology log 102 (Basin 1)

Outcrop B13 (Figure 5.1a) is located on the outskirts of Pitas Town, with a GPS coordinate of 06'42'10.4"N and 117'05'22.7"E. It is one of the most significant outcrops in the Bongaya basin territory, with a length of more than 35 meters and a height of more than 10 meters. This outcrop's lithology consists predominantly of sandstone and mudstone and thin to medium heterolytic bedding (Figure 5.1b & 5.1c). The bedding strike and dip is measured to be 220/28 NW, and it is observed to have a normal fault with strike and dip of 060/78 SW. The coals are bound to discover in lenses left by the previous plant traces such as root and stem (Figure 5.1d & 5.1e). Most sandstone has Ophiomorpha burrows (Figure 5.1f) and parallel and trough crossbedding (Figure 5.1g), suggesting shoreline deposition sediments. The intertidal flat lithofacies series is distinguished by repeated interbedding of sandstone and mudstone, while the mangrove area is distinguished by very thick mudstone with organic matter dispersion and small coal lenses. Figure 5.2 and Figure 5.3 display the sedimentology log of this outcrop.

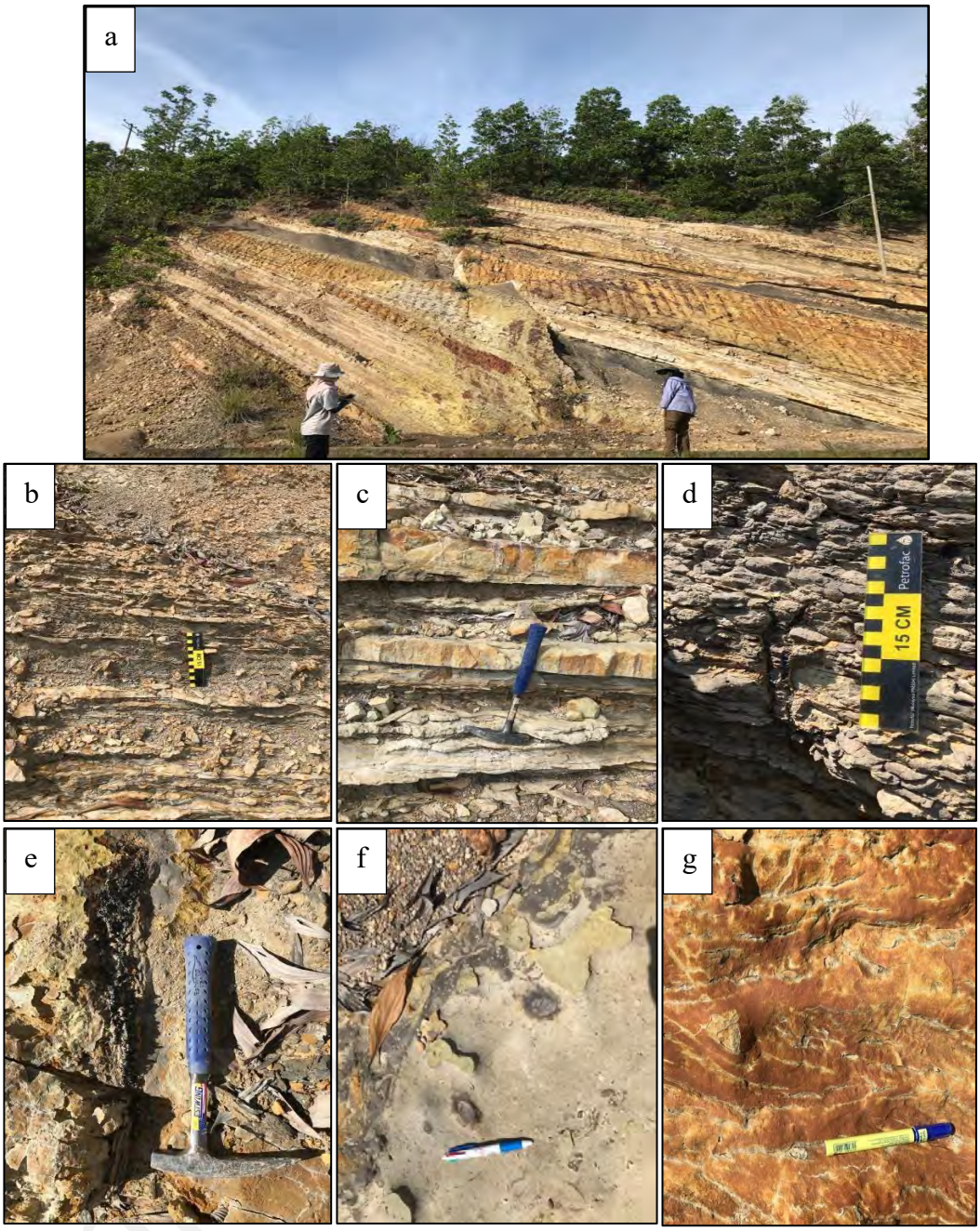

Figure 5.1: Field photograph and evidence to the lithofacies identification. (a) outcrop visual showing high composed of thick sandstone and shale. Picture (b) and (c) shows the different size of heterolithic bedding found in the outcrop. (d) and (e) are two types of coal found, probably originated from root or stem. (f) evident of *Ophiomorpha* burrow trace found whereas (g) is crossbedding marks as one of the common sediment structures found in this formation.

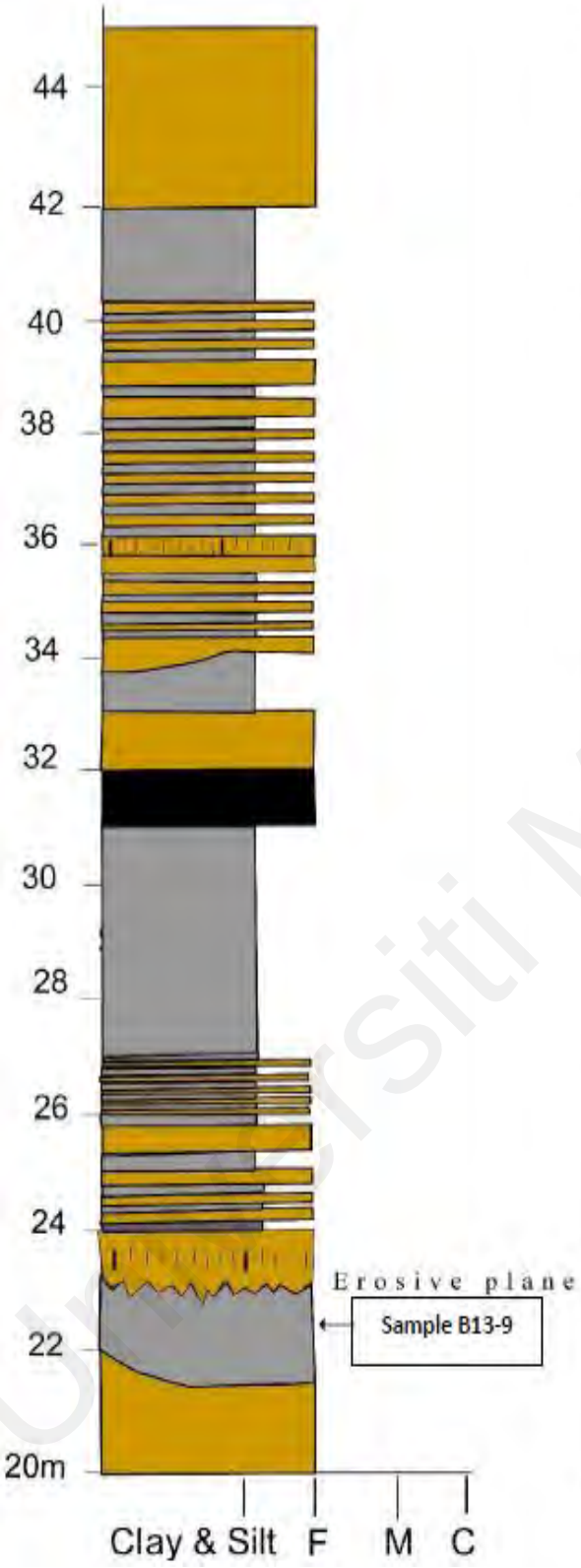

- Clean sand	Beach /shore
- Mud lenticular - Vertical coal penetration / root	Tidal flat
- Interbedded sandstone + mud - Thicker lenticular sand upward - Ophiomorpha burrow - Coal seam in sand	Intertidal flat
- Carbonaceous - coal seam / stem	Mangrove ???
- Paleosoil	Tidal flat
- Very thin lenticular	Intertidal flat
- Burrow - Erosive base	
	Mangrove /Tidal flat

Figure 5.2: Sedimentology log and their environmental interpretation in Outcrop 1.

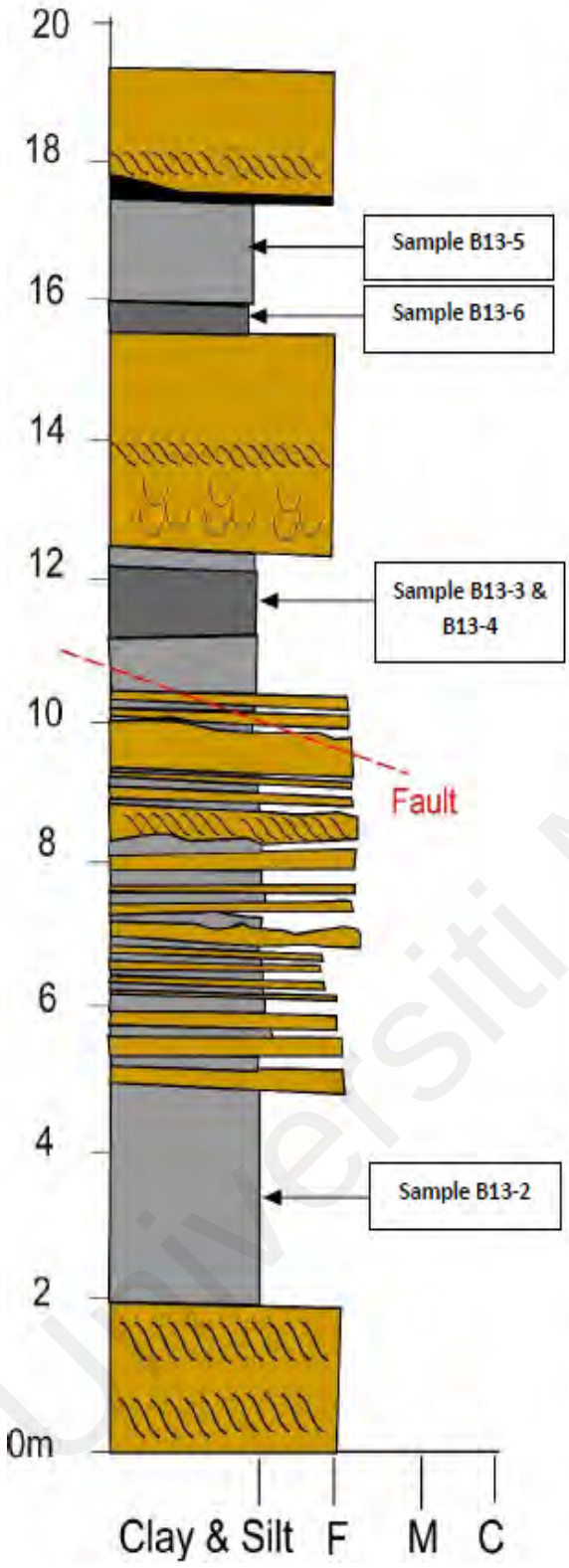

- Cross-bed	Shore
- Coal lenses - Bioturbation sand in between	Tidal flat / swamp?
- Parallel and trough cross-bed	Shore
- Mudstone (shale) - 13-3 & 13-4 (carbonaceous shale)	Tidal plain/ swamp
- Heterolytic bedding - Lenticular bed of sandstone and mudstone	Riverbank? Intertidal flat?
- Mudstone - Sample 13-2 (s)	Mangrove
- Bioturbation - Cross-bed	Shallow marine

Figure 5.2, continued.

5.2.2 Outcrop B11 (Basin 1)

This outcrop is the second-largest outcrop that was found in the study area. Outcrop 2 (Figure 5.3a) is located near the first outcrop (06'42'08.7"N and 117'05'05.5"E) having bedding and fault strike and dip of 250/30 NW and 040/ 89 SW respectively. The succession consists of very thick mudstone and sandstone layer up to 4 meters where the sandstone was coarse to fine sandstone, indicating channel succession. Figures 5.4 show the sedimentary log of this outcrop. The coal interference in this outcrop is considered small and some were found to originate from the root fossils of mangrove trees (Figure 5.3b). There is mud drip indication in between sandstone and mudstone layer indicating riverbank environment (Figure 5.3c).

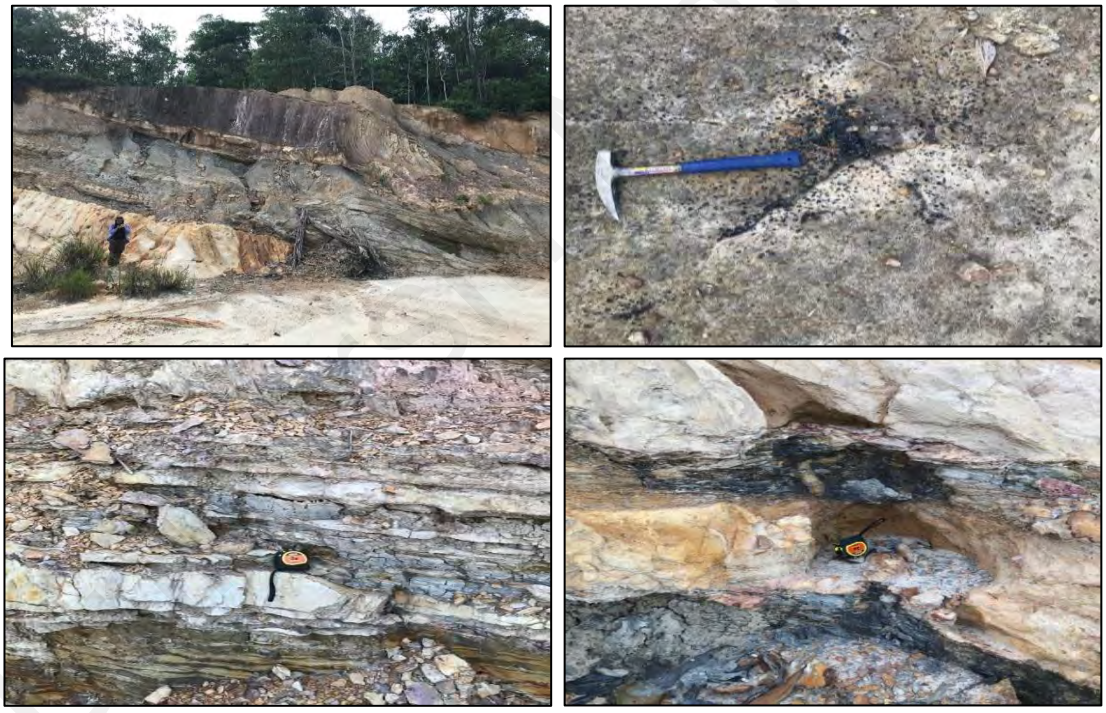

Figure 5.3: Field observation in outcrop 2. (a) outcrop view; (b) top view of coal made from plant stem; (c) trace of mud drip in sandstone and (d) Heterolithic bedding found in the outcrop showing different thicknesses of sediments layer.

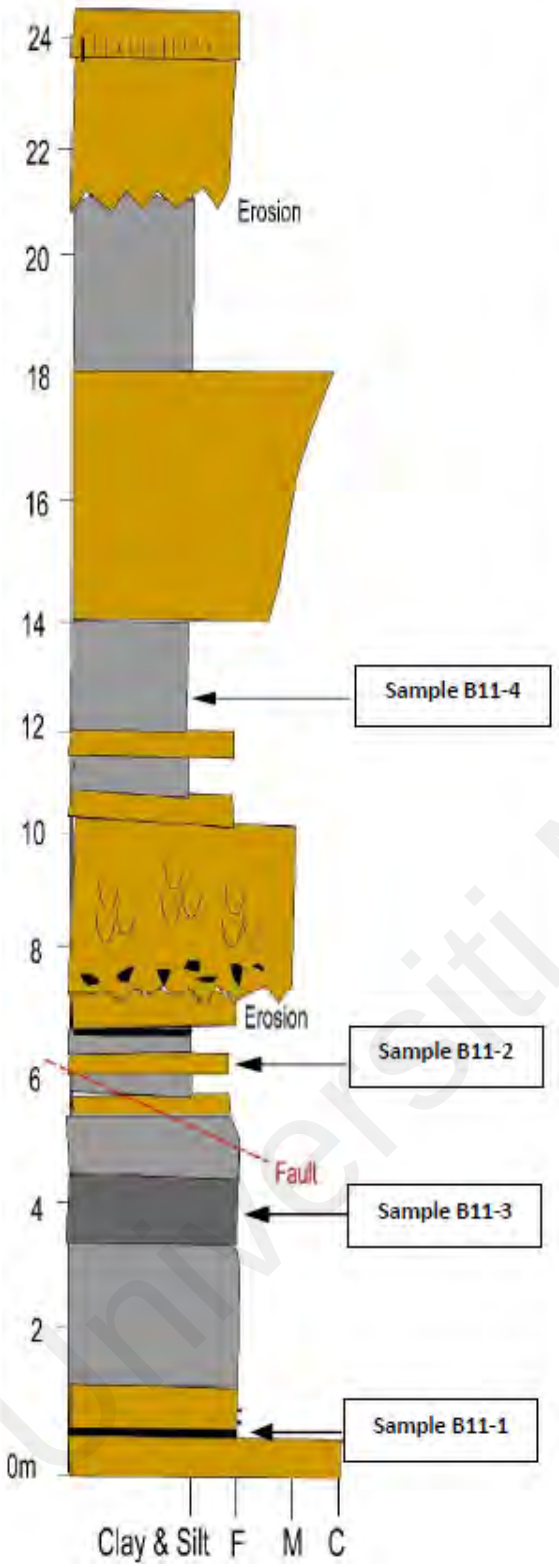

- Clean sand - Burrow trace - Erosion base	Shore/Shallow marine
- Thick mud	Swamp
- Coarsening upward sequence - Mud drip	Channel overbank
- Interbedded sandstone with mudstone	Intertidal flat
- Medium sand - Pebbles/ mud clast - Cross-bed / trough cross-bed	Channel
- Sand thickness increase - Heterolithic sequence - Coal	Intertidal flat
- Different type of mudstone	Mangrove /Tidal flat
- Coal seam /tree trunk - Oxidation trace (orangish substance)	Back mangrove
- Fining upwards	Channel

Figure 5.4: Analyzed sedimentology log of outcrop 2 that represents each layer structure and characteristics and their depositional setting.

5.2.3 Outcrop B14 (Basin 3)

This outcrop is near Kg. Telaga (on the road to Kg. Malubang) with latitude and longitude of 6°50'45.60"N and 117° 4'49.52"E, respectively. As shown in Figure 5.5 below, this outcrop is made entirely of almost loose upper fine-grain feldspar-rich sandstone (Arkose), where the sandstone is white. The strike and dip are 210/ 30 NW, and there are no faults or sedimentology structures visible here.

Figure 5.5: An overview of Outcrop B14 displaying thick amalgamated fine-grained white sandstone facies with people as a scale.

5.2.4 Outcrop B17 (Basin 4)

Outcrop 13 locality is located on the mangrove area at the shoreline (Figure 5.6a). This outcrop is a fold made entirely of coarse sandstone and rich in fossil; calcareous sandstone (Figure 5.6b). The folding direction is 10 ->209 E, where the north limbs were striking and dipping 232/18 NW, while the south limbs were in the direction of 036/70 SE.

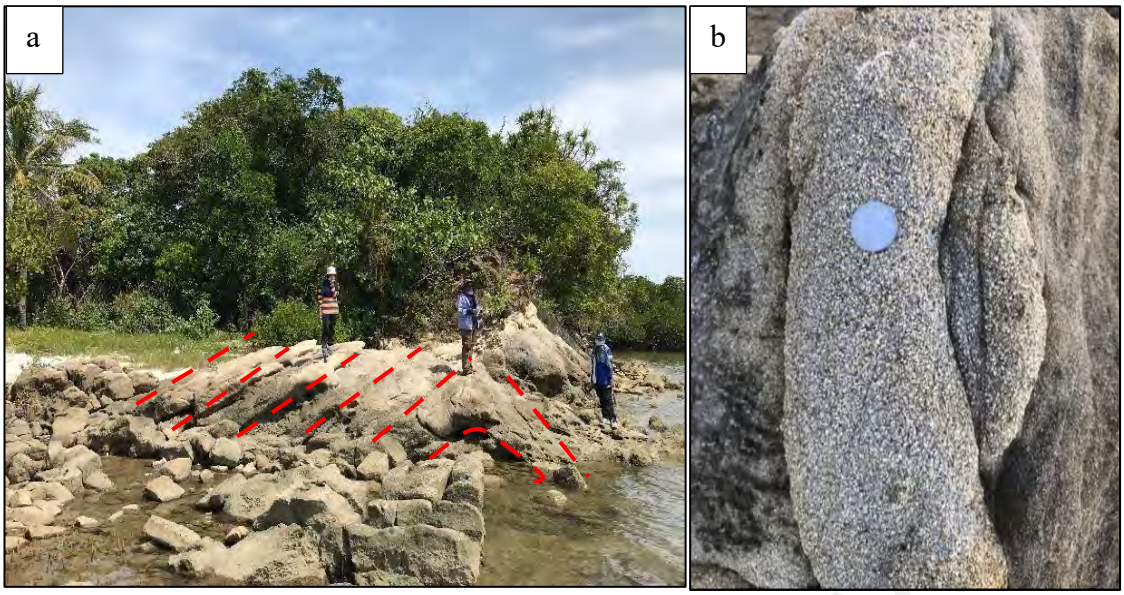

Figure 5.6: Field picture represents (a) the fold structure and their line of limbs direction and (b) close up of the coarse-grained calcareous sandstone in this outcrop.

5.2.5 Outcrop B20 (Basin 1)

This outcrop has not been indifferent with others since the primary sediments are sandstone with a slight inclusion of mudstone (Figure 5.7a). It is located at 6°47'28.46"N and 117° 5'35.82"E, as this is the only outcrop where a conglomerate was discovered. The conglomerate layer, which was found at the bottom of an outcrop's sequence, is a fine grain, approximately 2-4 mm granule (Fig 5.7b) and is only found in a small quantity in this formation. The existence of a minor fault trace, as shown in Figure 5.8c, suggests that slight displacement has occurred from the deformation.

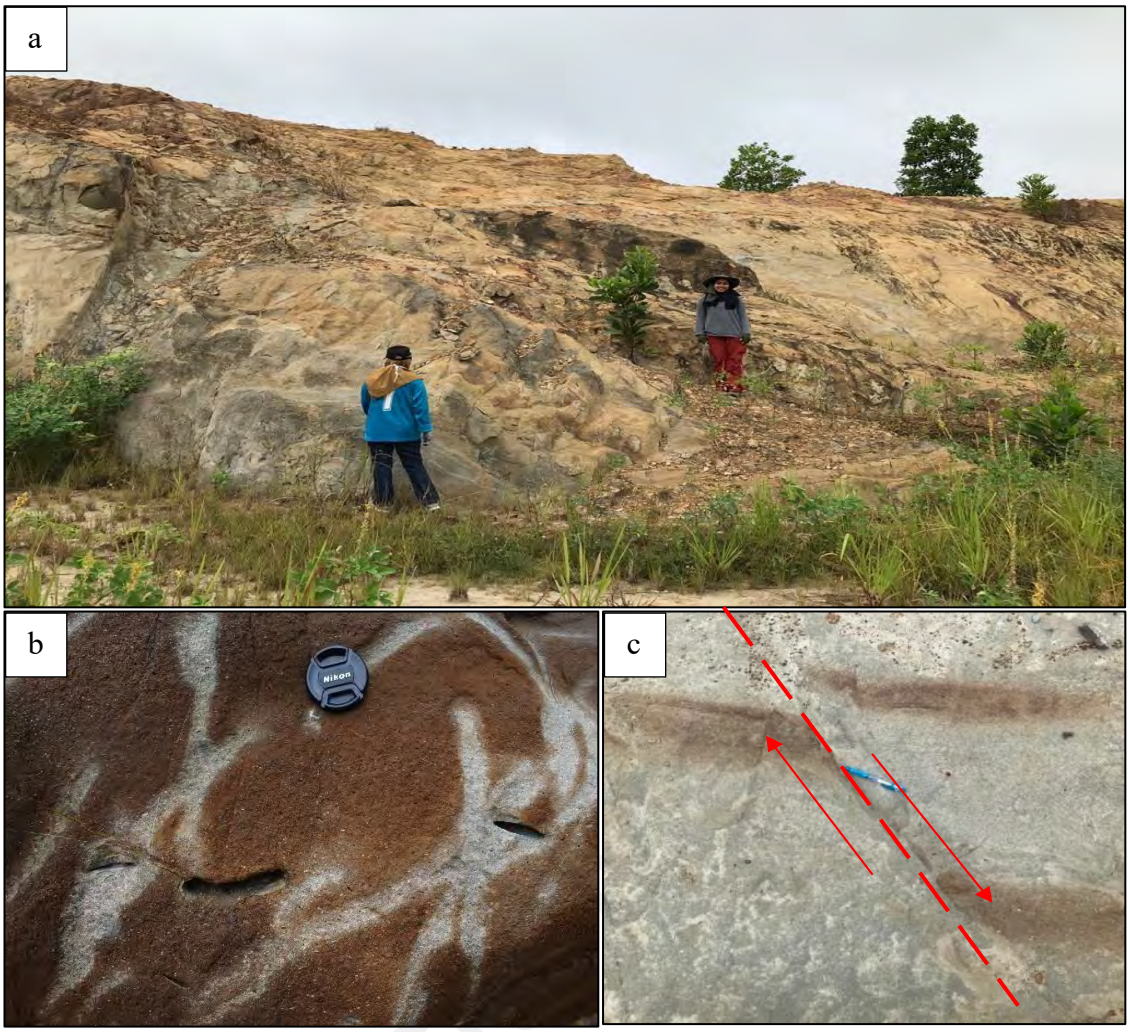

Figure 5.7: Outcrop 18 images are showing (a) the general view of this outcrop; (b) zoom picture of conglomerate sequence made of fine granule and (c) evidence of small displacement that was discovered in this outcrop.

5.2.6 Outcrop B21 (Basin 2)

Located at a latitude of 6°41'54.88"N and a longitude of 117° 1'58.31"E, this outcrop is in Basin 2 and consists of typical Bongaya Formation sediments, which are the thick sandstone and mudstone (Figure 5.8a). The top layer consists of conglomerate; however, it is interpreted to be another formation; might be The Timohing Formation. The sandstone sediments are full of cross-bedding structures, as shown in Figure 5.8b.

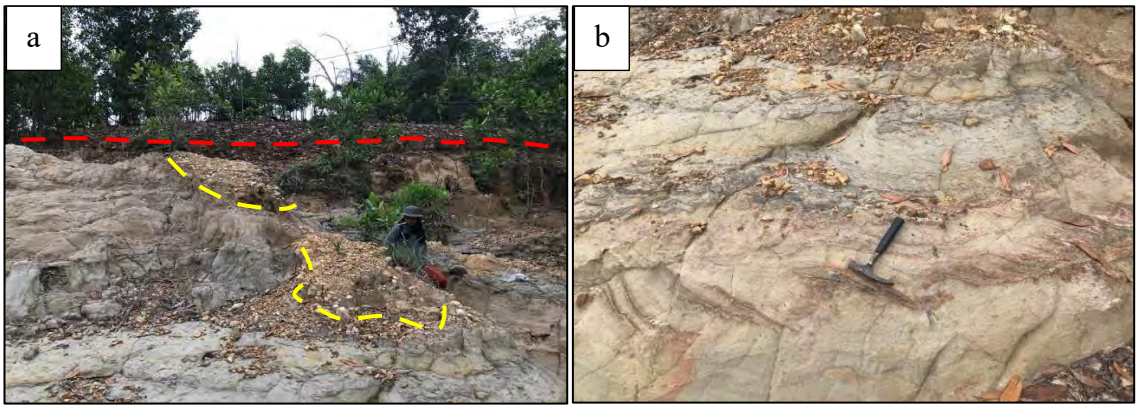

Figure 5.8: field observation of outcrop 19 representing (a) outcrop sediments composed of thick sandstone, mudstone, and conglomerate (weathered conglomerate separated by a red line and fresh conglomerate by the yellow line). (b) showing sandstone surface full of crossbedding structure.

5.3 Organic geochemistry

Several complementary experiments of organic geochemical study, such as bulk geochemistry and pyrolysis study, were carried out on selected samples to study the organic matter content, the type of kerogen, and the thermal maturity of the formation. Further analysis by gas chromatography was conducted to evaluate the depositional environment and paleo-condition of the Bongaya Formation. Around 70 samples were taken to represent the studied formation of the sand sediments (coal laminated with sandstone, clean sand, and sand with feldspar), the shaly sediment (shale and carbonaceous shale), the mudstone, and the coal in identifying the most potential rock sediments in promoting hydrocarbon.

The total organic carbon, source rock analysis, and extractable organic matter (EOM) yield were used to classify the organic richness in hydrocarbon generation. At the same time, the type of kerogen was assessed through the pyrolysis analysis (pyrolysis gas chromatography), maceral abundance in the samples, and through the source rock analysis. T_{max} results of source rock analysis and the vitrinite/huminite reflectance were

used to identify the maturity level of the rocks. Both gas chromatography mass-spectrometry and elementary composition analysis were done to reconstruct the paleoenvironment.

5.3.1 Extractable Organic Matter and Hydrocarbon Yield

A table summarizing the amount of bitumen extraction and their hydrocarbon yields is present below (Table 5.1). Generally, all samples contribute to an excellent quantity of organic matter regarding potential source rock, although some shale did show only an average amount (<1000 ppm). The extractable organic matter is high in coal samples, with an average of 13104 ppm to 61164 ppm compared to most other samples. The carbonaceous shale is also excellent by having more than 20 000 ppm organic matter followed by shale sediments. Also, in the same table 5.1, hydrocarbon concentration, including the aliphatic and aromatic and the NSO fractions, is shown. As expected of immature formation, the amount of NSO fractions is relatively high to the total hydrocarbon made of both aliphatic and aromatic. The aromatic fraction in the selected samples shows a much higher concentration than the aliphatic fraction.

Table 5.1: Bitumen extraction and column chromatography result in ppm

Sample ID	Lithology	EOM (ppm)	SAT (ppm)	ARO (ppm)	Hydrocarbon (ppm)
B1-4	Coal clast	53568	1811	4239	6051
B4-1	Coal clast	13394	711	1721	2432
B5-3	Coal clast	14634	162	779	941
B7-3	Coal clast		1138	11660	12798
B9-2	Coal clast	56709	117	820	937
B11-1		13104	127	2163	2290
B12-2	Coal clast	61164	449	3783	4231
B11-4	Carbonaceous shale	21102	1357	1639	2996
B13-6	Carbonaceous shale	20664	623	3007	3630
B2-1	Carbonaceous shale	6091	401	641	1042

B11-3	Carbonaceous shale	4338	269	372	640
B13-2	Carbonaceous shale	7235	158	742	900
B13-3	Carbonaceous shale	11519	449	1197	1646
B8-1	Shale	1931	207	253	460
B8-2	Shale	4200	989	1045	2035
B12-1	Shale	802	131	164	295
B13-1	Shale	4372	648	815	1464

5.3.2 Biomarker distribution

The hydrocarbon fraction extracted from column chromatography was taken for further analysis using Gas chromatography mass-spectrometry to identify the paleoenvironment, organic origin, and depositional condition. Some of them help to identify maturity. The saturate fraction was analyzed based on the distribution of n-alkanes and isoprenoid (m/z 85), Triterpenes distribution (m/z 191), and sterane distribution (m/z 217), whereas analysis of aromatic fraction used phenanthrene (m/z 178) and alkyl (m/z 192) derivatives.

5.3.2.1 The n-alkanes distribution and isoprenoid

Selected coal, shales, and carbonaceous shales samples' chromatograms were interpreted in identifying the abundance of n-alkanes, the CPI value, and acyclic isoprenoid. The aliphatic fraction n-alkanes of m/z 85 chromatograms and the peak distribution are given in Figure 5.9.

5.3.2.2 Carbon Preference Index (CPI)

Tissot and Welte (1984) discuss Carbon Preference Index (CPI) as a metric for detecting both the source of organic matter and maturity. In this study, the formulated CPI initially introduced by Bray and Evans (1961) was applied.

The CPI is influenced by the odd and even carbon preference that characterized source rock deposited in non-marine and marine depositional environments, respectively (Moldowan et., 1985; Palacas et al., 1984). This study shows that the selected samples are immature with a CPI value between 2.5 to 5.2 (Table 5.2). With the CPI value >1 and the abundance carbon mostly falling to be the odd-numbered n-alkane, the samples are correlated with land plant origin.

5.3.2.3 Acyclic isoprenoids

Besides the n-alkanes analysis, the most reliable isoprenoid alkanes are the Pristane (Pr) and Phytane (Ph) compounds that are associated with carbon 17 and carbon 18, respectively (Figure 5.9). Both isoprenoids act as a depositional environment and organic matter type indicator (Maxwell et al., 1972, 1973; Didyk et al., 1978; Brooks and Smith, 1969; Powell and Makriday, 1973; Chandra et al., 1994; Large and Gize, 1996). Both pristane and phytane being the biomarker derived from the phytol side chain of the chlorophyll, have contributed a lot in knowing the paleocondition during the burial of the organic matter. Calculated Pr/Ph results (Table 5.2) in values ranging from 0.33 to 2.55 indicate suboxic conditions to anoxic conditions, promoting Bongaya sediment to be deposited mostly under transitional environment sediment.

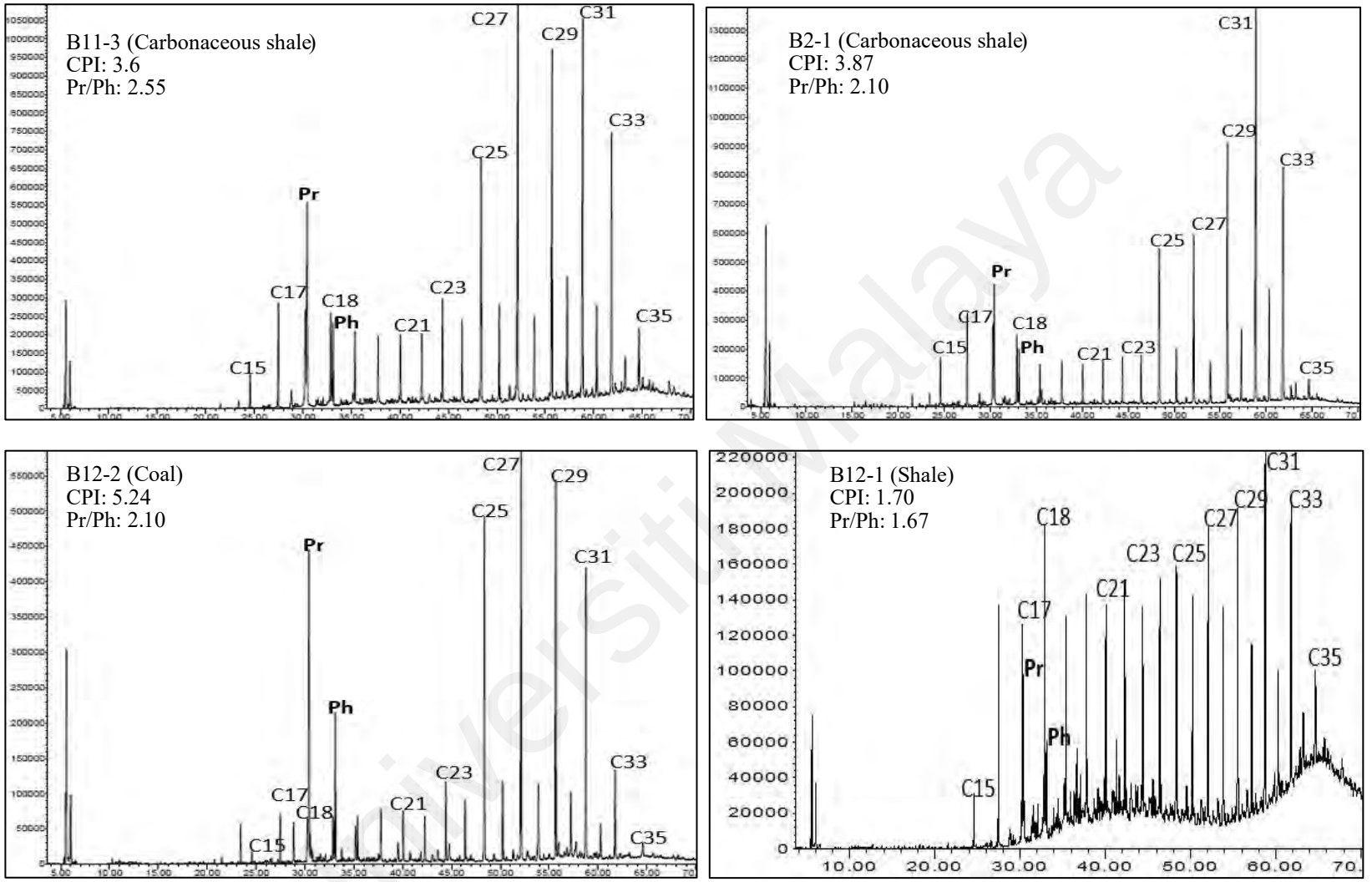

Figure 5.9: Representative of m/z 85 chromatograms showing the distributions of n-alkanes and isoprenoid. Pr=Pristane;Ph=Phytane.

Table 5.2: Biomarkers parameters for extracts of bitumen samples studied.

Sample	n-alkanes (m/z 85)					Hopane (terpenes)			Steranes			Phenanthenes and methylphenantherane		
	CPI (24-34)	Pr/Ph	Pr/C17	Ph/C18	Paq	Ts/Tm	Ts/ (Ts+Tm)	C29/C30	C27 (%)	C28 (%)	C29 (%)	P	9MP/(9MP+1MP)	MPI-1
B11-3	3.60	2.55	2.11	0.88	0.31	0.72	0.42	0.09	15.47	12.15	72.38	18.90	0.73	0.59
B13-2	4.90	1.64	2.57	1.10	0.17	0.47	0.32	0.35	11.27	25.00	63.73	20.80	0.51	0.09
B12-2	5.24	2.10	7.27	3.25	0.39	0.28	0.22	0.20	4.24	13.94	81.82	20.60	0.72	0.18
B2-1	3.87	2.10	1.42	0.81	0.17	0.50	0.33	0.36	12.87	24.75	62.38	20.90	0.44	0.19
B7-3	2.56	0.81	0.26	0.51	0.23	0.38	0.27	0.29	1.85	9.26	88.89	8.80	0.73	0.20
B13-3	3.78	0.89	1.04	0.78	0.22	0.75	0.43	0.43	9.20	19.16	71.65	20.60	0.56	0.22
B5-3	1.27	0.89	0.42	0.26	0.84	1.45	0.59	0.38	2.56	47.86	47.86	20.50	0.60	0.44
B11-1	1.29	0.33	0.25	0.33	0.7	0.27	0.21	0.22	10.99	39.01	50.00	19.80	0.53	0.62
B5-10	3.33	0.94	3.22	3.10	0.58	1.40	0.58	0.07	18.99	2.79	78.21	11.80	0.77	0.29
B9-2	1.33	0.67	0.33	0.21	0.25	0.50	0.33	0.37	9.28	8.25	82.47	20.70	0.71	0.25
B13-1	4.38	0.70	1.70	1.40	0.178	0.64	0.39	0.31	7.87	20.47	71.65	-	-	-
B1-4	2.08	0.50	0.75	0.50	0.96	0.25	0.20	0.06	14.08	21.13	64.79	11.6	0.70	0.80
B4-1	2.82	0.17	1.50	1.13	0.40	0.50	0.33	0.37	14.08	21.13	64.79	11.6	0.70	0.80
B8-1	2.09	1.57	1.05	0.74	0.23	0.40	0.29	0.41	13.14	8.76	78.10	16.2	0.50	0.60
B12-1	1.70	1.67	0.76	0.32	0.40	0.23	0.19	0.23	15.65	14.78	69.57	7.9	0.67	0.27

CPI = 0.5 x/[C25+C27+C29+C31+C33/C26+C28+C30+C32+C34] + [C25+C27+C29+C31+C33/ C24+C26+C28+C30+C32].

Paq= nC23 + nC25/ nC23 + nC25 + nC29 + nC31 – Alkanes

MPI-1 = 1.5 (2-MP + 3-MP)/ 0.69P + 1-MP + 9-MP

Pr/Ph: pristane/phytane.

Ts/Tm: trisnorneohopanes/trisnorhopanes ratios

5.3.2.4 Triterpenes Distribution

Apart from n-alkanes and isoprenoid study, the hopanoid distribution and related compounds of ions m/z 191 from saturated hydrocarbon are tracked and analyzed. The identified peaks are listed in the appendix.

Figure 5.10 displays peaks defined in the terpene fingerprint or m/z 191 mass chromatograms on the selected samples. The presence of C30 hopane and C29 norhopane dominates the samples, accompanied by a significant number of homophones of C31-C35, 17 (H)-trisnorhopane (Tm), 18 (H)-trisnorneohopane (Ts), and tricyclic terpenes. A significant peak of olanne can be found in some of the samples. Oleanane is a terrestrial angiosperm flowering plant marker or higher plant fingerprint that has been found in upper Cretaceous and younger sediment sequences (Peters and Moldowan, 1993; Peters et al., 2005; Mustapha et al., 2017). The presence of oleanane compounds indicates a large terrigenous organic input and good preservation conditions throughout the early deposition process (Murray et al., 1997; Peters et al., 2000). This approach necessitated a semiquantitative analysis that measured the area under the defined peak. The C29/C30, C31/C30, Ts/Tm, and Ts/(Ts+Tm) ratios were determined and listed in Table 5.2.

The results reveal a small range of C29 to C30 ratio, which is between 0.07 to 0.37. This mentioned ratio is widely used to identify the environmental setting of organic matters. The presence of 17 (H)-trisnorhopane (Tm) and 18 (H)-trisnorneohopane (Ts) compound area ratio was calculated in terms of Ts/Tm and Ts/ (Ts+Tm). The ratio indicates sediments maturity (Seifert and Moldowan 1978,1979; Moldowan et al.1985), with varying values of 0.27-1.45 for Ts/Tm while 0.21-0.59 for Ts/ (Ts+Tm). The value increases with increasing maturity.

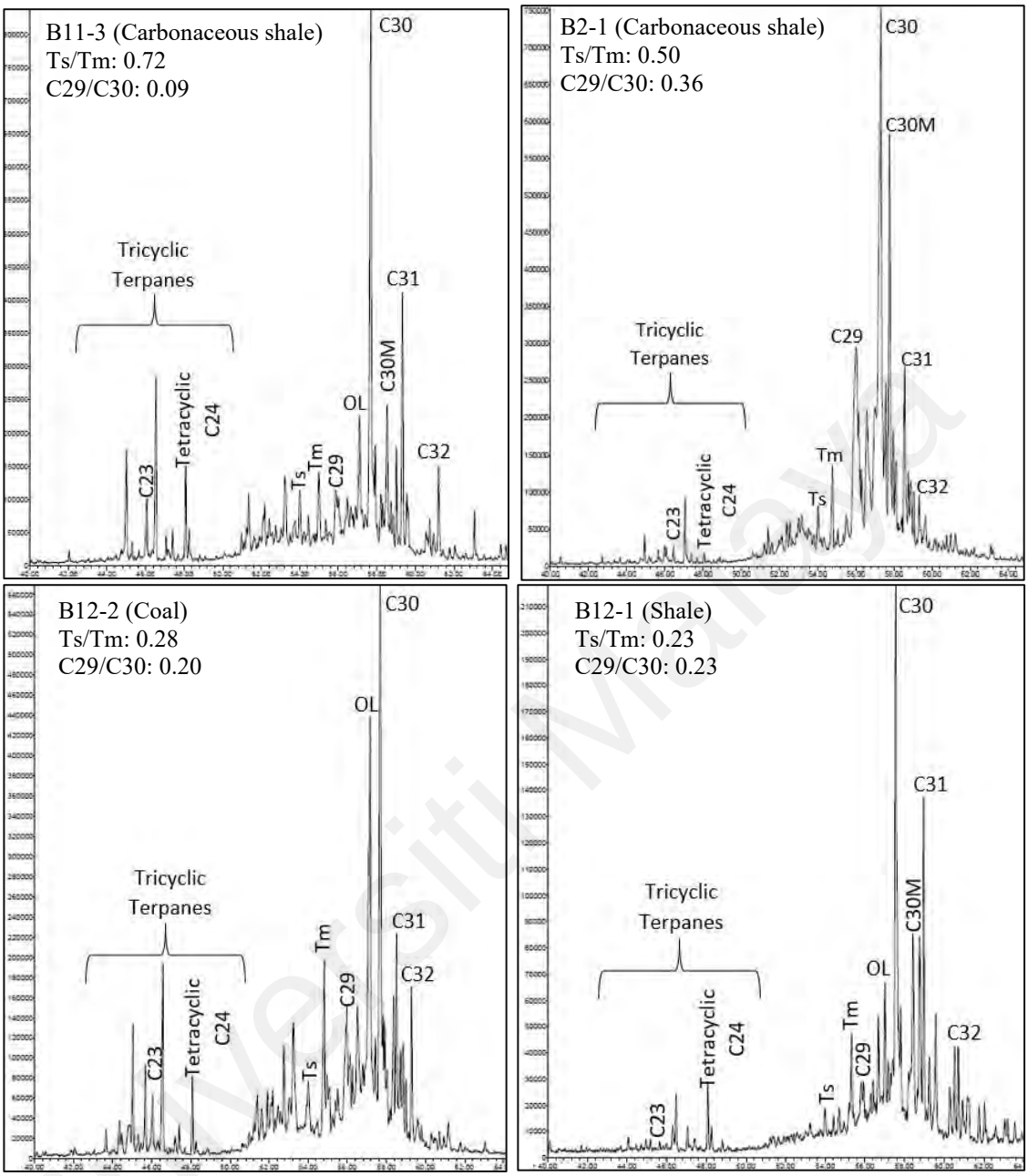

Figure 5.10: Representative of studied samples showing m/z 191 mass-chromatogram of saturated fraction and their respective peaks (refer to the appendix for compound abbreviation). Peak assignments refer to Appendix

5.3.2.5 Sterane Distribution

The m/z 217 ion chromatograms in Figure 5.11 present steroid distributions of significant biomarkers derived primarily from higher plants (Table 5.3) (Seifert and Moldowan 1978,1979). C27, C28, and C29 are important sterane compounds that are used to describe the environment of organic matter input. As shown in Table 5.2, the approach entailed using relative abundances between the identified steranes epimers (C27, C28, and C29) and was used in percentages form. In comparison to both C27 and C28 Steranes, a high proportion of C29 was discovered. In the discussion portion, this matter was further discussed.

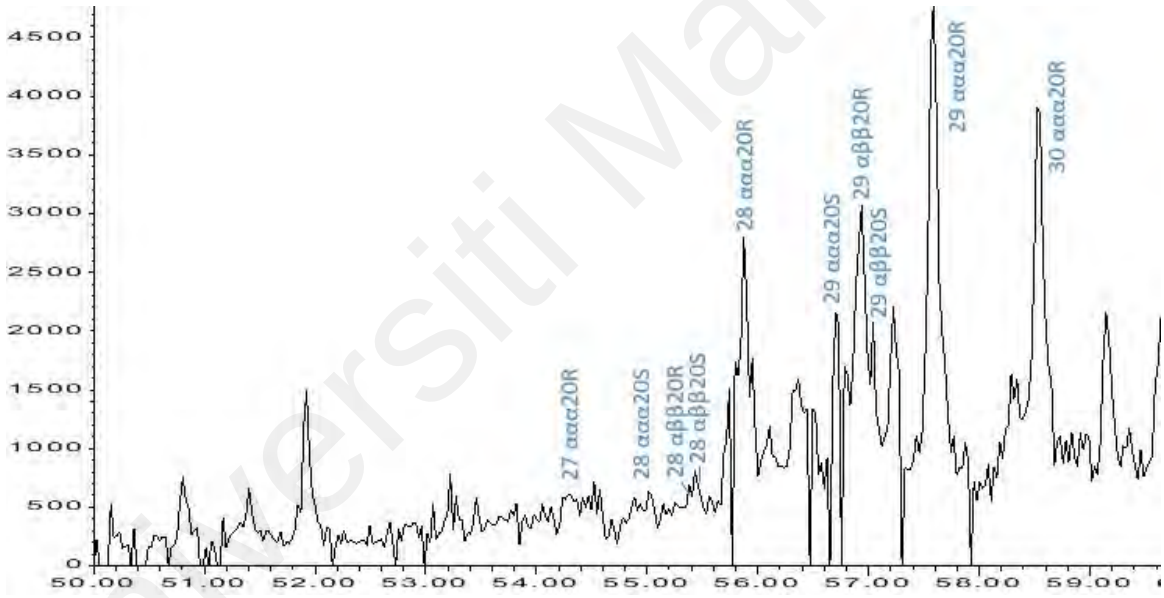

Figure 5.11: Representative of m/z 217 (from time retention of 50-59) showing the identified peak for paleoenvironment analysis.

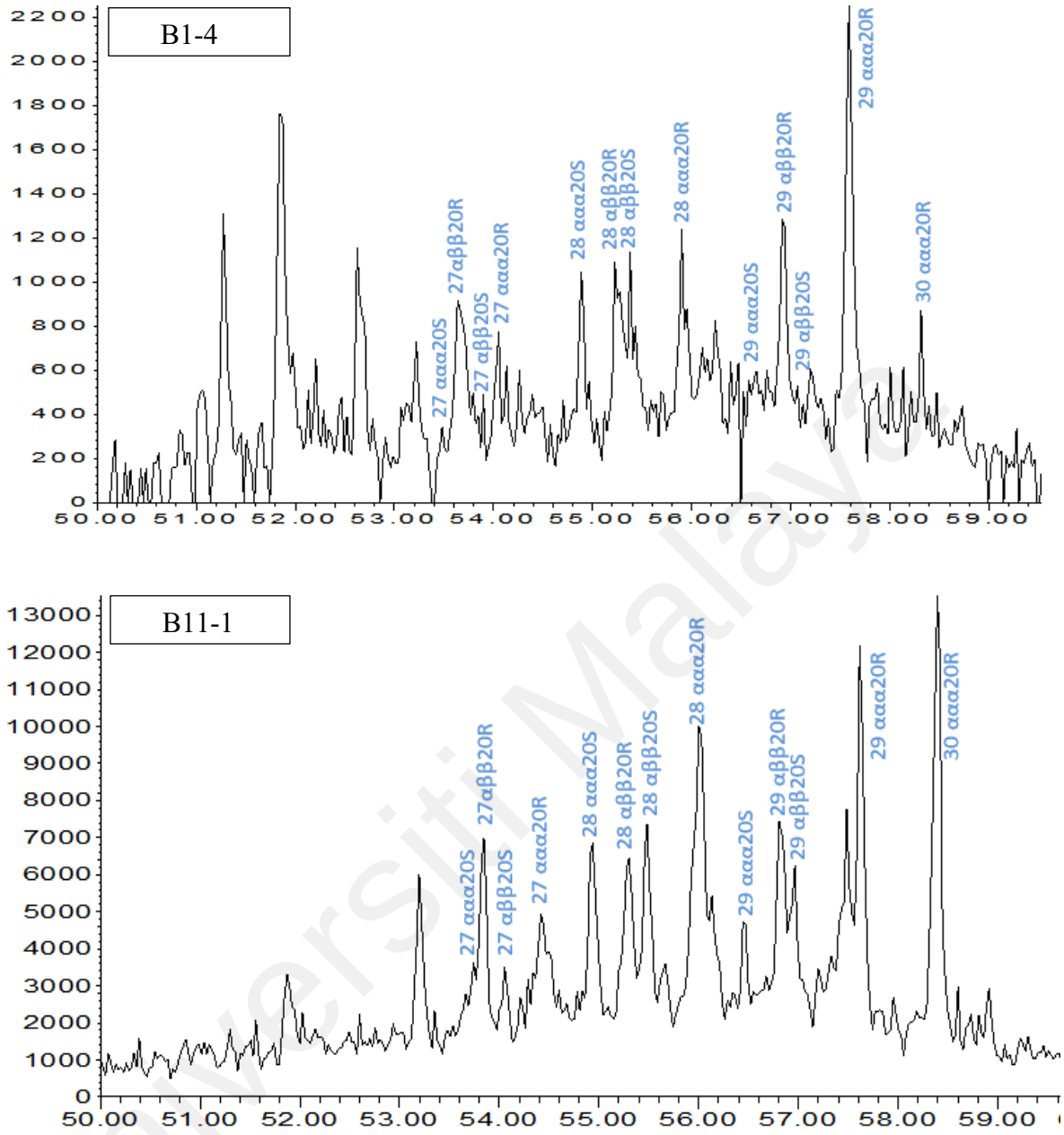

Figure 5.11. continued

5.3.2.6 Phenanthrene and alkyl derivatives.

Phenanthrene and alkyl derivatives of an aromatic fraction were extracted from the fragmentogram of m/z 178 and 192, as shown in Figure 5.12. The samples were studied to determine the thermal maturity and source input through the region of under phenanthrene and four methylphenantherane (MP) as measured in the chromatograms (Table 5.2). The

methylphenantherane ratio is determined as 9MP/(9MP+1MP). The ratio of MPI-1 displays increasing in value relative to the maturity increase (Sonibare et al., 2008).

5.3.3 Total organic carbon

A total of 53 samples was selected from various locations/outcrops and were conducted into a Rock-Eval-like analysis to identify their Total Organic Carbon (TOC). Total organic carbon (TOC) accompanied by SRA data quantifies the organic matter's amount to satisfy the essential requirement as source rock. TOC value (Table 5.3) was identified as excellent for most of the coals and some carbonaceous shale samples. The TOC value reached up to 63.1 wt%, coal particularly (51.8 until 63.1 wt%). Carbonaceous shale has a TOC level range between 18.3 to 30.8 wt% as the value is still above the threshold value of excellently rich organic matter content by Peter and Cassa (1994). Shale and coal laminated with sandstone have TOC values ranging from 0.9 to 4.9 wt% and 1.6 to 16.5 wt%, respectively. Consequently, most of them satisfy the average levels needed (TOC > 1.0 wt%) to be classified as conceivable hydrocarbon source rock (Hunt, 1996; Mustapha and Abdullah, 2013) except mudstone (0.7-0.8 wt%).

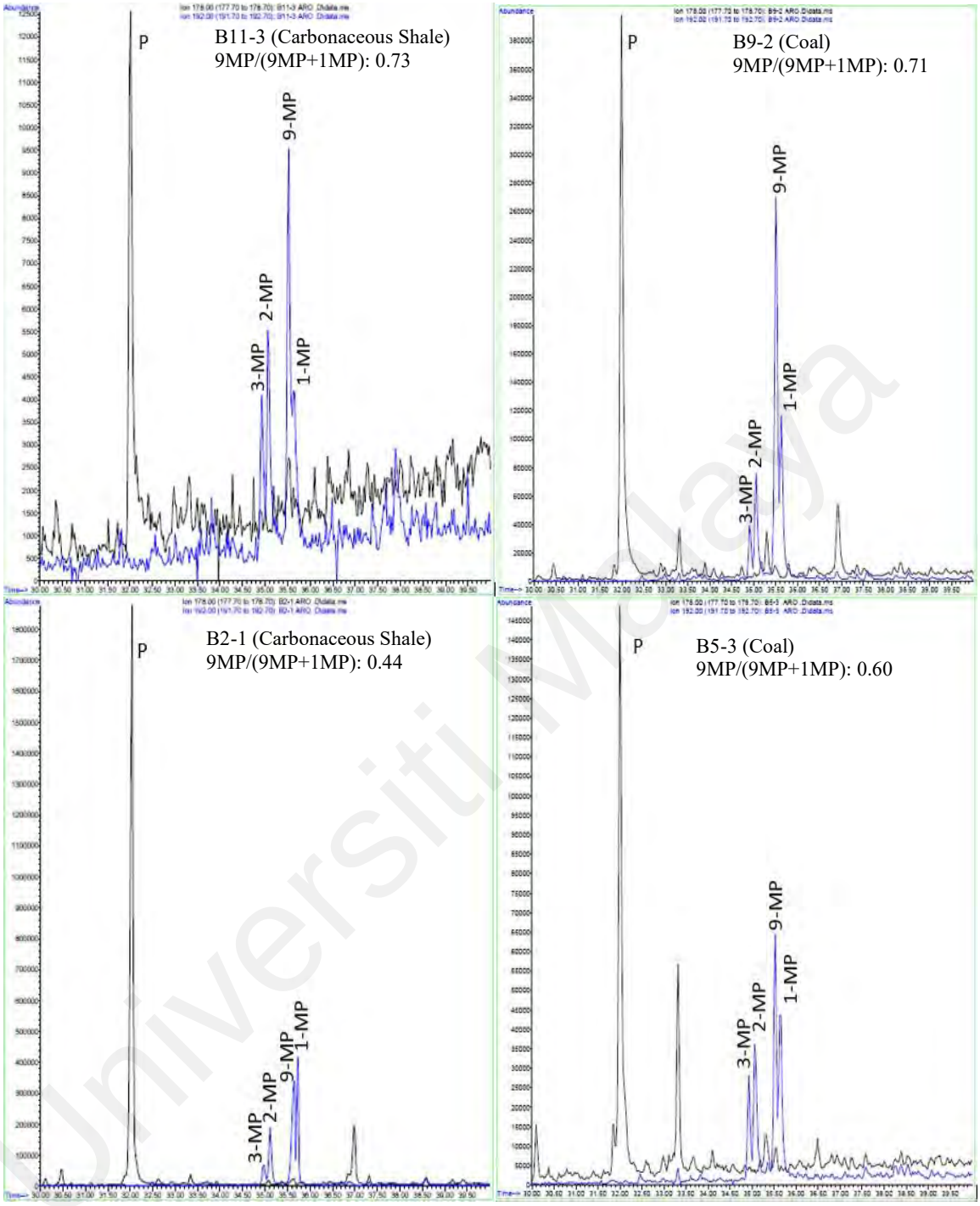

Figure 5.12: Representative of m/z 178 and 192 chromatograms from the aromatic fraction with identified phenanthrene and methylphenanthrenes compound peak (Blue chromatogram = Ion 192; Black chromatogram = Ion 178; Retention time = 30 to 40).

5.3.4 Source rock analysis

In conjunction with TOC amount by SRA pyrolysis, parameters such as free hydrocarbons (S1), the amount of hydrocarbon (S2), and CO_2 (S3) expelled from kerogen were calculated during the pyrolysis, and the results are shown in Table 5.3. Coal (2.45 to 282.1 mg HC/g) followed by some carbonaceous shale (16.32-30.8 mg HC/g) mainly possessed a very excellent S_2 value, exceeding the minimum required of 5 mg/g S_1 + S to meet the expectation of having good potential to produce hydrocarbons (Peter, 1986; Bordenave,1993). However, except for most carbonaceous shale (4.84 to 12.86 mg HC / g), which shows fair to very good hydrocarbons amount, shale, coal laminated with sandstone promoted S_2 value below 13.51 mg HC/g, indicates poor hydrocarbon potential. Though some of the coal laminated with sandstone do exceed above 9 mg HC/ g (good S_2 amount), it may be due to high carbon in the coal. In addition, a thermal maturity indicator represents by T_{max} values generally range between 371.6 to 437.3 as studied samples are still yet cracked to produce hydrocarbon. Coal samples, as compared to other samples, have lower T_{max} values (range between 371.6 to 421.5).

The hydrogen index (HI) values were derived from both the TOC amount and the S2 amounts. HI values are significantly linked to the amount of liptinite (high hydrogen material) as an oil presence indicator. Peter and Cassa (1994) developed an HI value that appointed gas, oil, and mixer prone as a reference, although there is no exact boundary to be clarified. The highest HI value presented by coal source rock (48.9 to 629.6 mg HC/g TOC) included the three highest values above 500 mg HC/g TOC (Table 5.3). Carbonaceous shales came in second highest with HI range from 45.7- 100.1 mg HC/g TOC where two of them have high HI, which are 89.2 and 100.1 mg HC/g TOC. Table 5.3 also includes HI values for coal laminated with sandstone (20.61-103.3 mg HC/g TOC), shale (28.4-67.3 mg HC/g

TOC), and mudstone (23.3-66.67 mg HC/g TOC). The results of the Production Index (PI) have ranged from 0 to 0.23. According to the HI value, most samples could potentially contribute as gas source rock with some oil. All parameters are combined to identify source rock quantity and quality at the Bongaya Formation and discussed further in the following chapter.

Table 5.3: Result of TOC (wt%) and SRA data of the analyzed samples along with their lithology

ID	lithology	TOC	S1 (mg HC / g rock)	S2 (mg HC / g rock)	Tmax (°C)	PI	HI (mg HC/ g TOC)
B1-1	Coal Laminated Sandstone	2.9	0.04	1.05	427	0.03	36.2
B1-2	Coal Laminated Sandstone	1.7	0.03	0.55	431.1	0.05	32.35
B1-3	Mudstone	0.8	0.04	0.25	433.2	0.16	31.25
B1-4	Coal Clast	63.1	0.08	90.66	422.1	0	143.7
B1-5	Coal Laminated Sandstone	1.6	0.05	0.56	433	0.08	36.1
B1-6	Coal Laminated Sandstone	3.3	0.03	0.68	415.3	0.04	20.61
B1-7	Mudstone	0.6	0.06	0.40	430	0.14	66.67
B1-8	Coal Laminated Sandstone	4.4	0.02	2.92	422.5	0.01	66.4
B1-9	Coal Laminated Sandstone	1.8	0.01	0.75	432.8	0.01	41.7

B1-10	Carbonaceous Shale	9	0.11	4.84	419	0.02	54.1
B1-11	Coal Laminated Sandstone	3.9	0.03	3.39	425.3	0.01	86.3
B1-12	Coal Laminated Sandstone	1.6	0.04	0.58	433.1	0.06	35.8
B1-13	Coal Laminated Sandstone	1.7	0.03	0.41	426.7	0.07	24.12
B1-14	Carbonaceous Shale	7	0.07	5.39	427.3	0.01	77.1
B2-1	Carbonaceous Shale	11.4	0.41	10.29	400.2	0.04	90.26
B3-1	Shale	1.1	0.06	0.46	423.4	0.12	41.4
B3-2	Mudstone	0.7	0.05	0.41	437.30	0.11	62.4
B4-1	Coal Clast	52.7	0.41	56.23	371.6	0.01	106.7
B4-2	Shale	2.9	0.1	0.81	409.4	0.11	28.4
B5-1	Paleosol	0.8	0.02	0.21	435.2	0.12	26.25
B5-2	Coal Laminated Sandstone	16.5	0.27	10.27	407.5	0.03	62.2
B5-3	Coal Clast (Root)	52.6	0.31	44.3	375.7	0.01	84.2
B5-4	Coal Laminated Sandstone	8.6	0.03	2.5	422.4	0.01	29.07
B5-5	Mudstone	0.7	0.05	0.17	426.3	0.23	23.3
B5-6	Coal Laminated Sandstone	4.8	0.11	2.94	428.2	0.04	61
B5-7	Coal Laminated Sandstone	3	0.1	3.1	419.6	0.03	103.3
B5-8	Coal Clast	52.3	0.19	25.59	421.5	0.01	48.9
B5-9	Shale	2.5	0.08	0.74	416.6	0.09	29.6
B6-1	Shale	1.6	0.07	1.05	428.8	0.06	67.3
B7-1	Shale	1.4	0.06	0.51	417.7	0.11	37.5
B7-2	Carbonaceous Shale	4.9	0.35	2.45	402.8	0.13	49.8

B7-3	Coal Clast	54.2	4.21	276.26	395.8	0.02	509.7
B8-1	Shale	2.8	0.08	1.11	426.4	0.07	40.1
B8-2	Shale	4.9	0.08	1.4	407.9	0.06	28.57
B9-1	Coal Clast (Trunk)	55.4	0.34	36.57	410.1	0.01	66
B9-2	Coal Clast	60.7	1.91	382.17	369.6	0	629.6
B9-3	Shale	3.2	0.07	1.21	412	0.05	37.81
B9-4	Carbonaceous Shale	14.9	0.72	11.98	411.5	0.06	80.4
B10-1	Shale	0.6	0.04	0.34	426.1	0.11	57.6
B11-1	Coal Clast (Trunk**)**	51.8	0.05	56.72	386.8	0	109.5
B11-2	Laminated Silt	0.8	0.04	0.17	423.4	0.22	21.25
B11-3	Carbonaceous Shale	15.4	0.47	12.86	411.9	0.04	83.5
B11-4	Carbonaceous shale	18.3	0.2	16.32	415	0.01	89.2
B12-1	Shale	0.9	0.02	0.41	432	0.05	45.7
B12-2	Coal Clast (Trunk)	62.5	1.27	330.09	396.7	0	528.1
B12-3	Carbonaceous Shale	8.3	0.41	7.36	406.9	0.05	45.7
B13-1	Shale	5.4	0.24	3.38	402.2	0.07	62.7
B13-2	Carbonaceous Shale	8.7	0.32	7.32	404.7	0.04	83.8
B13-3	Carbonaceous Shale	10.9	0.65	11.09	403.6	0.06	101.7
B13-4	Carbonaceous Shale	17.1	0.39	9.67	392.6	0.04	56.5
B13-5	Shale	1.4	0.07	0.52	425.3	0.13	37.14
B13-6	Carbonaceous shale	30.8	1.48	30.84	411.4	0.05	100.1
B13-7	Carbonaceous Shale	15.3	0.72	13.51	403.7	0.05	88.3

TOC= Total Organic Carbon, wt%; S1 = free hydrocarbons, mgHC/g rock; S2 =kerogen generation capability, mgHC/g rock; HI – hydrogen Index (S2x100/TOC), mgHC/gTOC; PI = Production Index (S1/ (S1+S2); Tmax = Temperature at maximum generation of S2, ^{O}C.

5.4 Pyrolysis Gas Chromatography

The pyrolysate analysis acts as an alternative way to assess the type of kerogen produced by the source rock as more details were deliberately discussed in determining the mixed kerogen types (Dembicki, 1983). Dembicki et al. (1983) and Dembicki (2009) discussed that the pyrolysate S_2 provides the composition of hydrocarbons generated by the thermal cracking of kerogen and deduces the nature kerogen type using both qualitative and quantitative analysis. The pyrograms of the analyzed samples display a unimodal distribution of methane peaks, followed by n-alkene/n-alkane doublets of up to n-C_{30} in several samples (Figure 5.14).

Generally, Bongaya Formation possessed mainly Type III kerogen gas-prone as n-alkane/alkene compounds are highly concentrated in low molecular carbon fraction ($<C_{10}$) as well as having an abundance of aromatic peaks (benzene, toluene, m(+p)-xylene and naphthalene) upsurge in between as highlighted by Dembicki (2009). However, the Py-GC results also display less significant n-alkene/alkane doublets extended beyond C30 suggesting little oil potential source rock (Hakimi,2018) indicated a mixed oil and gas potential, but mainly gas kerogen type.

Quantitative analysis, the C8/xy ratio, and the 'Type Index' (R) method were chosen to explain kerogen type determination as they are considered closely related to each other (Adegoke et al., 2015). Both C8/xy and 'type index' ratio (Fig. 5.13) provided relative measure between aromatic (represent by xylene) and aliphatic peak high (represent by n-Octane) in the pyrograms to determine their hydrocarbon potential and kerogen type, respectively. n-Octane and xylene ratio higher than 1.0 contribute to good petroleum potential (oil) while <1.0 ratio shows the potential of more gas prone rather than oil-prone.

Mustapha and Abdullah (2013) suggested that samples with less than 0.5 ratios were inferred to be gaseous. 'Type index' was measured by xylene over n-Octane fractionated to three indexes; <0.4 indicating Type I kerogen, whereas Type III kerogen takes range from 1.3 to over 20 indexes. Type II kerogen is an intermediate index (0.4 to 1.3). Figure 5.14 below shows the calculated C8/xy ratio and the 'Type Index' (R) that ranged from 0.2 to 1.3 and 0.8 to 6.5, respectively. Both results satisfy preliminary interpretation of Bongaya Formation is Type III kerogen. However, one sample, B1-4, shows some influence of oil mixture and Type II kerogen, indicating mixed Type II/III kerogen.

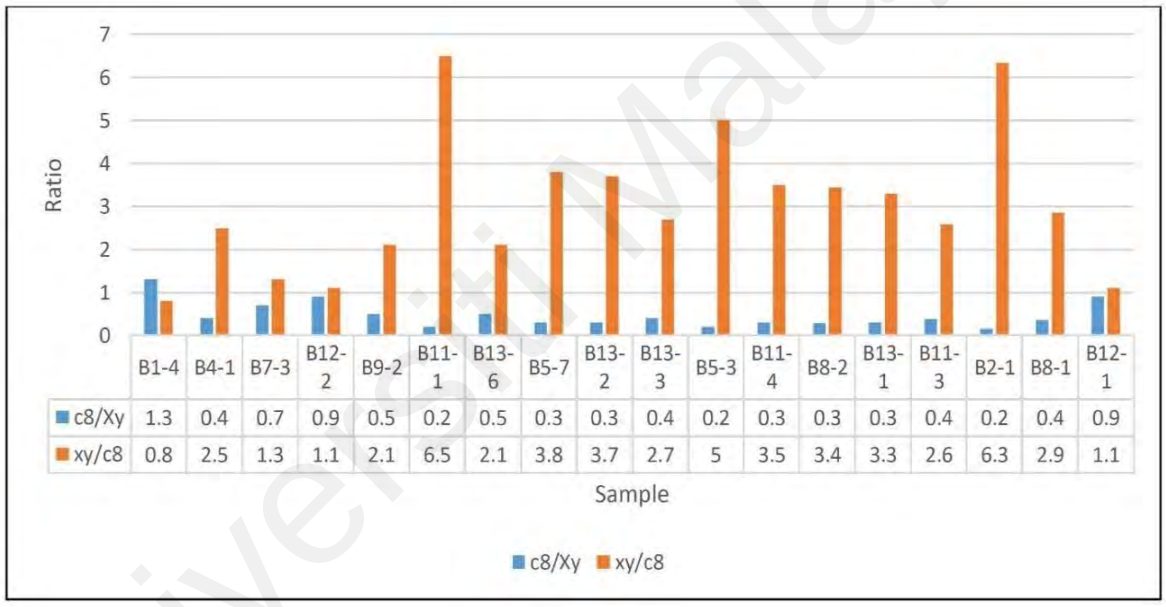

Figure 5.13: Histogram graph comparing the C8/xy and the "type index" ratios.

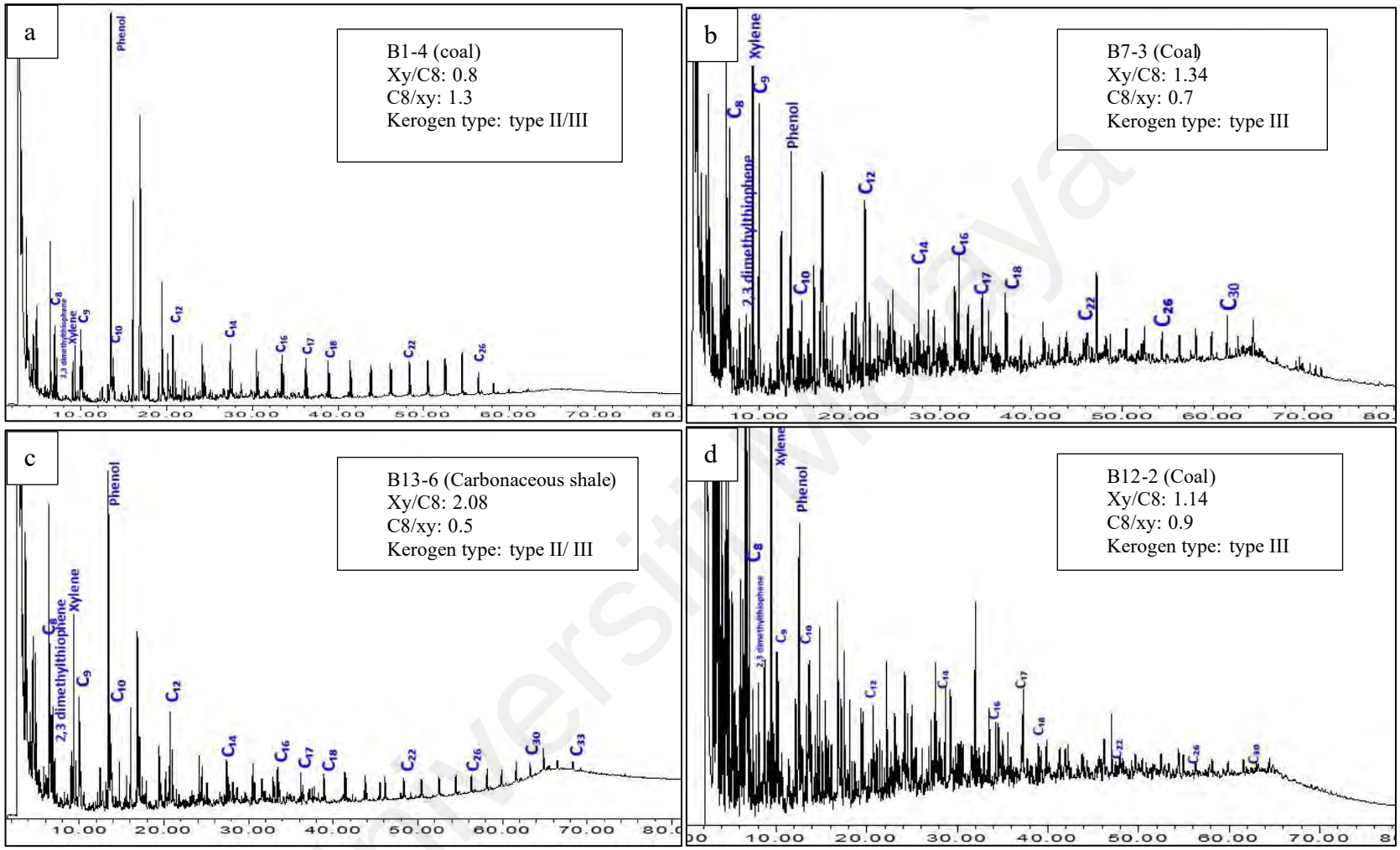

Figure 5.14: Representative of Py-GC chromatogram of coal and carbonaceous shale samples showing an abundance of aromatic peaks, doublets n-alkanes/alkenes, and compounds such as 2,3 dimethylthiophene, xylene, and phenol.

5.5 Petrographic Analysis

The petrographic analysis included vitrinite reflectance identification, maceral point counting, and fluorescence emission study of the liptinite in selected samples of Bongaya Formation, as reported in Table 5.4.

5.5.1 Vitrinite/Huminite Reflectance

Tissol and Welte (1984) believed that vitrinite/ huminite reflectance has now been considered the best indicator to identify the rank of coal and maturity of the samples, with considerations of preventing reworked vitrinites/huminite, hydrocarbon impregnation, and intermaceral effect. They mentioned that vitrinite/ huminite was commonly used for the scale due to its main occurrence. Considering the low-rank coal (lignite) in analysis, further discussion will use huminite nomenclature instead of vitrinite. A previous study by Peter & Cassa (1994) highlighted that vitrinite reflectance of 0.2%-0.6% shows low maturity in generating oil. In contrast, vitrinite reflectance in the range of 0.65%-0.9% is considered oil peak maturity, whereas, in this study, the samples' huminite reflectance ranges between 0.32 to 0.43 R_o% (<0.5), which is believed to be immature as proposed earlier.

5.5.2 Maceral counting

In a total of 15 samples, the relative amounts of macerals of the types huminite, liptinite, and inertinite were calculated (Table 5.4). The maceral examination found that huminite, liptinite, and mineral materials dominate the samples (depends on the type of source rock), with minimal inertinite maceral. The amount of huminite content varies from 10 to 98%, while a much lower amount was shown by liptinite (0 to 55%) and inertinite (0 to 33 %). Mineral matter content ranged between 2 to 90%. Pyrite and clay are the most abundant

mineral matter found. As noted, due to the inconsistent availability of the matter in each sample, the respective maceral and mineral matter percentages are so large and vary.

Table 5.4: The petrographic analysis of selected analyzed samples covers huminite reflectance (VR_o %) and maceral counting percentage, and mineral matter.

No	Sample ID	Lithology	VR_o (%)	Maceral composition (%)	Mineral matter (%)		
				Huminite	Liptinite	Inertinite	
1	B1-4	Coal	0.32	54	29	2	15
2	B1-10	Carbonaceous shale	0.36	29	0	0	71
3	B4-1	Coal	0.36	98	0	0	2
4	B5-3	Coal	0.35	53	10	28	9
5	B5-8	Coal	0.43	50	7	30	13
6	B7-3	Coal	0.33	50	46	0	4
7	B8-2	Shale	0.38	14	0	0	86
8	B9-2	Coal	0.32	53	43	0	4
9	B11-1	Coal	0.38	96	0	0	4
10	B11-4	Carbonaceous shale	0.37	24	7	0	69
11	B12-2	Coal	0.32	44	49	0	7
12	B13-1	Shale	0.38	10	0	0	90
13	B13-2	Carbonaceous shale	0.35	15	0	0	85

Huminite maceral was abundant in coal source rocks, with an average range of 44 to 98%, followed by liptinite maceral with a range of 0 to 49% (Table 5.4). Some of the coal was entirely comprised of huminite, while others had liptinite amounts comparable to the huminite maceral. Coal maceral analysis results in abundant resinite, sub-maceral of liptinite, found to be in the range between 2 to 55 % per sample. Resinite appears equivalently dominant with huminite in some coal, giving the predicted output of oil a waxy characteristic (Taylor et al., 1998), and they have fluoresced to a very bright yellow color. These resinites mostly aligned structurally to each other and enclosed huminite in separate globular bodies (Figure 5.15), showing a possibility of micro lamination (Petersen et al., 2013). Cutinite and

Sporinite are typical other liptinite macerals found in the coal samples besides resinite (Figure 5.16 (a) & (b)). As two naturally associated macerals, the cutinites and Sporinites were spotted to have their yellowish-green color which is less fluorescence compared with resinite. Cutinite always takes in a strand-like form, while Sporinite is present in a more ring agglomerated form (Pickel et al., 2017). A small portion of cell wall-like liptinite was also found, called Suberinite (Figure 5.16 (c)).

Nevertheless, two coals showed a profound amount of inertinite besides significant huminite existence. The inertinite occurrence indicates that the depositional environment is away from the shoreline; it may well be interpreted as a back mangrove environment. The significant representation of huminite and liptinitic macerals indicated that both liquid hydrocarbons of oil waxy and gas could be generated by these coals.

Two carbonaceous shale samples were discovered to have a small quantity of liptinite (7-10%), possibly resinite. However, most carbonaceous shale and shale samples are dominated by mineral matter (63-86%) and minimal huminite (12- 29%).

As predicted, mineral matter and less huminite dominated shale. In this study, both liptinite and inertinite are absent. Compared to mineral matter that dominated up to 86% and more, the proportion of huminite accounted for just 10% to 14%. This study shows that shale lacks organic matter, thereby reducing its hydrocarbon-producing capacity.

Most Bongaya sediments contain high huminite macerals revealed Type III kerogen occurrence. Some of the coals, particularly dominant with both liptinite and huminite, likely exhibit Type II/III kerogen. High saturated liptinitic resinite maceral would consider the production of high waxy oil from these samples.

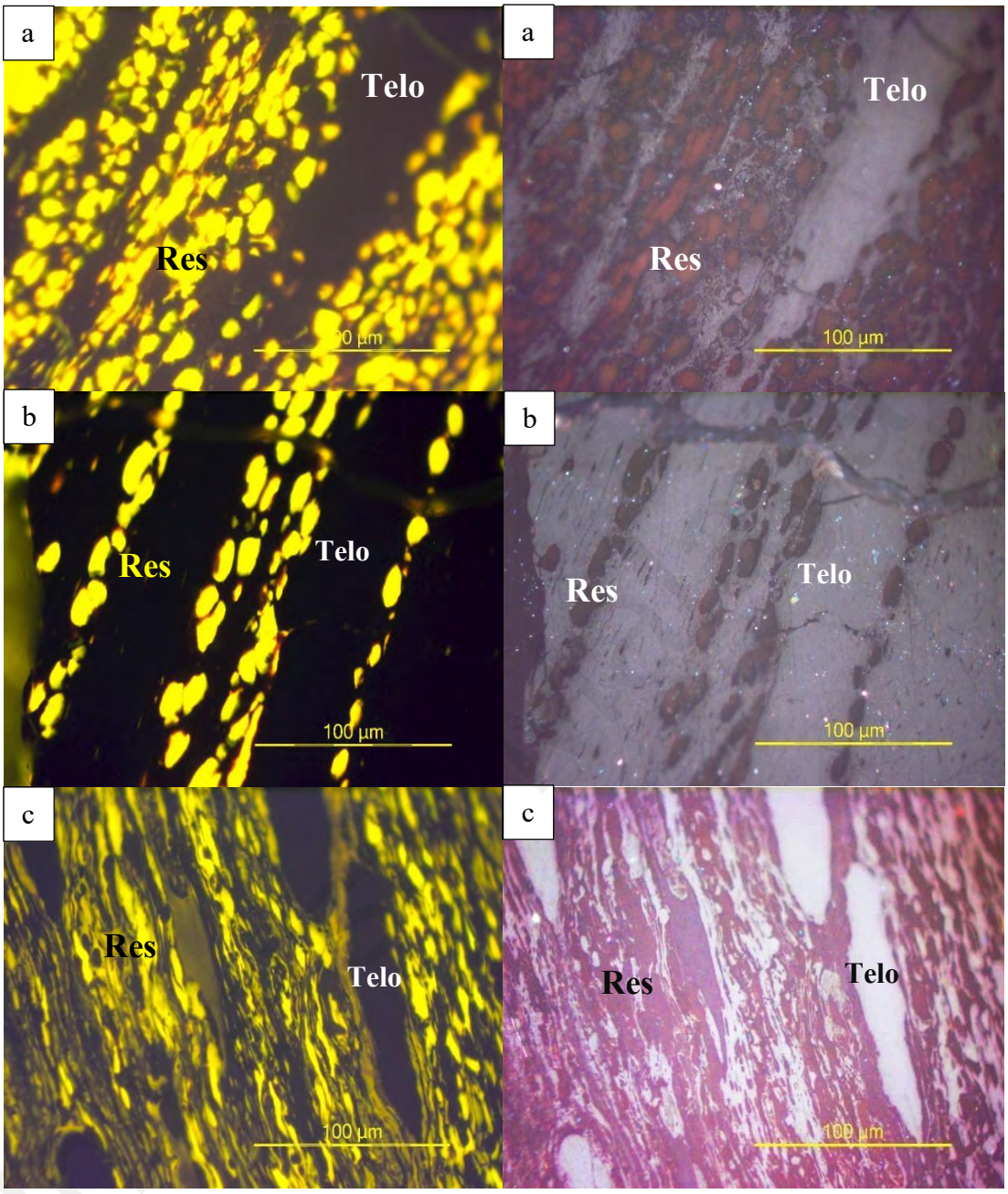

Figure 5.15: Coal maceral comparison under UV and white light, showing (a) B7-3 coal of resinite and huminite maceral, (b) high fluorescents of resinite aligned inside huminite maceral in sample B9-2, and (c) resinite appear much more compressed in sample B12-2, implying more burial force in the sample. Res=Resinite; Telo= Telocollinite (Huminite).

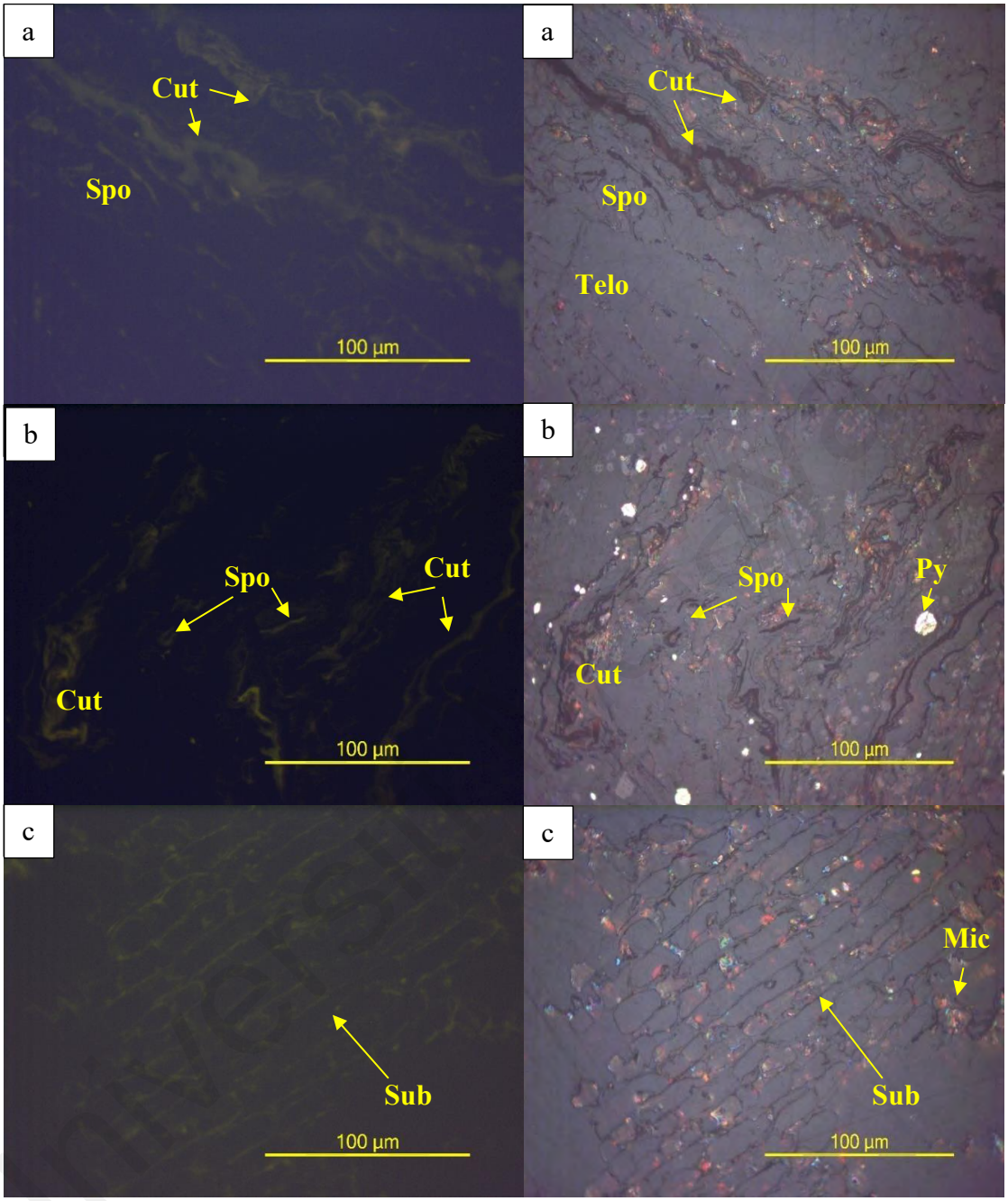

Figure 5.16: Photomicrograph of coal macerals (B1-4) under reflected white light (left) and ultraviolet light (right). (a) and (b) shows low fluorescence of sporinite and cutinite macerals alongside huminite and a little pyrite. (c) represents coal maceral of suberinite associated with micrinite. Cu= Cutinite; Spo=Sporinite; Sub= Suberinite; Py=Pyrite; Mic= Micrinite; Telo=Telocollinite.

5.5.3 Fluorescence observation

In evaluating hydrocarbon potential, liptinite maceral fluorescence is best established as an indicator of hydrogen-rich source rock, which is significant for oil generation (Taylor et al., 1998). The liptinite macerals revealed intense fluorescence in yellowish and yellowish-green color after being applied under UV light, as illustrated in Figures 5.16 and 5.17. This Miocene coal is expected to deliver oil, thus considered a potential hydrocarbon source rock, as it fulfilled Hunt's (1995) statement that at least 15-20% of liptinite constitute is needed in each sample.

5.6 Palynology

The palynological study is essential to petroleum geologists because they contribute to identifying the paleodepositional environment and, at the same time, assists in the general evaluation of the sedimentary basin's hydrocarbon potential (Combaz, 1964). The interpretation has been conducted based on the ecological preference of the palynomorphs and the distribution of palynological matter. The samples selected for this research are carbonaceous shale and shales, and their results are represented in table 5.5 as well as the photomicrograph of the spore and pollen (Figure 5.17).

The samples yielded abundant mangrove-source pollen, particularly *Rhizophora.* Also present were *Florschuetzia cf. levipoli, florschuetzia cf. meridionalis, Florschuetzia type, Brownlowia type, Nypa, and Avicennia type*. Morley (1978) highlighted that Florschuetzia group pollens identified in the samples are significant marker species for dating Miocene sediments of Borneo and the adjacent areas. The freshwater type was represented by *Elaeocarpus, Pometia, Barringtonia, Pandanus, Myrtaceae, Cyrtostachys type, Sapotaceae, Quercus, Melanorrhoea, Garcinia cuspidate, Calophyllum, Gonystylus, Lithocarpus type,*

Ilex type, Stemonurus type, Dactylocladus type, Calamus type, Blumeodendron, Palmaepollenites spp., Campnosperma, Chepalomappa, Timonius, Euphorbiaceae, Alchornea, Protaceae, Anacolosa, Arenga type, Ficus, Dacrydium, and Magnoliaceae. Besides, fern pollen is found most as other *Pteridophytes*, followed by *Stenochlaena palustris* and *Acrostichum aureum*. However, the herbs are represented by *Graminae* only.

The most abundant pollen type observed was Rhizophora type pollen, indicating that the main of this formation was a mangrove environment (averagely 11 Rhizophora pollen found in each sample). Since the Early Miocene till now, Rhizophora-type pollen has been a frequent mangrove plant. Furthermore, due to the occurrence of Nypa and Brownlowia type pollen, a palynology study suggests that the back mangrove area has little influence on the formation (Morley, 2000). Lastly, inland vegetation is represented by discoveries of pollen related to the freshwater zone. This zone is vital to identify inland vegetation influence in the paleoenvironment.

Table 5.5: Palynology data for selected coals and carbonaceous shale of Bongaya Formation.

BIL	Sample Id	Rhizophora Type	Florschuetzia Cf. Levipoli	Florschuetzia Cf. Meridionalis	Florschuetzia Type	Brownlowia Type	Nypa	Avicennia Type	Elaeocarpus	Pometia	Barringtonia	Pandanus	Myrtaceae	Cyrtostachys Type	Sapotaceae	Quercus	Melanorrhoea	Garcinia Cuspidata	Calophyllum	Gonystylus	Lithocarpus Type
1	**B13-1**	12			1							2	3			3					3
2	**B1-14**	3							1				1								1
3	**B5-10**	8				1		1		1		2	3	1		2					
4	**B2-1**	3	1					1	2						1	1					1
5	**B12-2**	21			2			1			1	1	1		1	1			1		2
6	**B7-1**	16	1	1	1				1			1	2								
7	**B13-5**	17			2				1			2	3								1
8	**B13-7**	8			2			1							3		1				
9	**B13-4**	3			1			1					1			1					
10	**B11-3**	6					1		2				4			1		1			
11	**B8-1**	15			1							2			1						2
12	**B5-9**	6			1							2	2			2					
13	**B9-4**	16			1			1	1		1	1				1		1			1
14	**B12-1**	10			2				5				2	1	1					1	1
15	**B3-1**	11				1			1					1							2
16	**B6-1**	17							2			1			2	2					1
17	**B8-2**	18							2		1		2	1	1	1					1

Table 5.5, continued

Bil	Sample Id	Ilex Type	Stemonurus Type	Dactylocladus Type	Calamus Type	Blumeodendron	Palmaepollenites Spp.	Campnosperma	Chepalomappa	Timonius	Euphorbiaceae	Alchornea	Protaceae	Anacolosa	Arenga Type	Ficus	Dacrydium	Magnoliaceae	Other Pteridophytes	Stenochlaena Palustris	Acrostichum Aureum
1	B13-1	2		2	2	1												1	5		
2	B1-14		1	1		2	1														
3	B5-10		1			3	3	1	1	1	1		1					1	4		
4	B2-1		3			5	1		1		2		1	1					5	2	
5	B12-2		1	2		1				1	1							1	3		1
6	B7-1	1		1	1	1	1							1				1	5		
7	B13-5			2		2		1					1						3	2	
8	B13-7			3	1	2												2	5	3	
9	B13-4							1													
10	B11-3				2	1		1			1		1		1			1	2		
11	B8-1				1		1												3	1	2
12	B5-9		1	3	1	1	2				2			1				2	2		
13	B9-4	1	1		1	1		1				1								1	
14	B12-1			1			1				1					1			2		
15	B3-1		1	1	1			1			1						1			4	
16	B6-1		1															2	1		
17	B8-2			2	1	2			1		1								3		

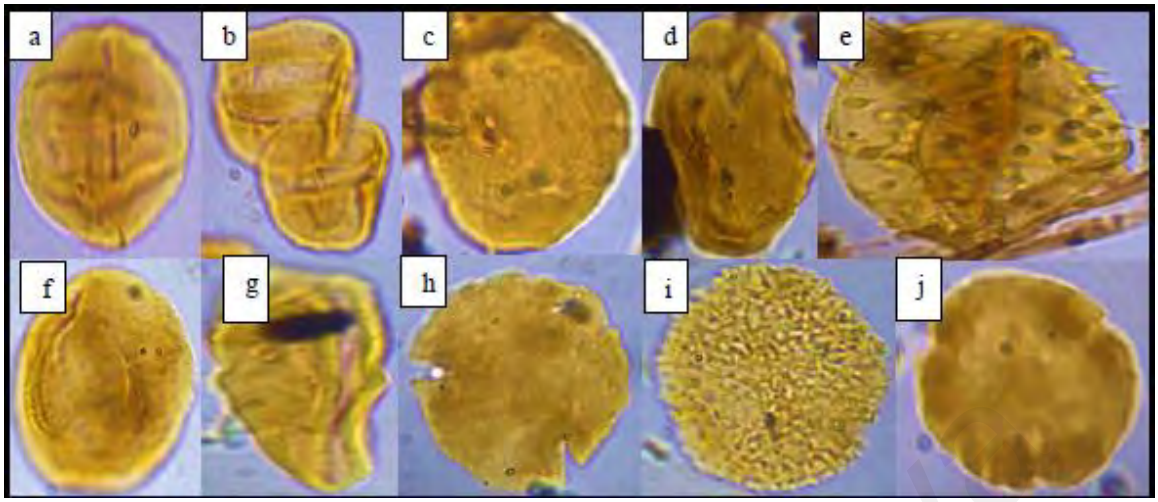

Figure 5.17: Photomicrography of representative spores and pollen in the analyzed samples, which were largely dominated by mangrove plant species (under x100 objective). a=*Avicenna*; b=*Rhizophora*; c=*Florschuetzia levipoli*; d=*Florshuetzia meridionalis*; e=*Nypa fruiticans*; f=*Calophyllum*; g=*Magnoliaceae*; h=*Brownlowia*; i=*Timonius*; j=*Alchornea*.

5.7 Elemental analysis

10 selected samples of six sandy materials and 4 shales (consisting of low total carbon) of the Bongaya Formation were sent for trace element analysis using the ICP-MS method. This external alternative is to reveal the depositional environment and the source input from less or non-organic sediments. The abundance and trace elements ratio have proved a success in determining both paleoenvironmental condition and the origin as different oxidation levels provide different geochemical behavior, thus altering the concentration of the element (Tribovillard et al. 2006). Significant trace elemental ratios such as cobalt/nickel (Co/Ni), vanadium/nickel (V/Ni), and V/(V/Ni) were usually used as one of the quantitative factors to identify the organic matter input, maturity, paleoredox condition, and their depositional

setting (Barwise 1990; Filby 1994; Alberdi-Genolet and Tocco 1999; Tribovillard et al. 2006; Akinlua et al. 2007, 2010).

The trace elements' concentration varies significantly in the range of 0.00015 to 145 ppm, as recorded in Table 5.6. Iron (Fe) dominates the element that exceeds the average reading of 44.99 ppm, making a huge gap with the following element: the Chromium (Cr) with a 3.43 ppm average. Nickel (Ni), being the third most abundant element in the sediments, gives an average 1.53 ppm concentration while the Manganese (Mn) followed with 0.89 ppm. The other elements, such as vanadium (V), Copper (Cu), and Cobalt (Co), has an average reading of 0.12, 0.13, and 0.05 ppm, respectively. In the future, the results of this experiment will need to be validated with Sandstone and Shale Certified Reference Materials (CRM) to ensure the precision of the measurements.

The trace element ratio is listed in Table 5.7 below. The ratio includes Vanadium (V) to Chromium (Cr) ratio, Vanadium (V) to Nickel (Ni) ratio, Cobalt (Co) to Nickel (Ni) ratio, and lastly, Vanadium over Vanadium plus Nickel ratio (V/(V+Ni)). V/Ni and Co/Ni ratio strongly influenced the organic matter input origin in the sediments (Lewan 1984; Barwise 1990; Udo et al. 1992; Akinluaet al. 2007), while V/Cr and V/(V+Ni) is widely used as an indicator of depositional condition and settings (McManus et al. 1999; Morford et al. 2001; Algeo and Maynard 2004; Harris et al. 2004; Akinlua et al. 2010; MacDonald et al. 2010; Fu et al. 2011). Many also implicated that the Vanadium to Nickel ratio gives reliable information on the paleoenvironment. The interpretation is further discussed in the discussion section.

Table 5.6: Results of trace elements concentration (ppm) and their average.

Sample ID	V	Cr	Mn	Fe	Co	Ni	Cu
B14-1	2.979	1.689	0.931	183.1	0.033	0.952	0.392
B20-1	11.9	15.93	256.1	6790	3.655	9.031	3.912
B21-3	3.464	1.714	0.996	346.1	0.034	0.766	0.994
B18-1	2.769	7.139	110.9	1393	1.429	3.345	2.667
B22-3	1.128	2.45	18.62	1662	1.336	3.539	3.382
B16-1	10.57	59.17	12.21	1863	1.977	29.20	5.556
B8-1	2.594	1.513	0.686	215.5	0.015	0.674	0.610
B13-1	28.85	9.341	217.9	10350	7.077	19.61	11.17
B15-1	25.39	523.7	64.21	7685	7.078	223.5	23.66
B22-1	34.9	2811	208.9	14500	25.98	1235	76.79
Average	12	343	89	4499	5	1530	13

Table 5.7: Ratio of trace elements concentration between Vanadium, Chromium, Nickle, and Cobalt.

Sample ID	Lithology	V/Cr	V/Ni	Ni/Co	Co/Ni	V/ (V+ ni)
B14-1	Sand	1.764	3.129	28.848	0.035	0.758
B20-1	Sand	0.747	1.318	2.4710	0.405	0.569
B21-3	Sand	2.021	4.522	22.529	0.044	0.819
B18-1	Sand	0.388	0.828	2.3410	0.427	0.453
B22-3	Sand	0.460	0.319	2.6490	0.378	0.242
B16-1	Sand	1.714	3.849	44.933	0.022	0.794
B8-1	Shale	3.089	1.471	2.7710	0.361	0.595
B13-1	Shale	0.048	0.114	31.577	0.032	0.102
B15-1	Shale	0.012	0.028	47.537	0.021	0.027
B22-1	Shale	0.179	0.362	14.770	0.068	0.266

5.8 Bulk Kinetic Energy

5.8.1 Activation energy distribution

The bulk kinetics method consists of the activation energy distribution and frequency factors analysis were conducted to represent six coaly samples, and the results were illustrated in Figure 5.18 and Table 5.8. The main objective in conducting this method is to

determine the petroleum capability and the capacity for hydrocarbon generation after maturing. Both the activation energy and the frequency factors will rise to different ranges depending on the type of organic matter assemblage inside the samples (Dieckmann, 2005). The majority of Bongaya formation samples exhibit broad range and high activation energy distributions, ranging from 36 to 73 kcal/mol with pre-exponential factors varying from 1.1352E+13/sec to 5.8663E+13/sec (Figure 5.18 and Table 5.8). The results indicate that the organic matter assemblage is a heterogeneous organic matter assemblage (Di Primio & Horsfield 2006; Hakimi, M. H et al. 2015). These samples of broad activation energy extending to 73 kcal/mol are having low HI (< 200 mg HC/ g TOC) were discussed to be derived from terrigenous organic matter and vitrinitic kerogen (Type III). However, one sample have relatively narrow activation energy distribution in a range of 42-60 kcal/mol is an indication of liptinitic kerogen with relatively high HI (>200 mg HC/ g TOC), which is interpreted to be Type II-III kerogen (Makeen et al., 2020).

5.8.2 Geological heating conditions

A linear geological heating rate of 3.3 °K/My is used as part of the derived kinetic properties to estimate the temperature and timing of bulk petroleum generation as this heating rate corresponds to the average heating rate in sedimentary basins (Schenk et al., 1997). Based on the described heating rate and the measured kinetic models (Figure 5.19), the coals of the Bongaya Formation reach petroleum generation window (TR 10%) at temperature ranges from the lower 88 °C to 125 °C while this formation will produce petroleum at its peak on temperature (geological Tmax) range from 104 °C to 146 °C (Table 5.9). In terms of the vitrinite reflectance, this Type II-III kerogen is predicted to enter the oil window at 0.47-0.72 %Ro and reach the peak on 0.58 – 0.92 %Ro (Table 5.10).

Table 5.8: Activation energy distributions (kcal/mol) for coaly Bongaya Formation source rock samples from Pitas, Sabah.

Samples /EA (kcal/mol)	37	38	39	40	41	42	43	44	45	46	47	48	49	50	51	52	53	54	55	56	57	58	59	60	61	62	63	64	65	66	67	68	69	70	71	72
BG001	-	-	-	-	-	0.2	-	0.2	0.2	0.2	0.5	0.3	1.2	4.4	9.1	13.8	18	18.5	8.8	5.5	3.6	3.5	1.6	3.2	-	2.6	1.4	-	-	3.2	-	-	-	-	-	-
G316	0.05	0.05	0.3	0.05	0.9	4.5	-	-	35	19.5	10	8.8	6.1	4.1	2	1.9	1	1.3	0.8	0.5	1.4	-	-	1.7	-	-	-	-	-	-	-	-	-	-	-	-
G323 (U)	-	-	-	0.2	-	0.2	0.2	-	-	1.4	5	5.6	7.5	7.4	8.4	8	7.25	6.3	4.5	6.3	1.8	7.4	-	5.7	4.85	-	-	12	-	-	-	-	-	-	-	-
G326	-	0.3	-	0.3	0.2	0.6		1.4	1.1	0.8	5.3	28.2	38.8	7.4	6.1	2.4	1.8	1	0.9	0.5	0.8	-	0.6	0.7	-	0.2	-	-	-	-	-	-	-	-	-	-
G237 (U)	-	-	-	-	-	-	-	-	-	-	-	-	1.4	0	0.6	2.75	4.45	6.85	7.4	8	7.8	7.4	6.8	6	4.4	4.6	1.8	6.45	-	5	2.2	0.75	6.8	0.55	-	-

Table 5.9: Results for Pre-Exponential factors of petroleum generation windows (TR 10~) for temperature ranges and vitrinite reflectance.

Sample ID	PreExponential Factors	TR 10%		Peak TR	
	A [1/S]	T (◦C)	Ro%	TR	T (◦C)
B1-4	5.866E+13	125	0.72	40	146
B4-1	2.888E+12	88	0.47	22	104
B7-3	2.160E+13	110	0.63	33.5	136
B12-2	1.135E+13	104	0.58	37.5	121
B9-2	2.947E+15	124	0.72	38.5	144
B11-1	1.938E+15	124	0.72	39	145

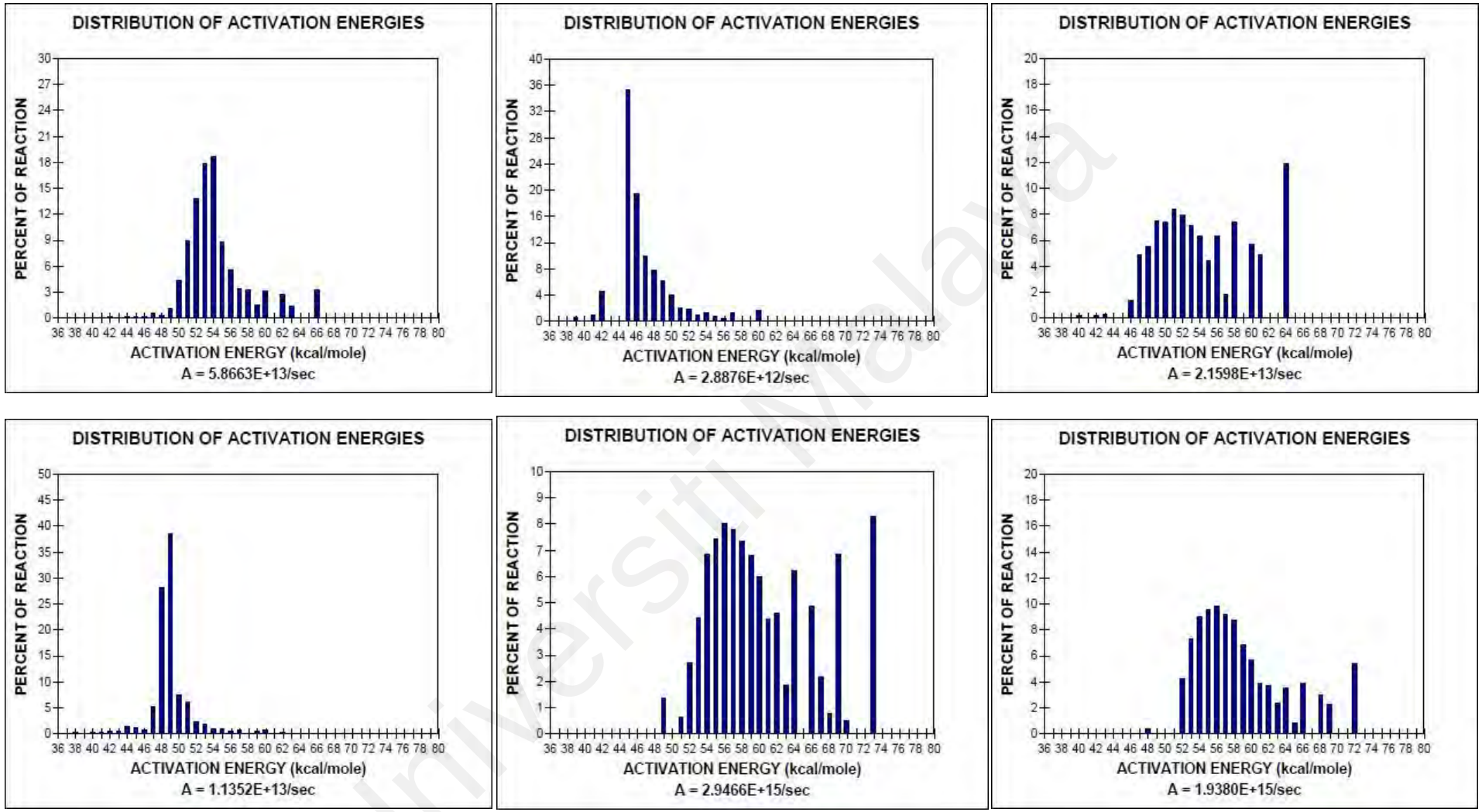

Figure 5.18: Activation energy distributions (kcal/mol) for coaly Bongaya Formation source rock samples from Pitas,

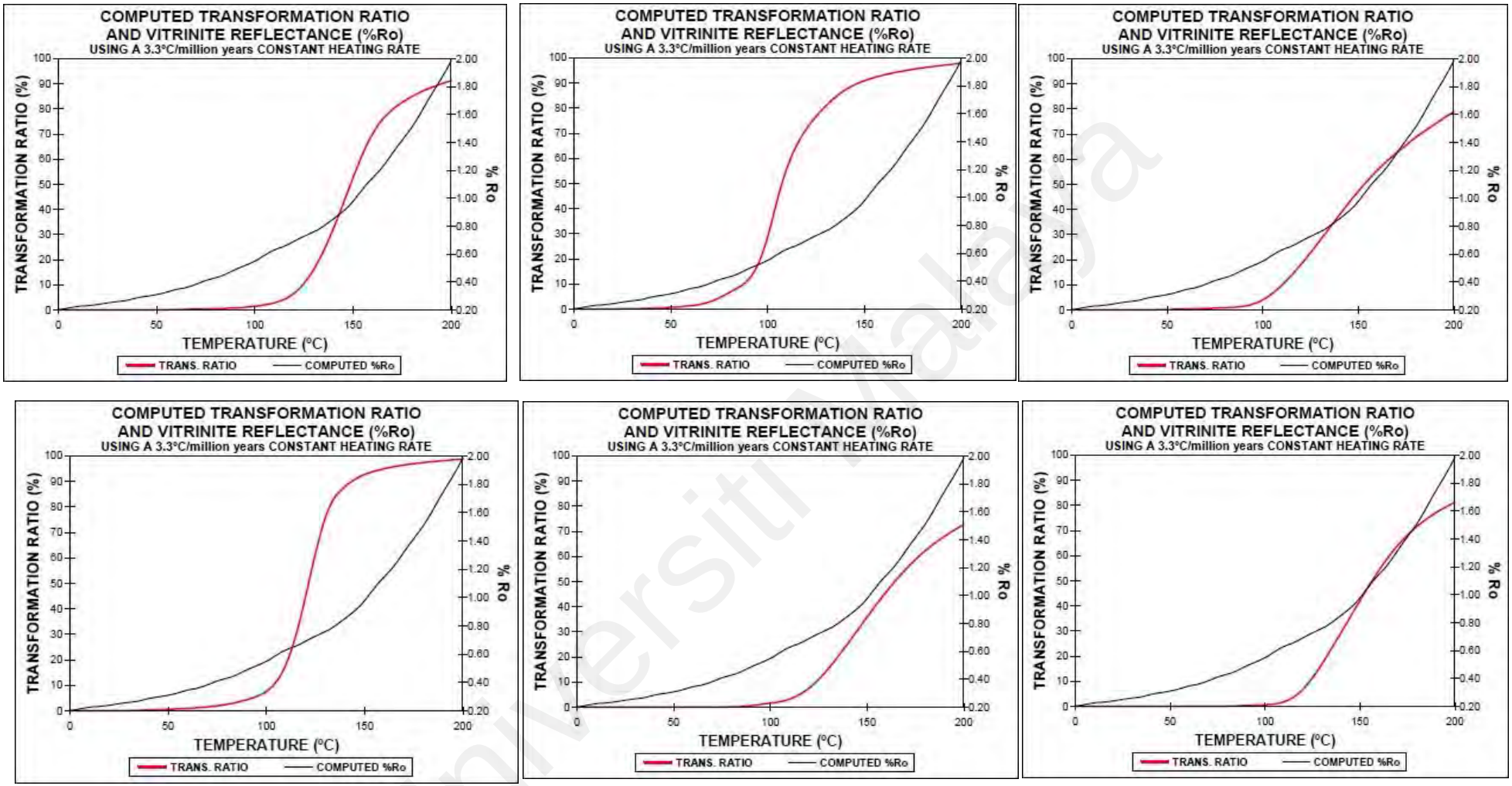

93

Figure 5.19: The results in terms of temperature versus transformation ratio curves for the organic facies of selected coal-bearing sediment from the Bongaya Formation, illustrating the onset (10% TR) and peak generation (Geol. Tmax) temperatures. 94

CHAPTER 6: DISCUSSION

6.1 Introduction

Chapter 6 discusses and interprets the relationship of all collected data (geochemical data, petrographical analysis results, palynology data, trace element data, and bulk kinetic data) to achieve optimal identification of the source rock characteristics and their potential contribution to the petroleum industry. Furthermore, organic matter preservation was considered by tracking the paleodepositional environment and its condition. More attention is being placed on evaluating coal, carbonaceous shale, and shale sediments in this Bongaya Formation sequences.

6.2 Source rock potential (organic richness).

The organic matter amount of each source rock is one of the most crucial factors for identifying a potential petroleum source rock. The previous researcher identified that the geochemical characteristics of total organic carbon (TOC) (as a percent weight) are used to calculate the organic richness of source rocks and their ability to produce petroleum during thermal maturity (Peters and Cassa 1994; Mustapha and Abdullah, 2013). 1 wt. % TOC content or above has completed the condition to be classified as a good potential source rock (Hunt, 1964), which gradually strengthens their ability to produce the hydrocarbon. As previously indicated, all Bongaya sediments, apart from mudstone, have a TOC value ranging from 0.9 to 63.1 wt.%, indicating sufficient organic matter. Coal consists of the highest TOC amount, followed by carbonaceous shale, coal laminated sandstone, and shale. Although TOC generally emphasizes the amount of organic matter, which are crucial generative factors, the petroleum yield results (pyrolysis S1 and S2) should also be complementary to it (e.g., Peters 1986; Peters and Cassa 1994; Dembicki 2009) when

referring to hydrocarbon production ability because they comprehend the hydrogen present in the rock. Selected samples in Figure 6.1a revealed that coal and carbonaceous shale has good to excellent generative potential while shale possessed only fair potential.

Furthermore, the bitumen extraction amount of chosen samples was consistent with high TOC content (Table 5.1), indicating considerable organic matter capable of producing petroleum at ideal thermal maturity levels. A cross-plotted figure that linked both TOC and bitumen extraction concentration to determine the petroleum potential shows coal and carbonaceous shale have higher productive potential than shale sediments. (Figure 6.1b).

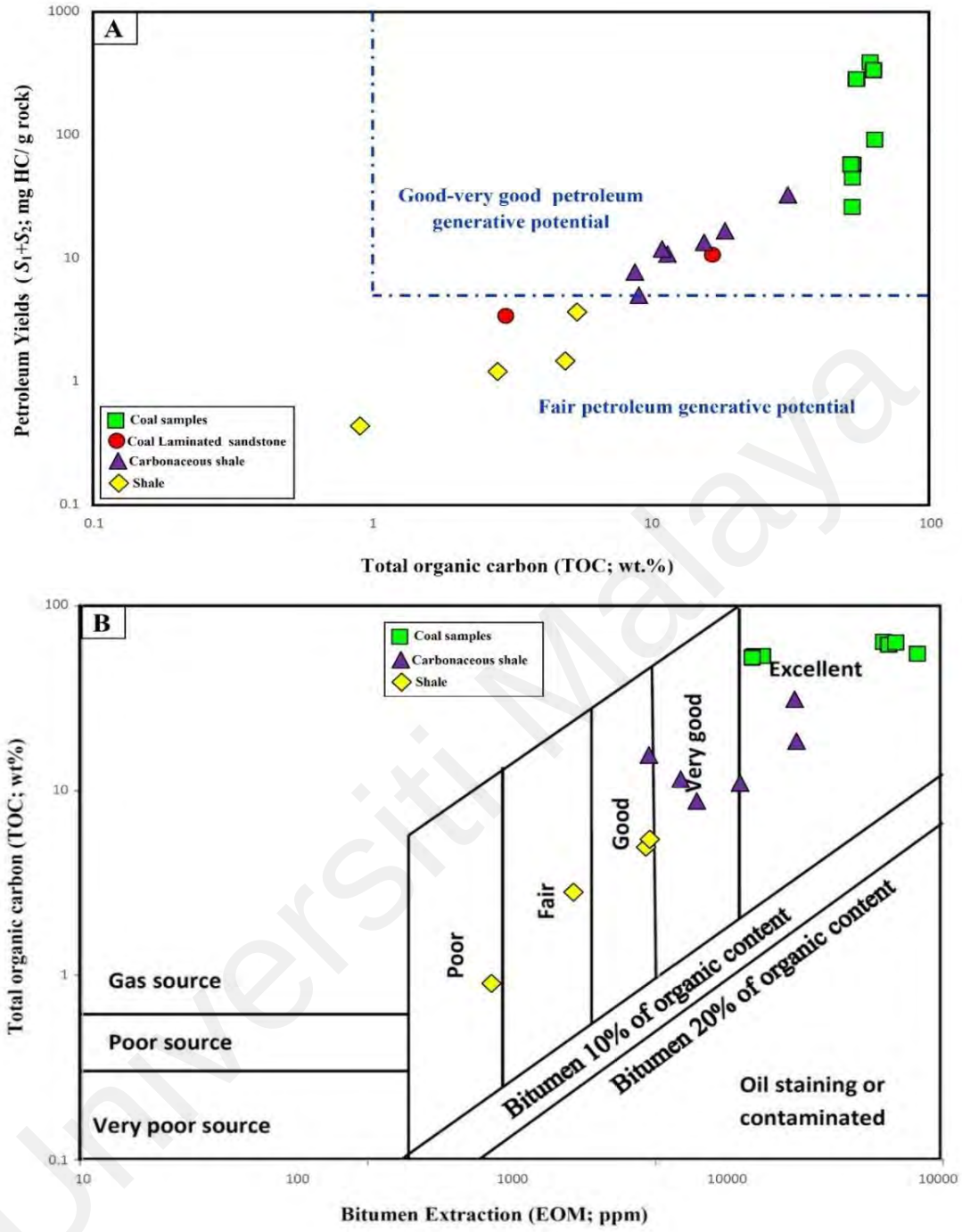

Figure 6.1: Plot between (a) petroleum yields (S_1 + S_2) versus total organic carbon (TOC) and (b) total organic carbon (TOC) versus bitumen extraction to indicate the hydrocarbon productive potential of each sample.

6.3 Type of organic matter- kerogen quality

Each kerogen type contains respective precursors that control hydrocarbon products, either oil or gas. Thus, the best source rock can be quantified throughout the research. In this study, central identification was made on geochemistry results, notably HI (Espitalie et al., 1985; Peters and Cassa, 1994; Hunt, 1996; Tissot and Welte, 1984; Mukhopadhyay et al., 1995), correlated with quantitative and qualitative pyrolysis results to improved prediction. Later, the results were interrelated with petrographic analysis.

As known, high HI value exceeds 500 mg HC/g TOC and is more considered as Type I or Type II oil-prone, whereas HI value below 300 mg HC/g TOC suggests a contribution of gas-prone source rock characterized to be Type III kerogen. However, Type IV kerogen did not possess any hydrocarbon production potential characterized to have HI value less than 50 mg HC/g TOC (Peter and Cassa, 1994). Referred to Table 5.3, the highest HI is from the coals (>500 mg HC/g 317 TOC); expected to be oil-prone source rock, by others lithology HI value did not even exceed 200 mg HC/g TOC; gas production samples.

Bongaya Formation sediments are dominated by HI values less than 200 mg HC/g TOC whereas three coal samples have high HI at least more than 500 mg HC/g TOC (510-630 mg HC/g TOC). A plot of HI value against T_{max} (Van Kravel Diagram) helps to determine each sample kerogen type (Figure 6.2a), where most samples are plotted in Type III kerogen except three coals (in Type II), suggesting oil-prone source rocks. Corroborate qualitative data by a diagram of pyrolysis S2, and TOC amounts (Mukhopadhyay et al., 1995) shows the dominance of Type III kerogen with low Type II kerogen contributions preferably explain an incorporated mixed organic matter (Figure 6.2b) that have dominant terrestrial organic matter contributions.

Nevertheless, quantitative pyrolysis (Py-GC) data were also correlated in this study as this analysis was referred to bring more accurate assessment in determining kerogen type (Horsfield, 1989; Abbassi et al., 2016). A ternary plot modified from Eglinton et al. (1990) was used to interpret the kerogen characteristics (Figure 6.3). This plot compared three main components of the pyrolysate, 2,3-diamethyldiophene, ortho-xylene, and carbon 9 percentages to identify the kerogen type (Keym et al. 2006). The plotted samples mostly fall on Type III kerogen, with some samples on border Type II and Type III, suggesting a mixed Type II/III kerogen (Figure 6.3). Supported by qualitative analysis of Py-GC chromatograms, most of the samples observed to have an abundance of aromatic peaks infraction less than carbon 10 (<C10) as stated by Dembicki (2009), it is an identification for Type III gas-prone source rock (Figure 5.14). However, the Py-GC data show less substantial n-alkene/alkane doublets beyond C30, indicating little oil potential generation (Hakimi,2018). The 'type index' value (Figure 5.13) from chapter 5 has indicated that the majority of the samples investigated have Type III kerogen characteristics (greater than 1.3) and that some samples are mixed Type II/III (0.8 to 1.3 value).

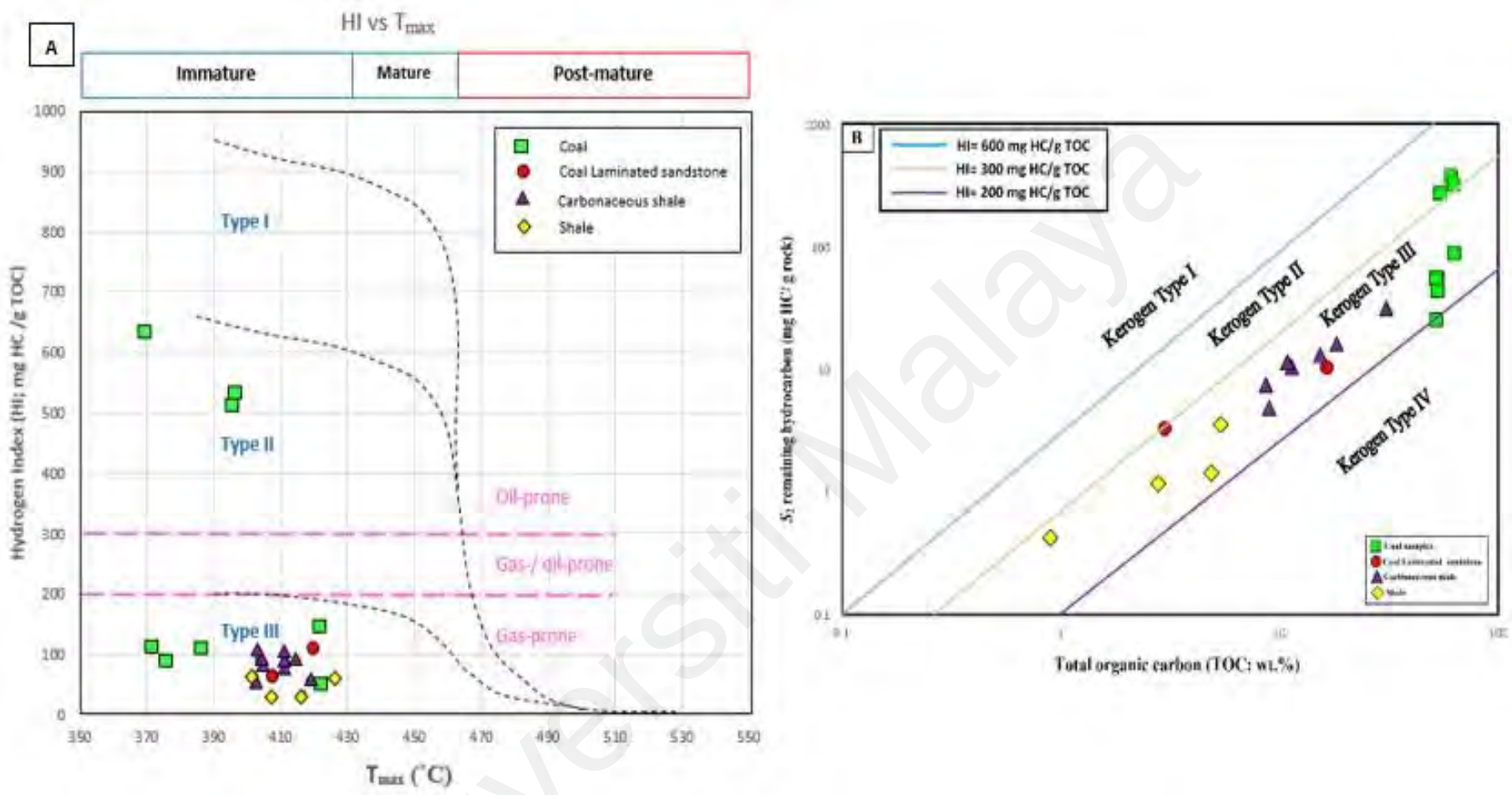

Figure 6.2: (a) Hydrogen Index versus T_{max} plot of the samples clearly shows each of their kerogen type along with their maturity stage (after Peter & Cassa, 1994) supported with (b) modified plot from Hakimi et al., (2020); S_2 remaining hydrocarbon versus total organic carbon (TOC).

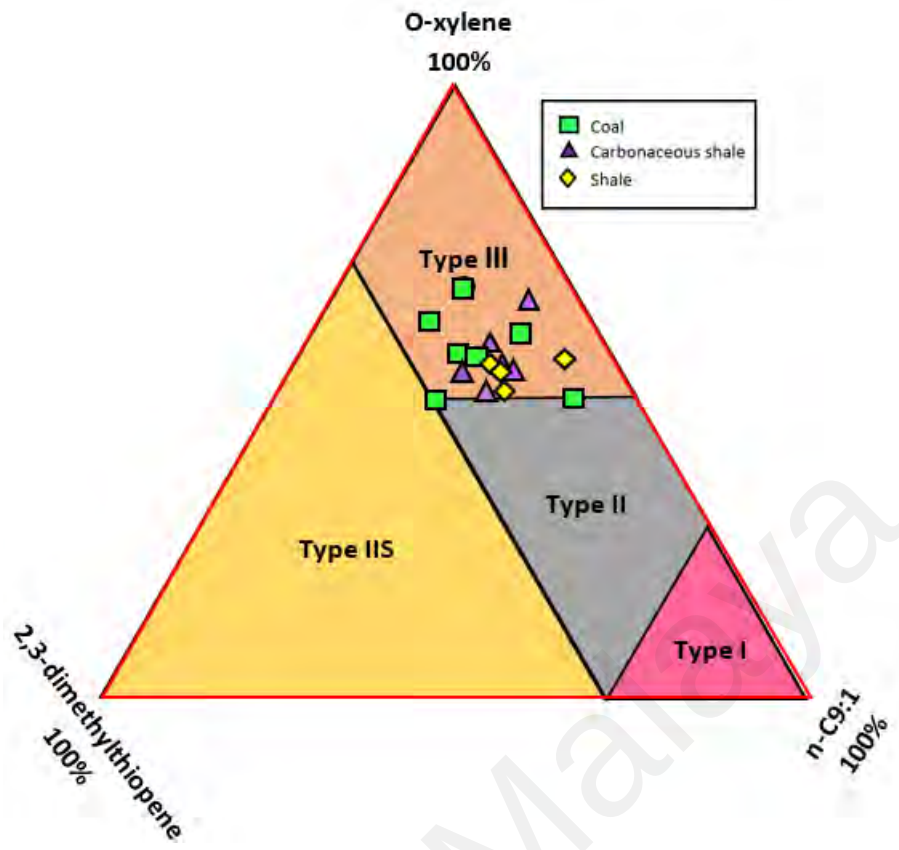

Figure 6.3: Ternary diagram of 2,3-diamethyldiophene, ortho-xylene, and carbon 9 (nC9:1), modified after Eglinton et al. (1990).

The petrographic analysis has been used to calculate the relative amounts of vitrinite, liptinite, and inertinite macerals, and it is a reliable method for determining kerogen properties (Cornford, 1979; Hakimi et al., 2020). The maceral study demonstrated that vitrinite dominates the samples, followed by liptinite and mineral material, with minimal inertinite occurrence. Table 5.4 summarizes the percentages, and the results were plotted in the ternary diagram used by Cornford (1979) to characterize the organic facies, as shown in Figure 6.4. Most Bongaya sediments exhibit high huminite plants that represent Type III kerogen. Type II/III kerogen is presumably present in the coals, notably prominent with both liptinite and vitrinite (Figures 5.15 and 5.16). The saturation of liptinitic resinite maceral would determine the formation of high waxy oil from these samples.

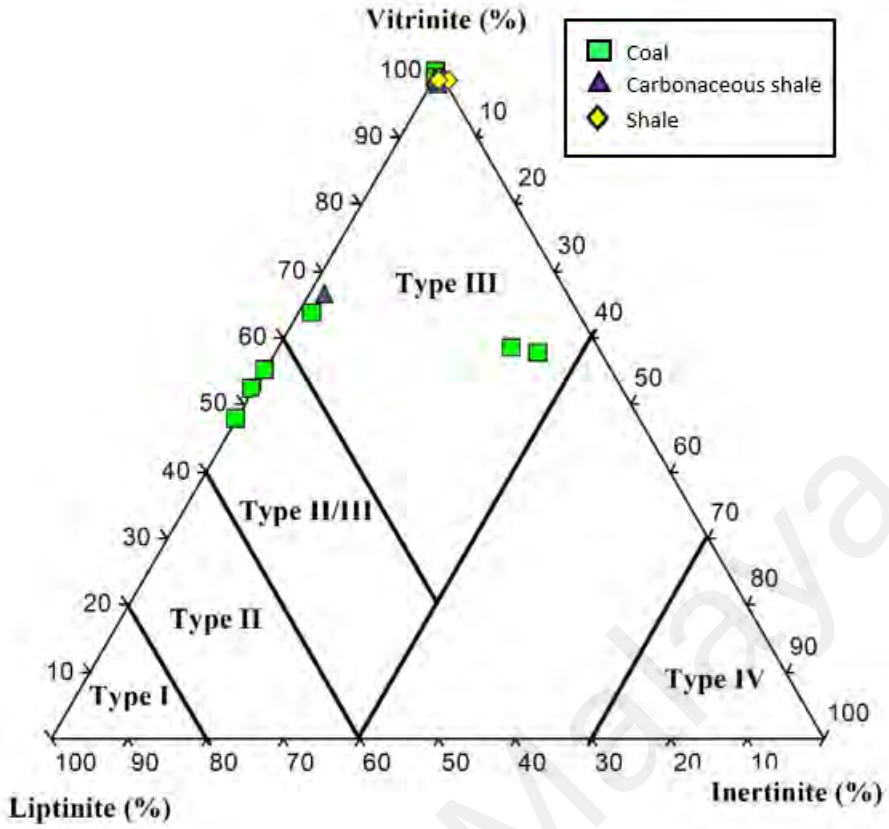

Figure 6.4: Ternary diagram representing liptinite, inertinite, and vitrinite/huminite percentage, after Cornford (1979) to identify kerogen type.

6.4 Thermal maturity

This study's thermal maturity assessment correlates with three leading indicators, including huminite reflectance, pyrolysis T_{max} data, and PI value. Table 5.3 recorded that all samples from Bongaya Formation possessed a T_{max} value between 369.6 to 437.3 °C. Tmax value that increases through maturity has proved to be a reliable evaluation method and was widely used in petroleum industry study (Peters, 1986; Tissot and Welte, 1984; Tissot et al., 1987; Bordenave, 1993). Based on Peter and Cassa's (1994) study, the T_{max} value below 435 °C is considered immature, as most of the Bongaya Formation samples were interpreted to be. These measures are equivalent to huminite reflectance (wt%) of the samples (coals, carbonaceous shale, and a shale) as they all ranged in between 0.32 to 0.43 R_o (Table 5.4); as suggested by Tissot and Welte (1984) also as immature samples

(<0.5 R_o). As illustrated in Figure 6.5a, a link between Tmax value and huminite reflectance was explored. Nonetheless, Production Index (PI) values below 0.10 are discussed and shown correlation to Tmax (Figure 6.5b), demonstrating a similar result between T_{max} and huminite reflectance, signifying that Bongaya organic matter is immature.

Aside from the parameters mentioned above, the carbon preference index (CPI) value was identified to deliver maturation information effectively. The CPI value of selected samples was found to be in the range of 2.5 to 5.2 (Table 5.2) with the prevalence of odd carbon number over even number, suggesting immature source rock level (>1.1) (Peters and Moldowan 1993). M/z 85 chromatogram also provides us with ratios of isoprenoids to n-alkanes where they were intensely used for maturation and biodegradation and source input (Ficken et al., 2002; Roushdy et al.,2010; Hunt, 1995). Figure 6.9 shows maturity level with relation to the biodegradation level as the Pr/n-C17 and Ph/n-C18 ratio decrease to maturation. The thermal cracking process results in n-alkanes production and eliminates Pr and Ph compounds (Tissot et al., 1971).

Furthermore, the concentration of EOM fractions can be used to estimate the level of thermal maturity. Immature source rock is known for having high Nitrogen, Sulphur, and Oxygen (NSO) levels, followed by aromatics, and finally saturates. As shown in Table 5.1, these characteristics were displayed by Bongaya Formation extraction samples.

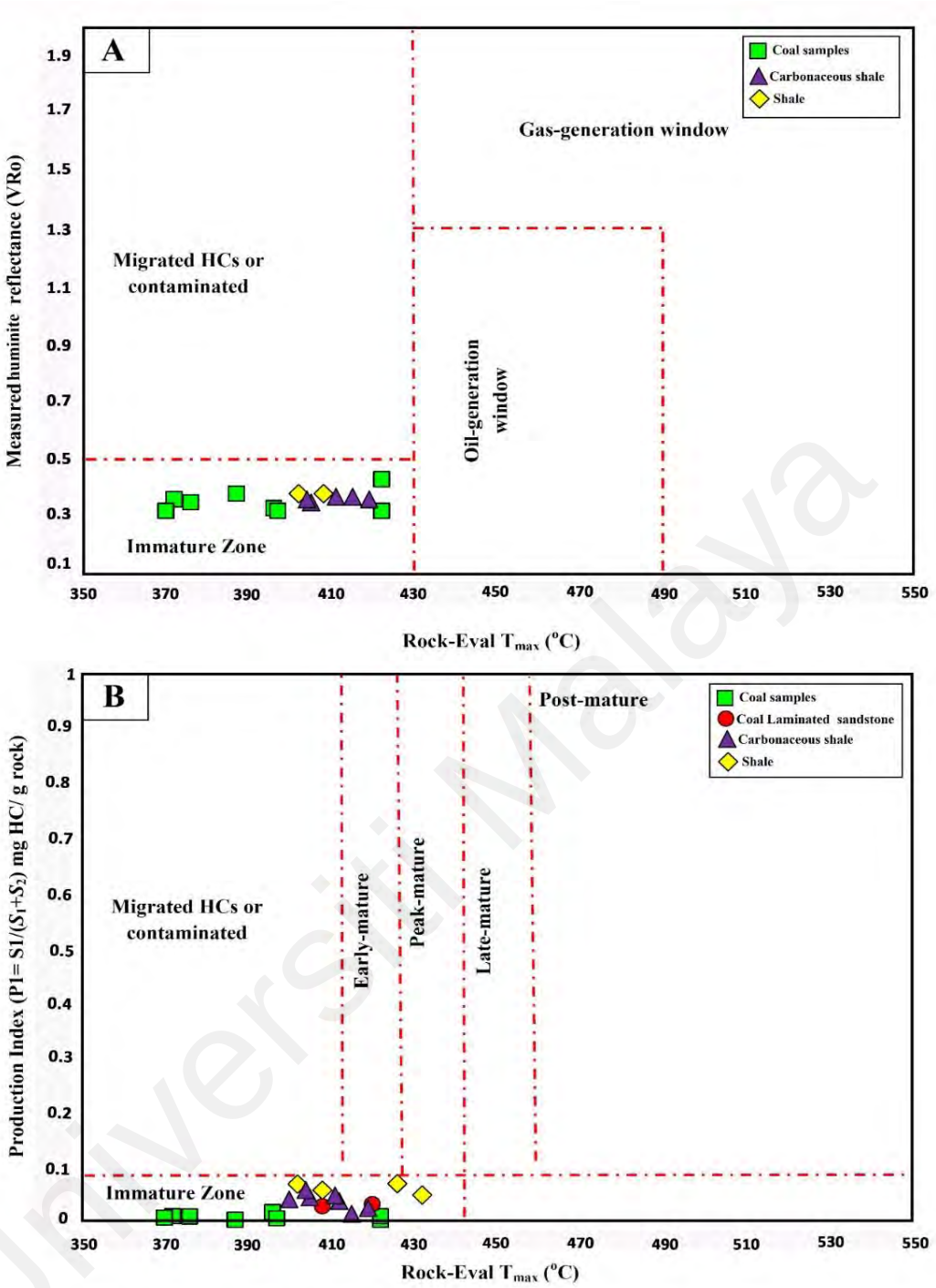

Figure 6.5: Plot between (a) petroleum yields (S1 + S2) versus total organic carbon (TOC) and (b) total organic carbon (TOC) versus bitumen extraction to indicate the hydrocarbon productive potential of each sample.

6.5 Organic matter input

The organic input of the Bongaya Formation was investigated based on molecular composition (n-alkanes, hopane, terpenes, and phenanthrenes) and element data interpretation.

The molecular composition of most samples shown high concentration on higher molecular weight alkanes (>C20) with odd predominance indicates originality from a terrigenous plant (Kolattudy, 1970; Powell and McKirdy, 1973; Tissot et al., 1977; Tulloch, 1976). In contrast, low molecular weight abundant distribution (<C20) with slight odd-predominance construed as a marine origin (Gelpi et al., 1970; Weete, 1976; Tissot and Welte, 1984; Peters and Moldowan,1993). According to the findings, the Bongaya Formation is a terrigenous organic source of origin. However, a sample (B7-3) may have been influenced by marine organic sources, most likely algal/bacterial, because the n-alkane peak was shown to be high in low molecular weight. Furthermore, the results are corroborated by CPI values greater than 1 (Table 5.2) associated with non-marine origin (Moldowan et., 1985; Palacas et al., 1984).

Further analysis based on molecular composition was used, namely the C29/C30 ratio and the relative proportions of C24 and C23. The ratios between C29 and C30 range from 0.07 to 0.37 (Table 5.2), reflecting that the organic matter from terrestrial source since the output is less than 1 (Fan et al., 1987 and Peters & Moldowan 1993). C24 tricyclic terpenes have a higher proportion than C23 tricyclic terpenes, which likewise have the same interpretation, indicating the samples are derived from terrestrial origin. Tricyclic terpenes are believed to develop markers in differentiating the various type of organic matter and depositional environment (Seifert and Moldowan, 1979; Walples and Machihara, 1991; Andrew et al., 2001; Peters et al., 2005).

Isomers 5a (H) and 5b (H), 14a (H), and 14b (H) of the saturated fraction distribution's ion 217 can be employed as organic inputs and maturity markers (Mackenzie and McKenzie, 1983). The semi-quantitative measurement of the proportions of C27:C28:C29 regular steranes, as in this work, often reflects the type of organic matter and its maturity (Moldowan et al., 1985; Philp et al., 1991). Terrestrial source input is distinguished through the abundance of C29 over C27, while marine organic input was reflected from the abundance of C27 over C29 isomers (Lijmbach, 1975; Huang and Meinschein, 1979; Palacas et al., 1984; Gonzalez-Vila, 1995; Hunt, 1995; Peters et al., 2005). Table 5.2 shows the corresponding percentages of the C27:C28:C29 isomers, and it was discovered that C29 steranes dominated over C27 in most samples suggested organic matter input has been derived from terrestrial plants (Figure 6.6).

According to Ficken et al. (2000), phenanthrenes can also be used as a source input indication. The aquatic macrophyte n-alkane proxy (Paq) was developed, with a value of 0.1 indicating pure terrestrial organic matter, 0.1-0.4 indicating emergent plant origin, and 0.4-1 indicating submerged plant origin. The interpretation was illustrated in the plot of 9MP/PMP+1MP ratios against Paq (Figure 6.7), which showed that most of the sample's source was terrestrial, with other source rocks having a marine inclusion.

Trace elements, particularly V, Ni, and Co, have proven to be reliable indicators in determining the organic matter origin based on their concentration (Lewan 1984; Barwise 1990; Udo et al. 1992; Akinlua et al. 2007). The previous study has commonly used trace element relative abundance and compared geochemical ratios like Ni/Co, Co/Ni, and V/Ni in source rock or oil studies. The Co/Ni ratios for shale and sandy samples from the Bongaya Formation ranged from 0.02 to 0.42 (Table 5.7). The majority of the samples revealed a considerable influence of terrestrial organic matter due to low Co/Ni ratios (less than 0.1), but four out of ten samples (B20-1, B18-1, B22-3, and B8-1) showed otherwise. They exhibit Co/Ni ratios higher than 0.1 where marine source input is

suggested (Udo et al. 1992). A relative abundance of Vanadium to Nickel also helps highlight diverse environmental circumstances. High nickel concentrations than Vanadium enhances terrestrial plants' effect in the samples (Lewan 1984; Barwise 1990). The V/Ni ratio was further categorized, with values larger than 3 indicating marine organic matter origin and less than 1.9 indicating terrestrial organic matter input (Galarrage et al. 2008). The ratio of V/Ni varied from 0.02 to 0.52, implying samples dominated by terrestrial organic matter with marine organic input for three sandy sediments.

A comparison of the ratios Ni/Co and V/Ni was used to undertake further research. The plot of the two ratios (Figure 6.8) revealed that Bongaya Formation is composed principally of terrestrial organic materials, with three of them indicating marine inclusion. The marine inclusion may be due to the transgression process in the environment that transport aquatic plant during the diagenetic process. It is worth noting that sandy sediments are not included in the source rock categorization because the goal here is to look at the overall organic matter input from the Bongaya Formation. The Bongaya Formation has high terrestrial organic inputs, yet there is no denying that it also has minor marine organic matter source influences.

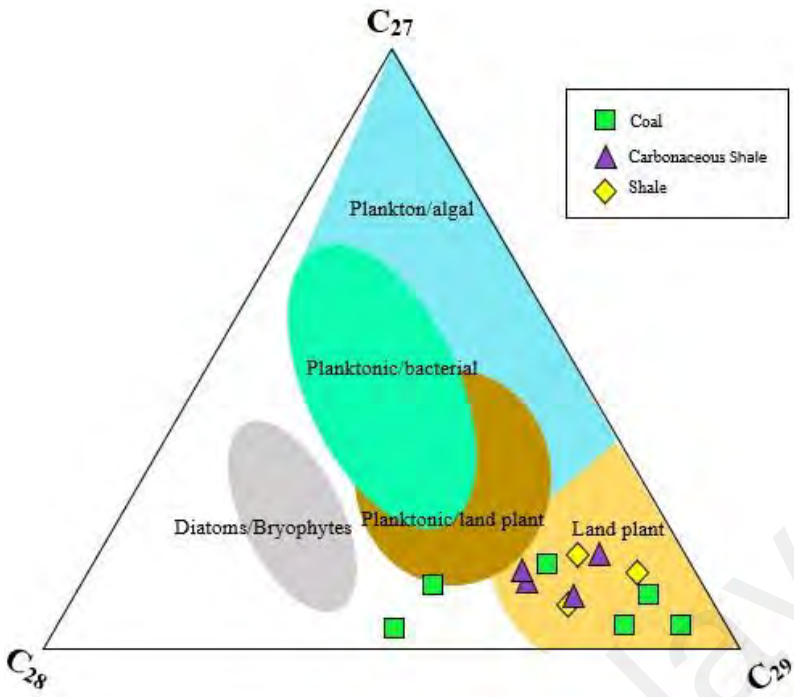

Figure 6.6: Ternary plot showing relative percentages of C29, C28, and C27 composition of ion m/z 217 chromatogram indicate studied samples derived from land plants.

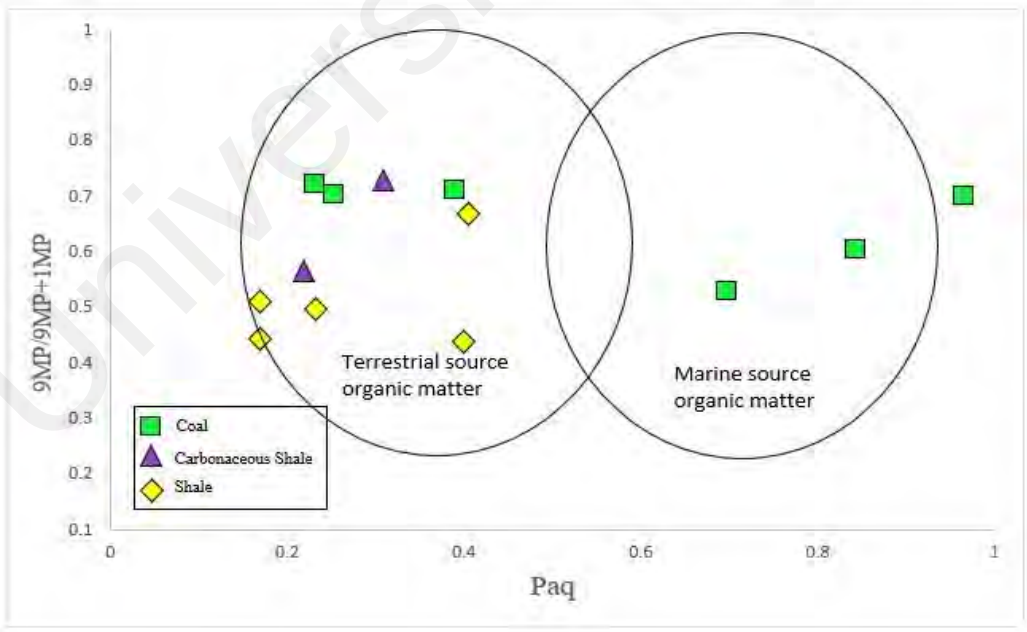

Figure 6.7: A modified plot by Ficken et al. (2000) correlated both Paq and 9MP/9MP+1MP ratio to identify source rocks' organic matter input.

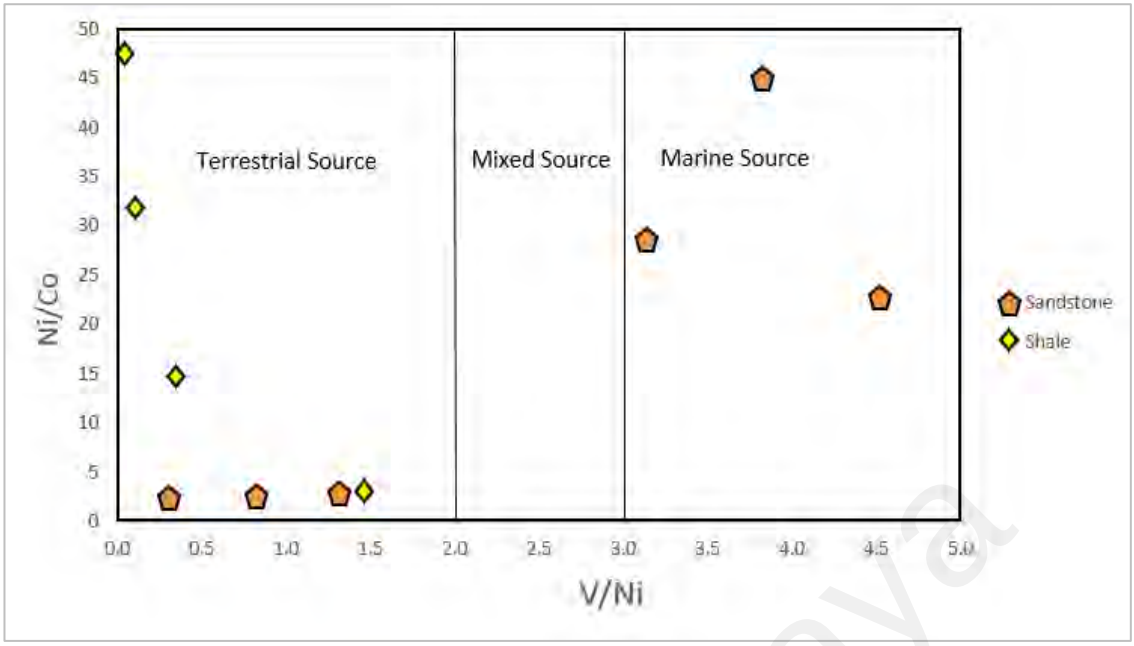

Figure 6.8: Plot Ni/Co versus V/Ni shows the classification of samples of different organic matter input from terrestrial and marine sources (modified after Jones and Manning,1994).

6.6 Depositional environment of the organic matter

As the organic matter influences are deduced previously, their depositional environment and condition reconstruction were also explored using various techniques, including petrographic analysis (palynology data), molecular composition, and element data interpretation (Pr/Ph & M/z 217).

The most essential and functional isoprenoid compounds, Pristane (Pr) and Phytane (Ph), are a worthy indicator for both depositional environment and source organic matter evaluation due to their well-known resistance to the diagenesis process. The Pr/Ph ratio above 3.0 indicates oxidizing conditions originating from the terrestrial environment, whereas the low ratio, below 0.8, indicates anoxic conditions originating from algae/bacteria. The suboxic state is an intermediate state with values ranging from 0.8 to 3.0. (Ten Haven et al., 1987; Amane and Hideki, 1997; Sarmiento and Rangel, 2004;

Basent et al., 2005). The calculated Pr/Ph values range from 0.33 to 2.55 (Table 5.2), reflecting that most source rock samples were deposited in a suboxic environment, while others did so in an anoxic environment. The ratios of Pristane/n-C17 and Phytane/nC18 (Figure 6.9) were purposefully employed as oil-source rock correlations to the extent of generation and maturity, confirming that the source rocks were deposited primarily in a transitional environment, with two of coals were found deposited in a reducing environment suggesting sea level inundation had influenced the depositional condition where anoxic conditions are promoted during high tides (Mustapha et al., 2017). All the samples have varying degrees of biodegradation and maturation (Figure 6.9).

Aside from profounding used as an organic matter origin indicator, the trace elements were also a reliable tool in detecting the depositional environment and the paleoredox condition based on their concentration variables (Lewan 1984; Barwise 1990; Akinlua et al. 2007, 2010). In this study, each trace element is analyzed due to its different behavior towards the sediment's geochemistry in different settings and depositional conditions. Iron was exceptionally high compared with other trace elements with an average of 44.99 ppm as it varies in ranges of 1.83 to 145 ppm (Table 5.7). The rich iron was due to high Fe oxyhydroxides input in organic matter as there are high terrestrial influences where they were well preserved under changing oxic and suboxic conditions (Byrne and Kester 1976; Froelich et al. 1979; Burdige 1993; Liu and Millero 2003). Generally, Copper concentration is low with an average of 0.13 ppm of all samples, which also suggests oxic-suboxic conditions as these elements were sensitively rich in redox conditions (Tribovillard et al. 2006). The interpretations are complementary to previous analysis by molecular compound where most of the samples were deposited in the suboxic settings with high terrestrial input.

A widely trace elements that are very useful in determining the depositional setting was the Vanadium and Nickel. For the majority of the examined samples, the relative fraction of high Nickel over Vanadium implies an oxic environment. A Vanadium and

Nickel plot shows that the majority of the samples were found in the marine terrestrial oxic-dyoxic environment (Figure 6.10), supporting the mixed condition environment with the significant oxidizing conditions. As mentioned by Adegoke et al., 2014, both V/Ni and V/(V+Ni) high and low ratios were frequently used to indicate reducing and suboxic environments. A high V/Ni ratio (>3) implicates a reducing condition, wherein in this study, there are only three samples (B14-1, B21-3, B16-1). The other samples significantly promoted the oxic condition environment. A ratio V/(V+Ni) plays a vital role in determining the deposition condition. The high value represents an anoxic condition (0.54-0.82), whereas a low value indicates oxic to dyoxic condition (<0.6) (Lewan 1984; Moldowan et al. 1985; Barwise 1990; Dai et al., 2020). The selected samples result in a V/(V+Ni) ratio ranging from 0.03 to 0.82 (Table 5.8), showing oxic and reducing influences on the samples with dominance on oxic-dyoxic settings. The concentration of Mn elements also depletes in sediments deposited in reducing conditions while rising in oxic-suboxic environments (Froelich et al. 1979; Lovley 1991; Burdige 1993; Morford and Emerson 1999), supporting the primary redox condition analysis. Generally, the Bongaya samples were interpreted to experience alternating oxic-anoxic paleodepositional conditions due to sea-level rise and low effect (Mustapha et al., 2017), as discussed earlier.

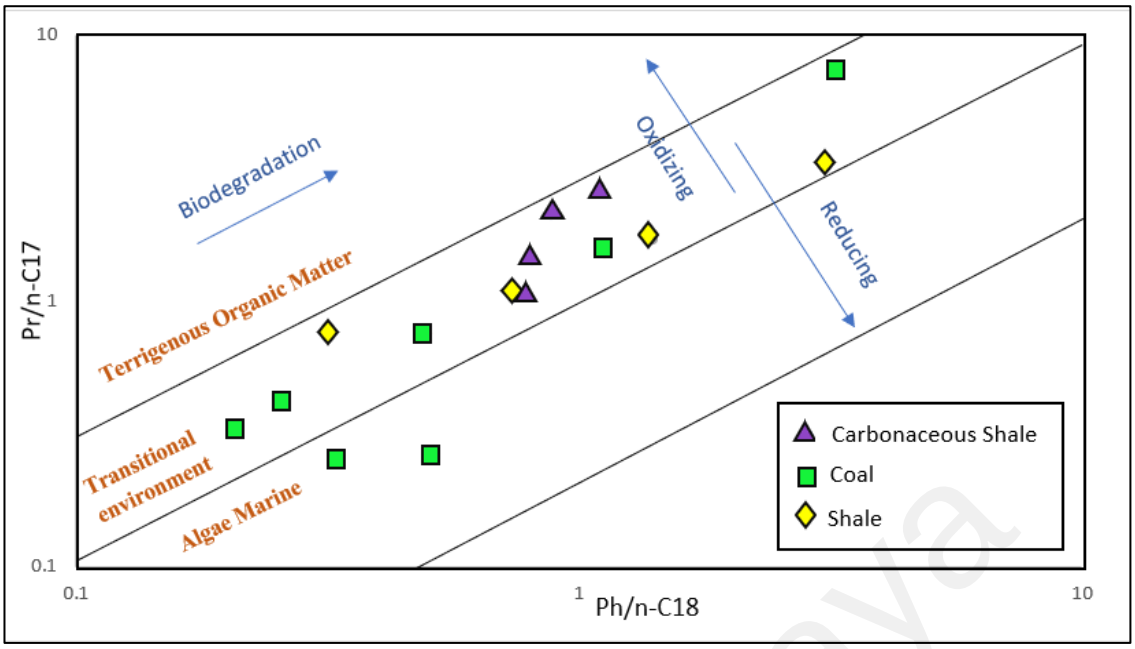

Figure 6.9: Plot between Pr/n-C17 and Ph/n-C18 indicates that most studied samples are preserved under a transitional environment, with two of them under reducing conditions.

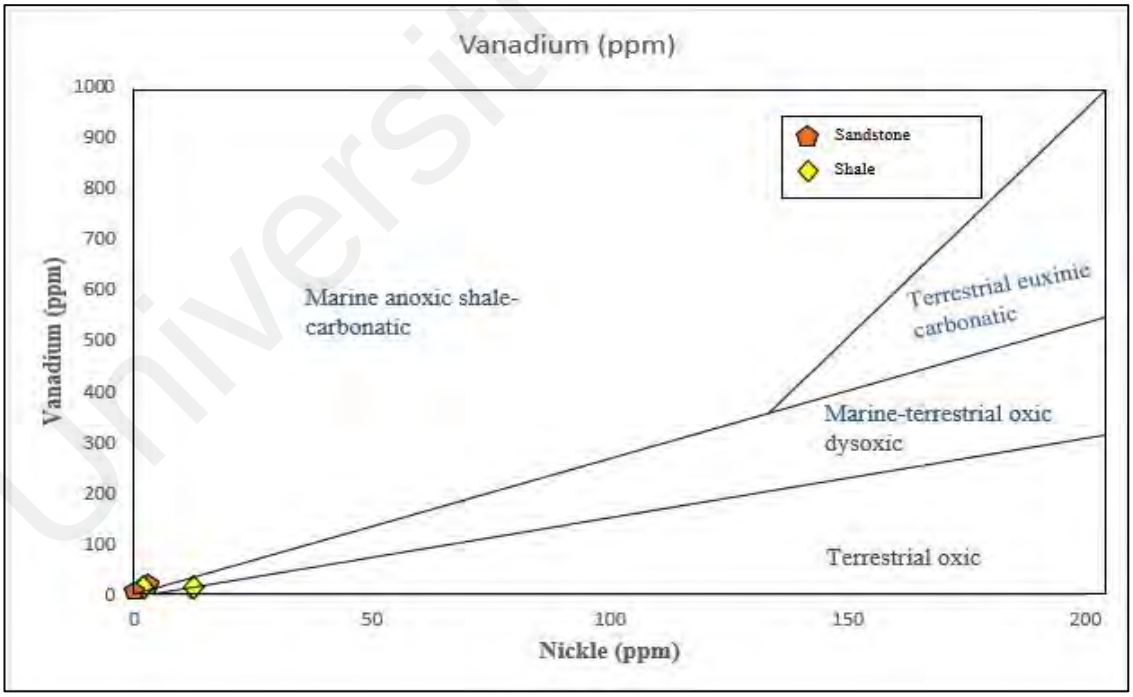

Figure 6.10: Plots of Vanadium against Nickel (modified after Akinlua et al. 2013).

The deposition environment and their condition interpretation were further verified by palynology analysis of Bongaya Formation carbonaceous shale and shale samples. It is

identified that three significant zones represented Bongaya Formation, i.e., (i) mangrove and (ii) back mangrove, and (iii) inland vegetation. This analysis result is greatly influenced by the high occurrence of Rhizophora type pollen and their well-preserved condition, suggesting the area was colonized by mangrove plants since the Early Miocene. Other associate mangrove species are also found such as Avicenna. A mangrove area is defined as an intertidal wetland ecosystem that implies an oxic/reducing condition, and at the same time undergoes high primary productivity, and is rich with organic carbon (Ping et al., 2012). Mustapha et al., (2017) discussed that the back mangrove zone consisted of Nypa and Brownlowia type pollen. The *Nypa* mangrove palm grows within tidal mudflats as back mangrove vegetation (Morley, 2000) and is tolerant to saltwater mangrove environment (Germeraad et al., 1968; Frederiksen 1985). Muller (1968) named the genus *Discoidites* after its discoid and colpate pollen, which are similar to those seen in the current genus *Brownlowia (Tiliaceae*). *Discoidites borneensis* is commonly used to explain the brackish environment in Southeast Asia's Tertiary depositional setting (Morley, 1991). Furthermore, a sedimentology logging study reveals that in the Bongaya Formation most coals and carbonaceous shale or shale were formed primarily in mangroves to the shallow sea environment and some were also found to be influenced by swamp area. This has confirmed the source rock's past deposition environment.

6.7 Petroleum Generating potential and Hydrocarbon prospectivity

The basic parameters of source rock characteristics, particularly the richness and type of organic content, as well as their maturation by geological temperatures, apply to determining the capacity of petroleum resources, whether oil or gas (Dow, 1977; Peters and Cassa, 1994; Hunt, 1996; Ardakania et al., 2017; Abdullah et al., 2017). A combination of these findings, generally from samples' bulk analysis, S2 pyrolysis, and heterogenous organic-rich characteristics, with bulk kinetic analysis generated further

information regarding the petroleum generating potential of Bongaya Formation source rock.

As noted, the Bongaya Formation was dominated by Type III kerogen, with minor contributions from Type II kerogen. Both geochemical findings and Py-GC quantitative analysis of S2 pyrolysate revealed that most studied samples contained gas-prone organic matter of Type III kerogen. In contrast, mixed organic matter of Type II and III kerogen suggested that both little oil and predominantly gas hydrocarbon were expected to be produced. The presence of numerous aromatic peaks seen between the alkanes and significant n-alkanes/alkenes doublets ranging up to C30 gives credence to the hypothesis. The quantitative Py-GC n-Octane (C8) and xylene ratio, as well as the 'Type index' (xy/C8), were employed to determine the kerogen type and its productive potential (Adegoke et al., 2015). The tested samples have a range of 0.2-1.3 (C8/xy) and 0.8-6.5 (xy/C8), consistent with the significant gas resource by Type III kerogen and oil and gas with mostly gas generation by a mixture of Type II and III kerogen.

The proportion of macerals visible under the microscope also contributes to the findings by bolstering the interpretation. It has been discovered that some coal samples contain some liptinite macerals, which are prone to delivering little oil. The oil constituents might have derived from the aliphatic cutinite and resinite found in these samples. Because of the abundance of resinite presence, significant amounts of high waxy oil should be considered (Horsfield et al., 1988).

Selected samples of a crossed plot between TOC vs. hydrogen index (mg HC / g TOC) demonstrate the petroleum potential of the Bongaya Formation (Figure 6.11). Coal possessed excellent TOC, has a good potential compared to others. Three of them are plotted in oil-present source rock, whereas the rest solely is shown to be good gas sources of this Miocene formation. On the other hand, shale and a coaly sandstone showed little potential to generate hydrocarbon due to the low total carbon present.

Currently, the maturity levels of the Bongaya Formation have demonstrated a lack of thermal energy, indicating that they have not yet attained a sufficient maturity level to generate oil or gas. The investigated samples revealed that all sediments were in the immature source rock stage of the oil-generation window. A bulk kinetic study of the plotted peak production temperature value versus the transformation ratios revealed that coal sediments had achieved at least a ~40% transformation ratio. Because of the difference in adsorption capabilities, the expulsion of hydrocarbons from terrigenous source rocks is expected to occur at a high transformation ratio of 60%, which is higher than that of marine source rocks (Pepper and Corvi, 1995; Hakimi and Abdullah, 2013). As a result, it is expected that the Bongaya Formation is able to generate and expel oil at temperatures ranging from 88°C to 146°C and with a Ro of 0.47-0.92%.

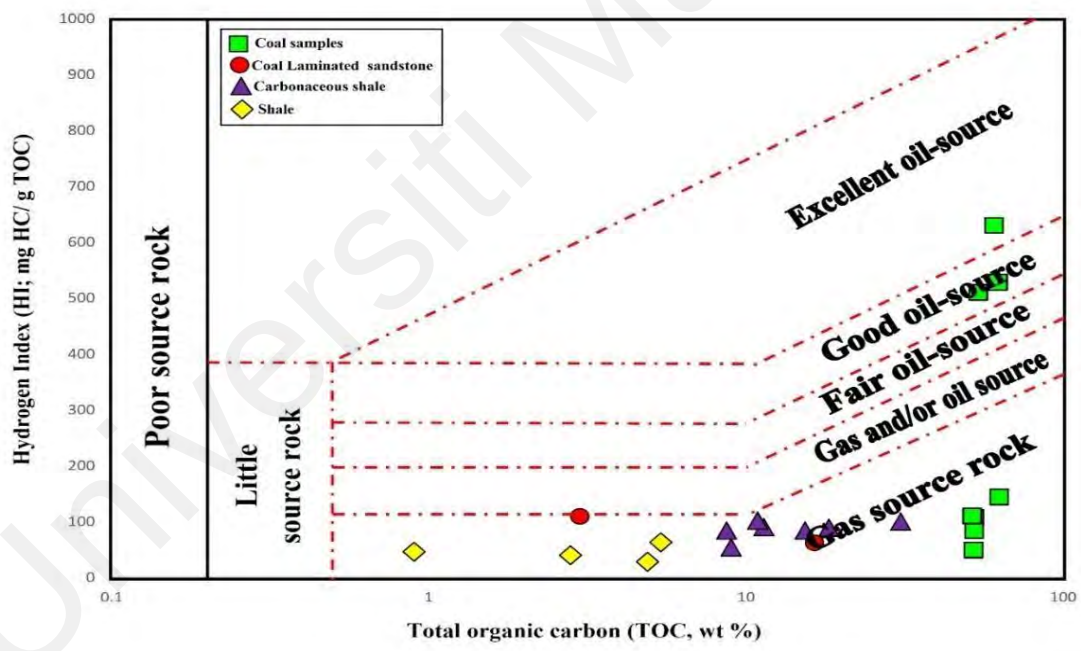

Figure 6.11: Geochemical correlation between hydrogen index (HI) and total organic carbon (TOC) showing gas type source rock for most samples with three coal sample exceptions. The three coals samples were expected to be able to generate little oil.

CHAPTER 7: CONCLUSION

This thesis entails geochemistry and petrology analyses to evaluate the Miocene deposits of the Bongaya Formation found in the Pitas area of Sabah for their potential as source rocks. The analyzed samples also include additional information about the source of organic matter in this formation and their depositional environment and condition settings. The results of this research are concluded as below:

1. The geochemical findings of the current study show that the Bongaya sediments have moderate to high TOC contents between 0.90 wt. %, and 63.1 wt. %, indicating favorable source-rock characteristics and satisfies the requirement to generate good hydrocarbon in the range from fair to excellent except mudstone. A complementary analysis with pyrolysis S2 yields revealed that coal has a very excellent potential while carbonaceous shale mostly shows good potential, leaving shale with poor to good hydrocarbon generating potential.

2. The selected Bongaya sediments are dominant in Type III kerogen, with HI values less than 200 HC/g TOC and thus, these sediments could be gas resources. Furthermore, several samples of coal and carbonaceous shale sediments are characterized to have mixed Type II/III kerogen as identified from Py-GC data and maceral types and they are considered to have mixed oil and gas source rocks, with significant amounts of high wax oil generation at sufficient maturity levels.

3. Both chemical and optical maturity results indicated that the Bongaya Formation is currently at an immature for hydrocarbon generation. Thus, the Type III and II/III kerogens in the analyzed Bongaya sediments have not been cracked by thermal alteration to release oil and/or gas.

4. Most of the analyzed Bongaya sediments have large contributions of terrestrial-derived organic matter, as mainly huminite organic matter are derived from plants and due to the abundance of high molecular weight alkanes. However, trace element analysis and Paq revealed that some of the samples analyzed had little marine organic matter interference (for some coals and sandy sediments). For coal source rock, this supported Type II/III kerogen mixed organic materials. The results are consistent with the bulk kinetic analysis that shows Bongaya Formation was derived from heterogeneous organic matter. Also, it is identified that the paleoenvironment is suboxic.

5. The source rock of the Bongaya Formation has been interpreted to be in a transitional environment where the paleoenvironment comprises back mangrove, mangrove, and freshwater environments. It is identified that the organic matter is mostly originated from the mangrove plant as the mangrove zone colonizes the area.

6. Although the sediments are potential source rocks, it is recommended to seek deeper stratigraphy or basins (possibly in the Offshore-Malawi Basins) to have better pressure and heat for hydrocarbon production which helps improve the opportunities and petroleum resource exploration approaches in the Sabah Basin.

REFERENCES

Abbassi, S., Edwards, D.S., George, S.C., Volk, H., Mahlstedt, N., di Primio, R., Horsfield, B. (2016). Petroleum potential and kinetic models for hydrocarbon generation from the Upper Cretaceous to Paleogene Latrobe Group coals and shales in the Gippsland Basin, Australia. *Organic Geochemistry, 91*, 54–67.

Abbassi, S., George, S.C., Edwards, D.S., di Primio, R., Horsfield, B., and Volk, H. (2014). Generation characteristics of Mesozoic syn- and post-rift source rocks, Bonaparte Basin, Australia: New insights from compositional kinetic modelling. *Marine and Petroleum Geology, 50*, 148-165.

Abdul Jalil, M., & Mohd Jamaal, H. (1992). Possible source for the Tembungo Oils: Evidences from Biomarker Fingerprints. *Geology Society of Malaysia, 32*, 213-232.

Abdullah, W. H., Togunwa, O. S., Makeen, Y. M., Hakimi, M. H., Mustapha, K. A., Baharuddin, M. H., Sia, S.G., & Tongkul, F. (2017). Hydrocarbon source potential of Eocene-Miocene sequence of western Sabah, Malaysia. *Marine and Petroleum Geology, 83*, 345-361.

Adedosu, T.A., Sonibare, O.O., Tuo, J., & Ekundayo, O. (2012). Biomarkers, carbon isotopic composition and source rock potentials of Awgu coals, middle Benue trough, Nigeria. *Journal of African Earth Sciences, 66*, 13-21.

Adegoke, A. K., Abdullah, W. H., Hakimi, M. H., & Yandoka, B. M. S. (2015). Geochemical characterisation and organic matter enrichment of Upper Cretaceous Gongila shales from Chad (Bornu) Basin, northeastern Nigeria: Bioproductivity versus anoxia conditions. *Journal of Petroleum Science and Engineering, 135*, 73-87.

Akinlua, A., Torto, N., Ajayi, TR., & Oyekunle, JAO. (2007). Trace metal characterisation of Niger Delta kerogens. *Fuel, 86*, 1358–1364

Akinlua, A., Adekola, S.A., Swakamisa, O., Fadipe, O.A., & Akinyemi, S.A. (2010). Trace element characterisation of Cretaceous Orange Basin hydrocarbon source rocks. *Applied Geochemistry, 25*, 1587-1595.

Alexander, T., Baihly, J., Boyer, C., Clark, B., Waters, G., Jochen, V., ... & Toelle, B. E. (2011). Shale gas revolution. *Oilfield review, 23(3)*, 40-55.

Algeo, T.J., & Maynard, J.B. (2004). Trace-element behavior and redox facies in core shales of Upper Pennsylvanian Kansas-type cyclothems. *Chemical Geology, 206*, 289–318.

Amane, W., & Hideki, N. (1997). Geochemical characteristics of terrigenous and marine sourced oils in Hokkaido, Japan. *Organic Geochemistry, 28*, 27–41.

Andrew, D.H., Bradley, D.R., David, Z.J., Moldowan, M., & Ulderico, B. (2001). Upper Oligocene lacustrine source rocks and petroleum systems of the northern qaidam basin, Northwest China. *American Association of Petroleum Geologist Bulletin, 85*, 601–619.

Anuar, A., & Abdul Jalil, M. (1997). A comparison of source rock facies and hydrocarbon types of the Middle Miocene sequence, offshore NW Sabah Basin Malaysia. In: Howes, J.V.C. and Noble, R.A eds, Proceedings of the IPA Petroleum Systems of SE Asia and Australia, 21-23 May 1997, *Indonesian Petroleum Association, Jakarta*, 773-786.

Arfaoui, A., Montacer, M., Kamoun, F., & Rigane, A. (2007). Comparative study between Rock-Eval prolysis and biomarkers parameters: A case study of Ypresian source rocks in central-northern Tunisia. *Marine and Petroleum Geology, 24*, 566-578.

Back, S., Morley, C. K., Simmons, M. D., & Lambiase, J. J. (2001). Depositional environment and sequence stratigraphy of Miocene deltaic cycles exposed along the Jerudong anticline, Brunei Darussalam. *Journal of Sedimentary Research*, *71*(6), 913-921.

Back, S., Strozyk, F., Kukla, P. A., & Lambiase, J. J. (2008). Three-dimensional restoration of original sedimentary geometries in deformed basin fill, onshore Brunei Darussalam, NW Borneo. *Basin Research*, *20*(1), 99-117.

Back, S., Tioe, H. J., Thang, T. X., & Morley, C. K. (2005). Stratigraphic development of synkinematic deposits in a large growth-fault system, onshore Brunei Darussalam. *Journal of the Geological Society*, *162*(2), 243-257.

Balaguru, A., & Hall, R. (2008). *Tectonic Evolution and Sedimentation of Sabah, North Borneo, Malaysia*. Paper presented at the Extended Abstract American Association of Petroleum Geologist International Conference Exhibition, Cape Town.

Balaguru, A., Nichols, G., & Hall, R. (2003). The origin of the 'circular basins' of Sabah, Malaysia.

Barwise, A. J. G. (1990). Role of nickel and vanadium in petroleum classification. *Energy & Fuels*, *4*(6), 647-652.

Basent, G.G., Rajendra, S.B., Ashok, K.B., Dinesh, K., Kusum, L.P., Adarsh, K.M., Jagdish, P.G., Gaur, C.D., & Nizhat, J.T. (2005). Geochemical characterization and source investigation of oils discovered in Khoraghat–Nambar structures of the Assam-Arakan Basin, India. *Organic Geochemistry, 36*, 161–181.

Bhattacharya, S., Dutta, S., & Summons, R. E. (2017). A distinctive biomarker assemblage in an Infracambrian oil and source rock from western India: Molecular signatures of eukaryotic sterols and prokaryotic carotenoids. *Precambrian Research, 290*, 101-112.

Bordenave, M. L. (1993). Applied petroleum geochemistry. Editions Technip, Paris.

Bray, E.E., & Evans, E.D. (1961). Distribution of n-paraffins as a clue to recognition of source beds. *Geochimica et Cosmochimica Acta, 22*, 2–15.

Brook, P.W. (1986). Unusual biological marker geochemistry of oils and possible source rock, offshore Beaufort – Mackenzie Delta, Canada, in D. Leythaeuser and J.

Rullkotter, eds., Advances in Organic Geochemistry 1985: Oxford, Pergamon, p. 401-406.

Brooks, J., & Smith, W.J. (1969). The diagenesis of plant lipids during the formation of coal petroleum and natural gas coalification and the formation of oils and gas in the Gippsland basin. *Geochimica et Cosmochimica Acta, 33*, 1183–1194.

Burnham, A. K., Braun, R. L., Gregg, H. R., & Samoun, A. M. (1987). Comparison of methods for measuring kerogen pyrolysis rates and fitting kinetic parameters. *Energy & Fuels, 1(6)*, 452-458.

Chandra, K., Mishra, C.S., Samanta, U., Gupta, A., & Mehrotra, K.L. (1994). Correlation of different maturity parameters in the Ahmedabad–Mehsana block of the Cambay basin. *Organic Geochemistry, 21*, 313–321.

Collenette, P. (1958). The geology and mineral resourcess of the Jesselton-Kinabalu area, North Borneo. *British Geological Survey, 6.*

Combaz, A. (1964). The palynofacies. *Revue de Micropaleontologie, 7 (3)*, 205-218.

Connan, J., Bouroullec, J., Dessort, D. & Albrecht, P. (1986). The microbial input in carbonate- anhydrite facies of a Sabkah paleoenvironment from Guatemala: A molecular approach. *Organic geochemistry, 10*, 29- 50.

Dai, S., Bechtel, A., Eble, C. F., Flores, R. M., French, D., Graham, I. T., ... & O'Keefe, J. M. (2020). Recognition of peat depositional environments in coal: A review. *International Journal of Coal Geology, 219,* Article#103383.

Dembicki Jr, H. (2009). Three common source rock evaluation errors made by geologists during prospect or play appraisals. *American Association of Petroleum Geologist Bulletin, 93(3)*, 341-356.

Dembicki Jr., Horsfield, H.B., & Ho, T.T.Y. (1983). Source rock evaluation by pyrolysis gas chromatography. *American Association of Petroleum Geologist Bulletin, 67*, 1094-1103

Di Primio, R., & Horsfield, B. (2006). From petroleum-type organofacies to hydrocarbon phase prediction. *American Association of Petroleum Geologist Bulletin, 90(7),* 1031-1058.

Didyk, B.M., Simoneit, B.R.T., Brassell, S.C., & Eglinton, G. (1978). Organic geochemical indicators of palaeoenvironmental conditions of sedimentation. *Nature, 272*, 216–222.

Dieckmann, V. (2005). Modelling petroleum formation from heterogeneous source rocks: the influence of frequency factors on activation energy distribution and geological prediction. *Marine and Petroleum Geology, 22(3),* Article#375e390.

Dow, W. G. (1977). Kerogen studies and geological interpretations. *Journal of Geochemical Exploration*, *7*, 79-99.

Eglinton, G. & Hamilton, R. G. (1967). Leaf epicuticular waxes. *Science, 156*, 1322–1344.

Eglinton, T. I., Damsté, J. S. S., Kohnen, M. E., & de Leeuw, J. W. (1990). Rapid estimation of the organic sulphur content of kerogens, coals and asphaltenes by pyrolysis-gas chromatography. *Fuel, 69(11)*, 1394-1404.

El Kammar, M. M. (2015). Source-rock evaluation of the Dakhla Formation black shale in Gebel Duwi, Quseir area, Egypt. *Journal of African Earth Sciences, 104*, 19-26.

Espitalié, J., Deroo, G., & Marquis, F. (1985). La pyrolyse Rock-Eval et ses applications. Deuxième partie. *Revue de l'Institut Français du Pétrole, 40(6)*, 755-784.

Espitalie, J., Marques, F. & Barsony, I. (1984). Geochemical logging. In: Voorhees, K.J. (Ed.), Analytical Pyrolysis-Techniques and Applications: Boston, Butterworth, p. 276-304.

Fan Pu, King, J.D., & Claypool, G. E. (1987**).** Characteristics of biomarker compounds in Chinese crude oils. In: Petroleum Geochemistry and Exporation in the Afro- Asian Region (R.K Kumar et al., eds.) Balkema, Rotterdam, p. 197-202.

Ficken, K.J., Li, B., Swain, D.L. and Eglinton, G. (2000). An n-alkane proxy for the sedimentary input of submerged/floating fresh water aquatic macrophytes. *Organic Geochemistry* 31 (7-8),745-749.

Frederiksen, N.O. (1985). Review of Early Tertiary Sporomorph Paleoecology. *American Association Stratigraphic Palynologist Contribution Series 15*, 97 pp.

Gelpi, E., Schneider, H., Mann, J., & OroAˆ , J. (1970). Hydrocarbons of geological significance in microscopic algae. *Phytochemistry, 46*, 1663–1671.

Germeraad, J.H., Hoping, C.A., & Muller, J. (1968). Palynology of tertiary sediments from tropical areas. *Review of Palaeobotany and Palynology, 6,* 189–348.

Gogou, A., Bouloubassi, I. & Stephanou, E. G. (2000). Marine organic geochemistry of the Eastern Mediterranean: 1. Aliphatic and polyaromatic hydrocarbons in Cretan Sea surficial sediments. *Marine Chemistry, 68*, 265-82.

Gonzalez-vila, F.J. (1995). Alkane biomarkers geochemical significance and application in oil shale geochemistry. In: Snape, C. (Ed.), Composition, Geochemistry and Conversions of Oil Shales. *Kluwer Academic Publishes*, pp. 51–68.

Guo, Y., & Bustin, R.M. (1998). Micro-FTIR spectroscopy of liptinite macerals in coal. *International Journal of Coal Geology, 36*, 259–275.

Hakimi, M. H., Abdullah, W. H., & Shalaby, M. R. (2012). Molecular composition and organic petrographic characterization of Madbi source rocks from the Kharir Oilfield of the Masila Basin (Yemen): palaeoenvironmental and maturity interpretation. *Arabian Journal of Geosciences*, *5*(4), 817-831.

Hakimi, M. H., Abdullah, W. H., Alqudah, M., Makeen, Y. M., Mustapha, K. A., & Hatem, B. A., (2018). Pyrolysis analyses and bulk kinetic models of the Late Cretaceous oil shales in Jordan and their implications for early mature sulphur-rich oil generation potential. *Marine and Petroleum Geology, 91*, 764-775.

Hakimi, M. H., Abdullah, W. H., Mustapha, K. A., & Adegoke, A. K. (2015). Petroleum generation modeling of the Late Cretaceous coals from the Jiza-Qamar Basin as infer by kerogen pyrolysis and bulk kinetics. *Fuel, 154*, 24-34.

Hakimi, M. H., Ahmed, A., Kahal, A. Y., Hersi, O. S., Al Faifi, H. J., & Qaysi, S. (2020). Organic geochemistry and basin modeling of Late Cretaceous Harshiyat Formation in the onshore and offshore basins in Yemen: Implications for effective source rock potential and hydrocarbon generation. *Marine and Petroleum Geology. 122*, Article#104701.

Hall, R. (1996). Reconstructing Cenozoic SE Asia. In: Hall, R., Blundell D.J. (Eds.), Tectonic Evolution of SE Asia. *Geological Society of London Special Publication 106*, pp. 153- 184.

Hazebroek, H. P., & Tan, D. N. (1993). Tertiary tectonic evolution of the NW Sabah continental margin. *Bulletin of Geologic Society of Malaysia, 33*, 195-210.

Hinz, K., Fritsch, J., Kempter, E. H. K., Mohammad, A. M., Meyer, J., Mohamed, D., ... & Benavidez, J. (1989). Thrust tectonics along the north-western continental margin of Sabah/Borneo. *Geologische Rundschau*, *78*(3), 705-730.

Horsfield, B. (1989). Practical criteria for classifying kerogens: Some observations from pyrolysis gas chromatography. *Geochimica et Cosmochimica Acta 53*.

Huang, W.Y., & Meinschein, W.G. (1979). Sterols as source ecological indicators. *Geochimica et Cosmochimica Acta 43*, 739–745.

Hunt, J.M. (1996). Petroleum Geochemistry and Geology, second ed. Freeman, San Francisco. pp. 408-411.

Hutchison, C. S. (1996). The 'Rajang accretionary prism'and 'Lupar Line'problem of Borneo. *Geological Society, London, Special Publications*, *106*(1), 247-261.

Hutchison, C. S. (1997). Tectonic framework of the Neogene basins of Sabah. Abstracts Geological Society of Malaysia Petroleum Geology Conference 1997.

Ingram, G. M., Chisholm, T. J., Grant, C. J., Hedlund, C. A., Stuart-Smith, P., & Teasdale, J. (2004). Deepwater North West Borneo: hydrocarbon accumulation in an active fold and thrust belt. *Marine and Petroleum Geology*, *21*(7), 879-887.

International Committee for Coal Petrology. (1971). International Handbook of Coal Petrography: Supplement to the 2nd Edition. Centre national de la recherche scientifique.

Jarvie, D. M., Weldon, W. D., Leroux, B., & Walker, P. R. (1996). Automated thermal extraction and pyrolysis total petroleum hydrocarbon and kinetic analysis using the

SR analyzer. In Pittsburgh Conference on Analytical Chemistry and Spectroscopy Abstracts, Chicago, Illinois, Paper (Vol. 785).

Jasin, B., & Tahir, S. (1988). Barremian radiolaria from the Chert-Spilite Formation, Kudat, Sabah. *Sains Malaysiana*, *17*(1), 67-79.

Jia, J., Liu, Z., Bechtel, A., Strobl, S. A., & Sun, P. (2013). Tectonic and climate control of oil shale deposition in the Upper Cretaceous Qingshankou Formation (Songliao Basin, NE China). *International Journal of Earth Sciences, 102(6),* 1717-1734.

Jones, B., & Manning, D.A.C. (1994). Comparison of geochemical indices used for the interpretation of paleoredox conditions in ancient mudstones. *Chemical Geology, 114*, 111–129.

Keym, M., Dieckmann, V., Horsfield, B., Erdmann, M., Galimberti, R., Kua, L. C., ... & Podlaha, O. (2006). Source rock heterogeneity of the Upper Jurassic Draupne Formation, North Viking Graben, and its relevance to petroleum generation studies. *Organic Geochemistry, 37(2)*, 220-243.

King, R. C., M. R. P. Tingay, R. R. Hillis, C. K. Morley, and J. Clark. (2010). Present-day stress orientations and tectonic provinces of the NW Borneo collisional margin. *Journal of Geophysical Research, 115* (B10).

Kirk, H. J. C. (1968). The igneous rocks of the Sarawak and Sabah. *Geological Survey Borneo Region, Malaysia, Bull*, *5*, 201.

Kolattudy, P.E. (1970). Plant waxes. *Lipids 5*, 259–275.

Large, D.J., & Gize, A.P. (1996). Pristane/phytane ratios in the mineralized Kupferschiefer of the Fore-Sudetic Monocline, Southwest Poland. *Ore Geology Reviews, 11*, 89–103.

Lee, D. T. (1988). Gunung Pock Area, Semporna Peninsula, Sabah, Malaysia: Explanation of Sheet 4/118/10. *Geological Survey of Malaysia, Sabah,* (Vol. 9).

Lee, T. (1980). Application of landsat images to regional geologic studies, with reference to the geology of central and west coast Sabah and adjacent areas.

Leong, K. M. (1998). Sabah crystalline basement: "Spurious" radiometric ages? Continental. *Warta Geologi, Geological Society of Malaysia Newsletter*, *24*, 5-8.

Leong, K. M., & KM, L. (1978). The" Sabah Blueschist Belt"; a Preliminary Note. *Warta Geologi, Geological Society of Malaysia Newsletter*, *4*, 45-51.

Leong, K.M., (1999). Geological Setting of Sabah. The Petroleum Geology and Resources of Malaysia. Petroliam Nasional Berhard (PETRONAS). Kuala Lumpur. 293-341.

Leong, K.M. (1974). The geology and mineral resources of the Upper Segama Valley and Darvel area, Sabah, Malaysia. *Geological Society of Malaysia Memoir 4*, 354pp.

Levell, B. K. (1987). The nature and significance of regional unconformities in the hydrocarbon–bearing neogene sequence offshore west Sabah.

Lewan, M.D. (1984) Factors controlling the proportionality of vanadium to nickel in crude oils. *Geochimica et Cosmochimica Acta, 48*, 2231–2238

Lewan, M. D. (1984). Factors controlling the proportionality of vanadium to nickel in crude oils. *Geochimica et Cosmochimica Acta*, *48*(11), 2231-2238.

Liechti, P., Roe, F. W., & Haile, N. S. (1960). The Geology of Sarawak, Brunei and the Western Part of North Borneo. *Kuching Sarawak: Geological Survey Department British Territories in Borneo.*

Lijmbach G. W. M. (1975). On the origin of petroleum. 9th World Petroleum Congress, Tokio Proc., Vol. 2, pp. 357-369

Lyons, T.W., Werne, J.P., Hollander, D.J., & Murray, R.W. (2003). Contrasting sulfur geochemistry and Fe/Al and Mo/Al ratios across the last oxic-to-anoxic transition in the Cariaco Basin, Venezuela. *Chemical Geology, 195*, 131–157.

Mackenzie, A. S. (1984). Application of biological markers in petroleum geochemistry. *In: Advances in Petroleum Geochemistry Vol.1 (J. Brooks and D. H. Welte, eds.), Academic Press, London*, p. 115-214.

Mackenzie, A.S., & McKenzie, D. (1983). Isomerization and aromatization of hydrocarbons in sedimentary basins formed by extension. *Geological Magazine, 120*, 417–470.

Makeen, Y. M., Hakimi, M. H., Abdullah, W. H., Mustapha, K. A., Hassan, M. H. A., Shushan, I. E., ... & Lashin, A. A. (2020). Basin modelling and bulk kinetics of heterogeneous organic-rich Nyalau Formation sediments of the Sarawak Basin, Malaysia. *Journal of Petroleum Science and Engineering,* 195, Article#107595.

Mann, A. L., Goodwin, N.S. & Lowes, S. (1987). Geochemical characteristic of lacustrine source rocks: A combined palynological/ molecular study of study of a Tertiary sequence from offshore China. *In: Proceedings of the Indonesian Petrol. Assoc., 6th Ann. Conv. Jakarta, Indonesian Petrol Assoc., Vol. 1*, p. 241-258.

Maxwell, J.R., Cox, R.F., Akman, R.G., & Hooper, S.N. (1972). In: Von Goertner, H.R., Wehner, H. (Eds.), Advances in Organic Geochemistry. Pergamon Press, p. 277.

Maxwell, J. R., Cox, R. E., Eglinton, G., Pillinger, C. T., Ackman, R. G., & Hooper, S. N. (1973). Stereochemical studies of acyclic isoprenoid compounds—II The role of chlorophyll in the derivation of isoprenoid-type acids in a lacustrine sediment. *Geochimica et Cosmochimica Acta, 37(2)*, 297-313.

Mazlan, M., Leong, K.M., & Azlina Anuar, (1999). Sabah Basin. The Petroleum Geology and Resources of Malaysia. Percetakan Mega, Kuala Lumpur, pp. 501-538.

Moldowan, J.M., Seifert, W.K., & Gallegos E.J. (1985). Relationship between petroleum composition and depositional environment of petroleum source rocks. *American Association of Petroleum Geologist Bulletin, 69*, 1255–1268

Morley, C. K., Back, S., Van Rensbergen, P., Crevello, P., & Lambiase, J. J. (2003). Characteristics of repeated, detached, Miocene–Pliocene tectonic inversion events, in a large delta province on an active margin, Brunei Darussalam, Borneo. *Journal of Structural Geology*, *25*(7), 1147-1169.

Morley, R. J. (1977). Palynology of tertiary and quaternary sediments in Southeast Asia. Proceeding of the 6th Annual Convention of the Indonesian Petroleum Association, pp. 255–276.

Morley, R.J. (2000). Origin and Evolution of Tropical Rain Forest. *John Wiley and Sons, Chichester*, 362 pp.

Morley, R.J. (1991). Tertiary stratigraphic palynology in Southeast Asia: Current status and new directions. *Geology Society Malaysia Bulletin, 28,* 1–36

Mukhopadhyay, P.K., Wade, J.A., & Kruge, M.A. (1995). Organic facies and maturation of Jurassic/Cretaceous rocks, and possible oil-source rock correlation based on pyrolysis of asphaltenes, Scotion Basin, Canada. *Organic Geochemistry, 22*, 85–104.

Mustapha, K. A., & Abdullah, W. H. (2013). Petroleum source rock evaluation of the Sebahat and Ganduman Formations, Dent Peninsula, Eastern Sabah, Malaysia. *Journal of Asian Earth Sciences, 76*, 346-355.

Nameroff, T.J., Calvert, S.E., & Murray, J.W. (2004). Glacial–interglacial variability in the eastern tropical North Pacific oxygen minimum zone recorded by redox-sensitive trace metals. *Paleoceanography, 19*(1).

Nor Azidin, N.F., Balaguru, A., & Ahmad, N. (2011). Structural Styles of the North West Sabah and West Sulawesi Fold Thrust Belt Regions and its Implication to the Petroleum System – A Comparison. PGCE, Kuala Lumpur.

Ourisson, G., Albrecht, P. & Rohmer, M. (1982). Predictive microbial biochemistry- from molecular fossils to prokaryotic membranes. *Trends in Biochemical Sciences*, 236-239.

Palacas, J.G., Anders, D.E., & King, J.D. (1984). South Florida basin prime example of carbonate source rocks of petroleum. *In: Palaces, J.G. (Ed.), Petroleum Geochemistry and Source Rock Potential of Carbonate Rocks AAPG, 18. Studies in Geology*, pp. 71–96.

Pepper, A. S., & Corvi, P. (1995). Simple kinetic models of petroleum formation. Part 1: Oil and gas generation from kerogen. *Marine and Petroleum Geology, 12,* 291-319.

Peters, K. E. (1986). Guidelines for evaluating petroleum source rock using programmed pyrolysis. *American Association of Petroleum Geologist Bulletin, 70(3),* 318-329.

Peters, K.E., & Cassa, M.R., (1994). Applied source rocks geochemistry, In: Magoon, L.B., Dow, W.G. (Eds.), The Petroleum System, from Source to Trap. *American Association of Petroleum Memoir, vol. 60*, pp. 93–120.

Peters, K.E., Moldowan, J.M. (1993). The biomarker guide: interpreting molecular fossils. In: Petroleum and Ancient Sediments. Prentice Hall, New Jersey, p. 363.

Peters, K.E., Walters, C.C., & Moldowan, J.M. (2005). The Biomarker Guide: Biomarkers and Isotopes in Petroleum Systems and Earth History, second ed. Cambridge University, pp. 476–625.

Petersen, H. I., Øverland, J. A., Solbakk, T., Bojesen-Koefoed, J. A., & Bjerager, M. (2013). Unusual resinite-rich coals found in northeastern Greenland and along the Norwegian coast: Petrographic and geochemical composition. *International Journal of Coal Geology, 109*, 58-76.

Philp, R.P. & Gilbert, T.D. (1986). Biomarker distributions in Austalian oils predominantly derived from terrigenous source material. *Organic Geochemistry, 10,* 73-84.

Philp, R.P. (1994). Geochemical characteristics of oil derived predominantly from terrigenous source materials. In: Scott, A.C., Fleet, A.J. (Eds.), Coal and Coal-Bearing Strata as Oil Prone Source Rocks. *Geology Society. Special Publication 77. The Geological Society, London*, pp. 71–91.

Philp, R.P., Fan, P., Lewis, C.A., Li, J., Zhu, H., & Wang, H. (1991). Geochemical characteristics of oils from Chaidamu, Shanganning and Jianghan basins, China. *Journal Southeast Asian Earth Science, 5*, 351–358.

Pi, D.H., Cong-Qiang, L., Shields-Zhoud, A.G., & Shao-Yong J. (2013). Trace and rare earth element geochemistry of black shale and kerogen in the early Cambrian Niutitang Formation in Guizhou province, South China: constraints for redox environments and origin of metal enrichments. *Precambrian Research, 225*, 218–229.

Pickel, W., Kus, J., Flores, D., Kalaitzidis, S., Christanis, K., Cardott, B. J., & Crosdale, P. (2017). Classification of liptinite–ICCP System 1994. *International Journal of Coal Geology, 169,* 40-61.

Ping, W., Tun-Hua, W., & Yong, Z. (2012). Monitoring and visualizing of PAHs into mangrove plant by two-photon laser confocal scanning microscopy. *Marine Pollution Bulletin, 64*,1654–1658.

Powell, T.G., & Makriday, D.M. (1973). Relationships between ratio of pristine to Phytane, crude oil composition and geological environments in Australia. *Nature, 243*, 37–39.

Rangin, C., & Silver, E. (1990). Geological setting of the Celebes and Sulu Seas. In *Proceedings of the Ocean Drilling Program, Initial Reports, 124,* 35-42.

Riboulleau, A., Baudin, F., Deconinck, J.-F., Derenne, S., Largeau, C., & Tribovillard, N. (2003). Depositional conditions and organic matter preservation pathways in an epicontinental environment: the Upper Jurassic Kashpir Oil Shales (Volga Basin, Russia). *Palaeogeography, Palaeoclimatology, Palaeoecology, 197*, 171–197.

Rimmer, S.M. (2004). Geochemical paleoredox indicators in Devonian– Mississippian black shales, Central Appalachian Basin (USA). *Chemical Geology, 206*, 373–391.

Rimmer, S.M., Thompson, J.A., Goodnight, S.A., & Robl, T.L. (2004). Multiple controls on the preservation of organic matter in Devonian–Mississippian marine black shales: geochemical and petrographic evidence. *Palaeogeography, Palaeoclimatology, Palaeoecology, 215,* 125–154.

Riquier, L., Tribovillard, N., Averbuch, O., Joachimski, M. M., Racki, G., Devleeschouwer, X., & Riboulleau, A. (2005). Productivity and bottom water redox conditions at the Frasnian-Famennian boundary on both sides of the Eovariscan Belt: constraints from trace-element geochemistry. In *Developments in Palaeontology and Stratigraphy*. *Elsevier, 20,* 199-224.

Sageman, B.B., Murphy, A.E., Werne, J.P., Ver Straeten, C.A., Hollander, D.J., & Lyons, T.W. (2003). A tale of shales: the relative roles of production, decomposition, and dilution in the accumulation of organic-rich strata, Middle–Upper Devonian, Appalachian Basin. *Chemical Geology, 195*, 229–273.

Sandal, S. T. (Ed.). (1996). *The geology and hydrocarbon resources of Negara Brunei Darussalam.* Muzium Brunei.

Sarmiento, L.F., & Rangel, A. (2004). Petroleum systems of the Upper Magdalena Valley, Colombia. *Marine Petroleum Geology, 21*, 373–391.

Schenk, H. J., Horsfield, B., Krooss, B., Schaefer, R. G., & Schwochau, K. (1997). Kinetics of petroleum formation and cracking. *Petroleum and Basin Evolution*, *Springer,* 231-269.

Scherer, F.C. (1980). Exploration in East Malaysia over the past decade. In: Halbouty, M.T., ED., Giant Oil and Gas Fields of the Decade 1968-1978. *American Association of Petroleum Geologist Memoir, 30*, 423-440.

Seifert, W.K., & Moldowan, J.M. (1980). The effect of thermal stress on source-rock quality as measured by hopane stereochemistry. *Physics and Chemistry of the Earth, 12*, 229-37.

Seifert, W.K., & Moldowan, J.M. (1978). Applications of steranes, terpanes and monoaromatics to the maturation, migration, and source of crude oils. *Geochimica et Cosmochimica Acta*, 42, 77–95.

Seifert, W.K., & Moldowan, J.M., (1979). The effect of biodegradation on steranes and terpanes in crude oils. *Geochimica et Cosmochimica Acta, 43,*111–126.

Simoneit, B. R. T. (2004). Biomarkers (Molecular fossils) as geochemical indicators of life. *Advances in Space Research, 33*, 1255-61.

Slater, S. M., & Wellman, C. H. (2016). Middle Jurassic vegetation dynamics based on quantitative analysis of spore/pollen assemblages from the Ravenscar Group, North Yorkshire, UK. *Palaeontology, 59(2),* 305-328.

Sonibare, O., Alimi, H., Jarvie, D., & Ehinola, O. A. (2008). Origin and occurrence of crude oil in the Niger delta, Nigeria. *Journal of Petroleum Science and Engineering, 61(2-4),* 99-107.

Stauffer, P. H. (1967). Studies in the Crocker Formation, Sabah. *Geological Survey of Malaysia, Borneo Region Bulletin*, *8*, 1-13.

Stephens, E. A. (1956). *The geology and mineral resources of the Kota Belud and Kudat area, North Borneo* (Vol. 5). Kuching : Geological Survey Department.

Sweeney, J.J., & Burnham, A.K. (1990). Evaluation of a simple model of vitrinite reflectance based on chemical kinetics. *American Association of Petroleum Geologist Bulletin, 74*, 1559–1570.

Tan, D.N.K. (1982). The Lubuk Antu Melange, Lupar Valley, West Sarawak. A lower Tertiary subduction complex. *Bulletin of Geologic Society of Malaysia, 15*, 31-46.

Taylor, G.H., Teichmüller, M., Davis, A., Diessel, C.F.K., Littke, R., & Robert, P. (1998). *Organic Petrology.* Gebrüder Borntraeger, Berlin, Stuttgart.

Ten Haven, H.L., De leeuw, J.W., Rullkotter, J., & Sinninghe, D.J.S. (1987). Restricted utility of the pristane/phytane ratio as a palaeoenvironmental indicator. *Nature, 330*, 641–643.

Tissot, B. P., & Welte, D. H. (1984). *Petroleum Formation and Occurrence.* Springer-Verlag, Berlin, Heidelberg.

Tissot, B., Califet-Debyser, Y., Deroo, G., & Oudin, J. L. (1971). Origin and evolution of hydrocarbons in early Toarcian shales, Paris Basin, France. *American Association of Petroleum Geologist Bulletin*, *55(12)*, 2177-2193.

Tissot, B., Pelet, R., RoucacheAˆ, J., & Combaz, A. (1977). Utilisation des alkanes comme fossiles geochimiques indicateurs des environments geAˆ ologiques. In: Campos, R., GonA¨ i, J. (Eds.), *Advances in Organic Geochemistry*, 117–154.

Tjia, H. D. (1974). Sense of tectonic transport in intensely deformed Trusmadi and Crocker sediments, Ranau-Tenompok area, Sabah. *Sains Malaysiana*, *3*(2), 129-166.

Tongkul, F. (1997). Polyphase deformation in the Telupid area, Sabah, Malaysia. *Journal of Asian Earth Sciences*, *15*(2-3), 175-183.

Tongkul, F. (1987). The sedimentology and structure of the Crocker Formation in the Kota Kinabalu area, Sabah. PhD thesis, University of London (unpublished).

Tongkul, F. (1990). Structural style and tectonics of Western and Northern Sabah. *Geological Society of Malaysia Bulletin, 27*, pp. 227-239.

Tongkul, F. (1991). Basin development and deposition of the Bongaya Formation in the Pitas Area, Northern Sabah. *Geological Society of Malaysia Bulletin, 29*, p 183-193.

Tongkul, F. (1994). The geology of Northern Sabah, Malaysia: Its relationship to the opening of the South China Sea Basin. *Tectonophysics, 235(1-2),* 131-147.

Tribovillard, N., Algeo, T. J., Lyons, T., & Riboulleau, A. (2006). Trace metals as paleoredox and paleoproductivity proxies: an update. *Chemical geology*, *232*(1-2), 12-32.

Tribovillard, N., Averbuch, O., Devleeschouwer, X., Racki, G., & Riboulleau, A., (2004a). Deep-water anoxia over the Frasnian– Famennian boundary (La Serre, France): a tectonically-induced oceanic anoxic event? *Terra Nova, 16*, 288–295.

Tribovillard, N., Ramdani, A., & Trentesaux, A. (2005). Controls on organic accumulation in Late Jurassic shales of northwestern Europe as inferred from trace-metal geochemistry. In: Harris, N. (Ed.), The Deposition of Organic-Carbon-Rich Sediments: Models, Mechanisms, and Consequences. *SEPM Spec. Public.,82*, 145–164.

Tulloch, A. P. (1976). Chemistry of waxes of higher plants. *Chemistry and biochemistry of natural waxes*, 235-287.

Tyson, R. V. (1995). Abundance of organic matter in sediments: TOC, hydrodynamic equivalence, dilution and flux effects. *Sedimentary organic matter, Springer,* 81-118.

Udo, O.T., Ekwere, S., & Abrakasa, S. (1992). Some trace metals in selected Niger Delta crude oils: application in oil-oil correlation studies. *International Journal of Mining and Geological Engineering, 28*, 289–291.

Villar, H. J., Püttmann, W., & Wolf, M. (1988). Organic geochemistry and petrography of Tertiary coals and carbonaceous shales from Argentina. *Organic geochemistry, 13(4-6),* 1011-1021.

Volkman, J.K. (1986). A review of sterol biomarkers for marine and terrigenous organic matter. *Organic Geochemistry 9*, 83-99.

Volkman, J. K. (1988). Biological marker compounds as indicators of the depositional environments of petroleum source rocks. *Geological Society, London, Special Publications*, *40*(1), 103-122.

Walples, D.W., & Machihara, T. (1991). Biomarkers for geologists: A practical guide to the application of steranes and triterpanes in petroleum geology. *Geology magazines, 9*, Article#91.

Wan Hasiah A. (1999). Oil generating potential of the Tertiary coals and other organic rich sediments of the Nyalau Formation, onshore Sarawak. *Journal of Asian Earth Science, 17*, 255-267.

Wang, Z., Yang, C., Yang, Z., Brown, C. E., Hollebone, B. P., & Stout, S. A. (2016). Petroleum biomarker fingerprinting for oil spill characterization and source identification. *Standard handbook oil spill environmental forensics*, 131-254.

Weete, J. E. (1976). Algal and fungal waxes. *Chemistry and biochemistry of natural waxes*, 349–418.

Werne, J.P., Lyons, T.W., Hollander, D.J., Formolo, M.J., & Sinninghe Damsté, J.S. (2003). Reduced sulfur in euxinic sediments of the Cariaco Basin: sulfur isotope constraints on organic sulfur formation. *Chemical Geology, 195*, 159–179.

Wilson, R.A.M. (1961). The geology and mineral resources of the Banggi Island and Sugut River Area, North Borneo. *Borneo Geological Survey Memoir, 15*, pp 143.

Wood, G.R., Gabriel, A.M., & Lawson, J.C. (1996). Palynological techniques processing and microscopy. In: Jansoniun, J., McGregor, D.C. (Eds.), Palynology: Principle and Application. *American Association of Stratigraphic Palynologist Foundation*, 29–50.

Yensepbayev, T., Izart, A., Joltaev, G., Hautevelle, Y., Elie, M. & Suarez-Ruiz, I. (2010). Geochemical characterization of source rocks and oils from the eastern part of the Precaspian and Pre-Uralian Basins (Kazakhstan): Palaeoenvironmental and palaeothermal interpretation. *Organic Geochemistry, 41*, 242-62.

Zhao, J., Jin, Z., Jin, Z., Geng, Y., Wen, X., & Yan, C. (2016). Applying sedimentary geochemical proxies for paleoenvironment interpretation of organic-rich shale deposition in the Sichuan Basin, China. *International Journal of Coal Geology, 163*, 52-71.